Chapter 5
Physical Chemistry of Intercalated System

The driving force of development of intercalation chemistry is significant improvement of properties of fabricated nanocomposites and design of materials with new properties. Forming hybrid structures (sometimes called "ship-in-the-bottle") define important functional characteristics: improved mechanical strength (increase in modulus), enhanced stiffness, heat resistance (decrease in thermal expansion coefficient), heat stability, and other thermal physical properties, water resistance, interesting barrier properties for gas separation, high flame and fire resistance, electric and electrochemical behavior, size stability, chemical stability, different from the simple additive properties [1–20].

Hybrid-phase nanocomposites [21] are not only of academic, but of commercial interest, because they posses improved mechanical and thermal properties as compared with the same content of conventional fillers (such as carbon soot or deposited silica gel). The methods of production of hybrid nanocomposites from polymer solutions or polymerization in situ in combination with delamination and exfoliation were already studied at the end of the last century (for example, [22, 23]). However, there were technological drawbacks: these methods had low correlation with polymer production and demanded great amounts of organic solvents. At the beginning of 1990s more convenient technique appeared on the basis of PEO (polyethylene-oxide) and MMT (montmorillonite), which advantageously demonstrated the intercalation process in the polymer melt, as well as potential applications of the obtained products in solid phase electrolytes of recharged lithium batteries.

However, highly promising commercial strategy in this problem was formulated after the group of researchers of Toyota company [24–26] had found extraordinary strengthening of mechanical properties of polymer-layered nylon-based nanocomposites, which was caused by extremely large surface contacts of the ingredients and high aspect ratio reached in the intercalation/exfoliation process, and by homogenous dispersion of silica plates in the polymer matrix [27, 28]. On the one hand, these functional materials have a relation to nanocomposites via

A.D. Pomogailo, G.I. Dzhardimalieva, *Nanostructured Materials Preparation via Condensation Ways*, DOI 10.1007/978-90-481-2567-8_5

nanosized galleries of layered silicates (1—5 nm), distances between networks and layers formed by polymer and inorganic components, on the other hand, via the value of their exfoliated fragments [29].

Most widely known hybrid organic-inorganic nanocomposites are polymer-clay ones, which combine organic polymers with smectites. MMT is the most convenient layered silicate for application into intercalation systems, because their natural reserves are unlimited, substitution of their inlayer inorganic cations by organic ones, such as ammonium groups with long hydrocarbon chains, is easy. Such a modification provides better compatibility of a silicate with a polymer matrix [30, 31]. Polymer is inserted into interlayer space of a smectite via penetration from a solution, melt with following delamination (layering) or exfoliation (peeling) with in situ formation of mineral nanoparticles, which are uniformly distributed in the polymer. Intercalation of inorganic component into organic materials having limited interlayer distance with preserving of their layered structure is, on the one hand, a perfect way of structuring of organic-inorganic nano-ensembles [9], and, on the other hand, it provides additional possibilities for studying physical-chemical properties of these systems. These are supramolecular formations with original molecular architecture (see, for example, [9]).

Rigid crystalline matrices of these materials (*hosts*) with regulated system of percolation pores and nanosized layers can be filled with atomic or molecular *guest* structures: molecules of organic matters, not only monomer links, but also solvents, alkyl amines, crown ethers, cryptands, etc., and also clusters, nanoparticles, inorganic coordination polymers of $(CdS)_x$ type, large molecules, like C_{60} fullerenes. For example, intercalation of buckminsterfullerene functionalized with ethylene diamine into mica-like silicate of hectorite type was found [32].

Most substantial are other problems, whose solutions are closely connected to intercalation physical chemistry of periodic mesoporous structures: sorption and phase transitions; ion exchange and complex formation; formation of metal, oxide, sulfide, and semiconductor clusters and nanowires; covalent inoculation of ligand and functional groups to a *host*; finding of a composition and structure of hybrid materials, obtained via in situ assembling, condensation, polymerization, or insertion of primarily prepared macromolecules in the interlayer space, finding of topochemistry of individual stages of reactions, etc. Numerous studies concerning intercalation of organic metal organic and inorganic compounds, and properties of the formed products are published (previous studies on the subject were considered in our reviews [33, 34]. The great surge of the studies relates to the last decade and concerns mostly “bridges constructing” between inorganic materials having intercalation properties and intermediates forming, as well as to characteristics of hybrid-phase nanocomposites.

5.1 Composition, Structure, and Intercalation Properties of Layered Materials

From four thousands of known minerals hundreds are of zeolite type (amphoteric silicates) [35, 36]. Layered silicates or smectites, smectite clays are groups of clay rock minerals, 2D layered aluminosilicate, phyllosilicate, such as MMT are crystal formations of natural origin and produced by various synthetic methods (including hydrothermal, sol-gel synthesis, etc.). This is the most important type of solids with interesting functional and structural properties, whose special feature is a weak bond between individual layers. Natural Na-MMT clay of intercalation purity modified by long-chain ammonium cations, for example, trimethyl octadecyl ammonium chloride has exchange capacity 1.2 mg-eq/g, contains 56.3 mass.% of inorganic component, basal distance is $d_{001} = 2.07$ nm, aspect ratio, length to thickness ratio, is AR = 1/c from 80 to 1,120, average AR is 320. For comparison, we shall consider oxide content of the native montmorillonite (%): SiO_2 62.9, Al_2O_3 19.6, TiO_2 0.009, FeO 0.32, Fe_2O_3 3.35, MnO 0.006, MgO 3.05, CaO 1.68, Na_2O 0.153, K_2O 0.53, exchange capacity is 0.76 mg-eq/g. For non-modified MMT thickness of one structural layer is about 1 nm (0.96 nm), surface of the plates reaches 800 m^2/g, aggregates consist of tens of such plates, their size in nm is: saponite 50–60, MMT 100–150, hectorite 200–300, for the latter AR is also high [30].

Most widely known are also other natural materials used due to their prominent intercalation abilities: hectorite, laponite, nontonite, beidelite, volkonskoite, sepiolite, stevensite, sauconite, swinfordite, kenyaite, bentonite, in particular, bentonite clay containing predominantly MMT, $(Na,Ca)_{0.33}(Al,Mg)_2Si_4O_{10}(OH)_2 \cdot (H_2O)_n$, $d_{001} = 1.206$ nm, product of volcanic ash erosion, layered mica silicates, including vermiculite, illite and close to them hydro-mica tubular attapulgite, a kind of palygorskite, the mineral with tubular structure formed owing to corrugation of structural layers, etc. The structure and composition of the layered silicates, their physical-chemical properties, the origin of active surface have been studied in detail for a long time, their models and properties of intercalation systems were considered in many reviews (see, for example, just one of them [37]). These are specific materials, whose interlayer space includes sandwich OH- groups of octahedron aluminum hydroxide and oxygen atoms of tetrahedron silica sheets: the crystals consist of altering layers of cations and negatively charged silicates in the 2:1 ratio. Their main structuring blocks are $Si(O, OH)_4$ tetrahedrons and $M(O, OH)_6$ octahedrons, in which $M = Mg^{2+}$, Al^{3+}, $Fe^{2+,3+}$. In kaolin (M = Fe and Mg) tetrahedrons and octahedrons are condensed in a monolayer with the ratio 1:1. In many minerals there is isomorphism, which is due to substitution of Si^{4+} ions in tetrahedral or Al^{3+} or Mg^{2+} in octahedral layers. In these cases a lattice can acquire charge depending on a valence state – from electrically neutral, in the mineral groups of pyrophyllite, talc to $x + y = 0.25$–0.6 (layered silicates with such a charge are particularly called smectites), 0.6–0.9 in vermiculites, synthetic clays of hectorite

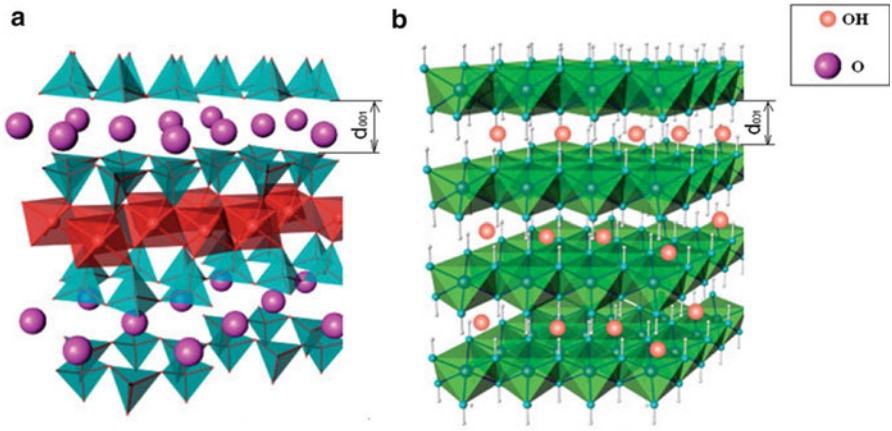

Fig. 5.1 The chemical general structures are respectively for: 2:1 phyllosilicates (**a**) and LDH (**b**), with the schematic representation of the tetrahedra (T) and octahedra (O) occupancies, substitution elements (Y), and interlayer ions (Z) in natural and synthetic layered nano-fillers. (a) Talc (T = Si, O = Mg (occupancy 3/3), Z none; hectorite: T = Si, O = Mg (occupancy 3/3); Y = Li, Z = Na^+/Mg^{2+}; saponite: T = Si, O = Mg (occupancy 3/3), Z = Na^+/Mg^{2+}, Y = Al; montmorinollite: T = Si, O = Al (occupancy 2/3), Z = Na^+/Mg^{2+}, Y = Mg; beidellite: T = Si, O = Al (occupancy 2/3), Z = Na^+/Mg^{2+}, Y = Al. б) brucite: O = Mg (occupancy 3/3), T = Z = Y none; gibbcite: O = Al (occupancy 2/3), T = Z = Y none; hydrotalcite: O = Mg/Zn etc., Z = Cl^-, CO_3^-, NO_3^-, T = Al

type, as $MgO(SiO_2)_s(Al_2O_3)_a(AB)_b(H_2O)_x$ (AB is a ionic pair of NaF type) and even 1 for mica. Oxide composition of Na-hectorite is $Na_{0.33}Mg_{2.67}Li_{0.33}Si_3O_{10}F_2$ and that of potassium tetrasilicate mica is $KMg_{2,5}Si_4O_{10}F_2$.

Idealized 2:1 structure of the layered silicate is presented by two tetrahedral sheets, which are condensed with octahedral sheets (the ratio is between tetrahedral and octahedral layers). The native silica gallery is usually filled with hydrated cations of alkali metal. The parameter, which characterizes intercalation activity of clay minerals can change depending on natural form of smectite clays, which is a crystal structure of aluminum silicate, a size of exchanging anions and aqua portion in the interlamellar space (Fig. 5.1).

In synthetic layered silicates (LHD) only octahedral and framing elements (Al, Mg, Zn, etc.) exist. General formula of dioctahedral minerals (pyrophyllite, vermiculite, and others) formed by Al-octahedrons, can be presented as follows $(Si_{8\text{-}x}M_y)^4(Al_{4\ -\ 'y})^6(OH)_4O_{20}M''_{(x+y)/n}(H_2O)_w$ (content of oxides in vermiculite is, mass.%): SiO_2 38.8, Al_2O_3 13.8, TiO_2 1.97, FeO 1.11, Fe_2O_3 6.25, MgO 18.3, foreign oxides MnO 0.03, Cr_2O_3 0.01, ZnO 0.01, NiO 0.12, CoO 0.01, cation capacity of this silicate is 1.36 mg-eq/g), and for Mg-octahedron based trioctahedral minerals (talc, saponite, biotite, hectorite, etc.) the formula is $(Si_{8\ -\ x}M_x)^4(Mg_{6\ -\ y}M'_y)^6(OH)_4O_{20}M''_{(x+y)/n}(H_2O)_w$, where x is a portion of isomorphic substitution.

Some characteristics of the surface and porosity of the most widely known alumosilicates[1] [38] are presented in Tables 5.1 and 5.2.

In the presence of water molecules in the MMT gallery it is difficult to obtain clear evidence of intercalation process. In the system dry MMT/PEO, MMT-B34 the intercalation process, for example, with PEO, is found by various physical chemical methods, for example, by X-ray powder diffractometry (XRD),[2] wide-angle X-ray scattering (WAXS), differential scanning calorimetry (DSC), etc.

We shall demonstrate this using as an example magadiite modified with long chained phosphorus-containing [39] surfactant (tributylhexadecylphosphonium bromide), which by its intercalation properties is close to organomodified MMT (OMMT)(Fig. 5.2).

In majority of layered systems basal (interlayer) space is no more than ~5 nm, a layer thickness in perovskite, for example, varies from 0.5 to 2.2 nm, dehydrated Na-MMT the space between the neighbor layers is approximately 1.0 (0.96 nm). It can increase from 1.25 nm to 1.50–1.55 or even to 1.80–1.90 nm, when mono-, bi-, and trimolecular water layers are inserted into the lamellar space. Layered

[1] As a rule, for scientific researches Swy-1 County Creek, Wyoming USA standard clays, or highly iron-concentrated smectite, Gafsa, Tunisia, supplied by Source Clay Repository, Clay Minerals Society or other suppliers (see, for example, [38]), Na-MMT - University of Missouri-Columbia (USA), Cloisite organic silicates, Benahavis (Málaga, Spain) vermiculite are used. MMT- Closite 30B is supplied by Southern Clay Products Inc (Texas, USA), Tokyo Kasei Industries Ltd, Na^+-MMT is supplied by Zhe-Jiang Fenghong Clay Company(China), modifier, N- diamine octadecyl ammonium chloride supplied by Zhejiang Chemi-520 Agent Company (China). It should be noted that also widely used are clays from Angrensk, Glukhovets national deposits, vermiculite from Kovdorsk deposit, etc. In the vermiculite from Kovdorsk deposit between mica packages $(Si_3{}^{4+}Al)O^{2-}{}_{10}(Mg^{2+})_6(OH^-)^{4-}$ hydrated layer is inserted, Mg ions are surrounded by 12 water molecules forming double-layer shell of Mg^{2+}. If an interlayer magnesium cation is replaced by univalent cations, the initial mineral is split into separate layers, bond strength between them depends on water state, its molecular mobility. First Mg^{2+} ions are substituted by Na^+ (via boiling in saturated NaCl solution), at the second stage sodium ions are substituted by $RNH_3{}^+$ (during boiling in 20–40 % aqua solution of respective alkyl ammonium chloride), cation exchange capacity is 1.7 mg-eq/g, after intense one-dimensional swelling, the mineral is dried in air. Water content in the dry product is 15–20 mass.%.

[2] Powder samples of organic silica were scanned to reflect in the angular range $2\theta = 2–10°$. The interlayer distance of the organic silicate is calculated using Wulf-Bragg equation by position of the d_{001} peak in the diffraction pattern $\lambda = 2d \sin\theta$, $\lambda = 0.1542$ nm is wavelength for Ni-filtered Cu K_α-radiation, d is interplanar distance, θ diffraction angle. After subtraction of background scattering, intensity of scattering distribution is implanted by azimuth angle and presented as dispersion function of q-vector in space:

$$q = \frac{4\pi}{\lambda}\sin\frac{2\theta}{2} \quad \text{and} \quad d_{001} = \frac{2\pi}{q}$$

$$d_{001} = \frac{1}{2}\frac{\lambda}{\sin(2\theta/2)}$$

Table 5.1 Characteristics of some aluminum silicates [395]

Silicate	Annealing temperature, °C	S_{sp} BET, m^2/g	V_{gen} porous, cm^3/g
Montmorillonite	Initial	50.0	0.081
	450	368	0.392
	500	382	0.402
	550	360	0.382
Vermiculite	Initial	23	0.043
	450	484	0.427
	500	471	0.396
Silicate			
Minerals	450	517	0.340
	500	600	0.398
	550	584	0.388

Table 5.2 Characteristics of some modified MMT [396]

Organosilicate[a]	Modifier ammonium cation[b]	2θ, deg	D_{001}, nm	Concentration of modifier, mg-eq/g
Cloisite® 10A	$(CH_3)_2(HT)(CH_2C_6H_5)$ N^+	4.38	2.01	1.25
Cloisite® 6A	$(CH_3)_2(HT)_2$ N^+	2.38, 4.34	3.7	1.40
Cloisite® C20A	$(CH_3)_2(HT)_2$ N^+	2.42		
Cloisite® 30B	$(CH_3)_2(T)$ $(CH_2CH_2OH)_2$ N^+	4.72	1.87	0.90

[a]Cation exchange capacity of the non-modified silicate is 0.926 mg-eq/g
[b]T(tallow) are amines of fatty acids of hydrated tall oil (~65 % C_{18}, ~30 % C_{16}, 5 % C_{14})

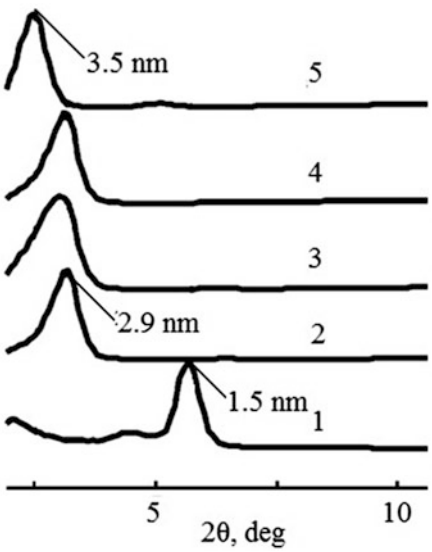

Fig. 5.2 WAXS of the magadiite powder (peak at $2\theta = 5.7°$ corresponds to a basal spacing of 1.5 nm) (*1*); organomodified magadiite (peak at $2\theta = 3.0°$ corresponds to 2.9 nm) (*2*); organomagadiite after melt annealing at 160 °C for 30 min (*3*); organomagadiite in PS microcomposites (*4*); and organomagadiite in PCL nanocomposites (peak at 2.58 corresponds to 3.5 nm) (*5*) [39]

perovskites are easily exfoliated into separate single nanosheets. From this point of view exfoliation can be regarded as the ultimate case of intercalation.

The longitudinal size of disc particles of clay is governed by the methods of its preparation: clays obtained by grinding have a typical plate shape with longitudinal size 0.1–1.0 μm. Taking into account the fact that their colloid sizes are characterized by extraordinary high length-to-thickness ratio, for example, AR = 25–27 for synthetic laponites, the exfoliated clays have extremely developed surface. For the AR to be AR > 25 is a mandatory demand for good intercalating properties of materials, which are of interest for the technology of fabrication of polymer nanocomposites (thickness of exfoliated plates is 0.7–2.5 nm) with far better characteristics of materials. In contrast to mica, cations in natural forms of smectite clays easily exchange as a result of isomorphic substitution of Al^{3+} by Mg^{2+} in $Si_8(Al_{3.34}\ Mg_{0.67})(OH)_4O_{20}M^+_{0.67}$ MMT, including replacement by the transition metal ions.

Exchange cation capacity depending on a crystal structure of aluminum silicate reaches 0.64–1.50 mg-eq/g (for MMT it is 1.10, for hectorite it is 1.20, for saponite it is 0.87 mg-eq/g, etc) [40]. A negative charge appears in the octahedral layer, it is compensated by metal cations in the interlayer space, which may be Na^+, Ca^{2+}, Mg^{2+} or Al^{3+}. Apart from non-stoichiometric octahedral substitution the natural MMT can also have tetrahedral isomorphic substitutions (in particular, Al^{3+} instead of Si^{4+}), and also excess negative charge on the side surfaces of the crystals and OH^- groups of the basic character. When M^{2+} cations are substituted by M^{3+} (Fe, Al, Ga) or by Zr^{4+}, Sn^{4+} in the layered materials, for example, LDH, exchange anion capacity can reach significant value, 2–4 mg-eq/g (Fig. 5.3) [41].

One important property of MMT is their tendency to swelling in polar reagents of ionic (water) and non-ionic (monoatomic and polyatomic alcohols, amines, nitro

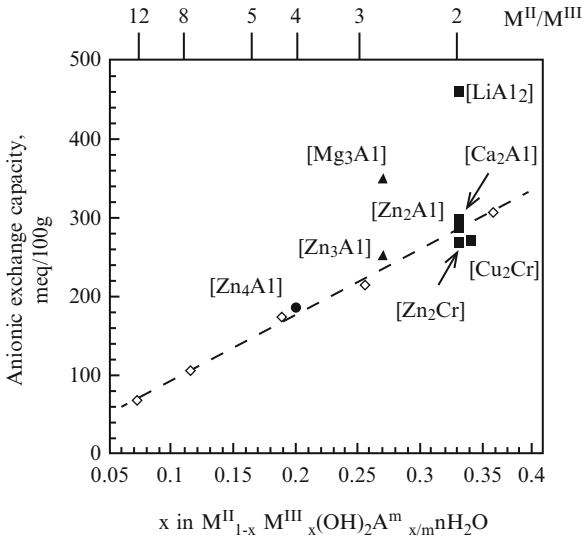

Fig. 5.3 Anionic exchange capacity *versus* layer charge for some LDH compositions [43]

methane, acetonitrile, ketones, aromatic hydrocarbons, etc.). They insert between aluminum-silica-oxygen layers and easily draw them apart. These molecules, though they form ion-dipole, Van der Waals, hydrogen bonds, may be substituted by others which can penetrate into interlayer distances. In the natural MMT interlayer distance is filled with metal cations, which impede dispersion of silicates in a polymer matrix. Substitution of metal ions by alkyl ammonium cations is a widely used method for enhancement of silicate dispersion in a polymeric matrix and for improvement of compatibility with the matrix.

Interlayer compensating cations of the layered silicates can be also replaced by various organic cations, the most interesting are ammonium cations with hydrocarbon chain C_1–C_{18}. Most often cation surfactants are used, such as octadecylamine (modification of MMT surface 15–30 mass.%), hexadecylamine, decylamine, and dodecylamine, hexadecyltrimethylammonium chloride, and also ammonium cations of amines of higher fatty acids of hydrated tallow oil, such as methylenbis (2-hydroxyethyl)tallow (2M2HT), alkylammonium [$CH_3(T)N(C_2H_4OH)_2^+$/MMT], consisting of ~65 % C_{18}, 30 % C_{16} and 5 % C_{14}, intergallery cation with exchange capacity 0.9–1.25 mg-eq/g, tetralkyl ditallow ammonium modifier B34 in bentonite increases *d*-basalt space by 25 % [42] (sometimes the latter named by trade name Nanometer 1.30 T). We should also note di(2-oxyethyl)-12alkano-3-methyl-aminochloride,

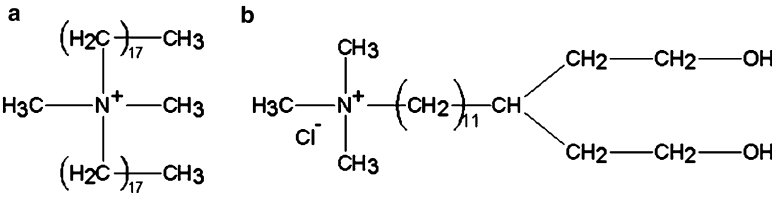

aminoundecanoic acid, more rarely, chiral L-leucine $(CH_3)_2CHCH_2CH(NH_2)COOH$ and many others. Thus, exchange capacity of MMT increases to 1.14 mg-eq/g in the case of modifying with 3-(acrylamidopropyl)trimethylammonium chloride. In this case d_{001} depends on a chain length in the cation of the modifying amine (Fig. 5.4).

Interplanar distance increases almost linearly with an increase in a number of carbon atoms in the primary amine $C_nH_{2n=1}NH_2 \cdot HCl$, intercalated in a layered silicate (Fig. 5.4), in this case the correlation equation is approximated as follows: d_{001} (nm) = 0.998 + 0.052n, the correlation score is $r = 0.980$ [43]. In other words, each CH_2- group increases d by 0.1 nm.

Degree of intercalation of a modifier is calculated taking into account interplanar distance D_F in a composite, with account for widening of the gallery (from 3.2 to 4 nm), and the magadiite sheet thickness (L = 1 nm) [39].

$$D_F = \frac{[(d_{001}(\text{organomagadiite}) - L) - (d_{001}(\text{magadiite}) - L)]}{[(d_{001}(\text{magadiite}) - L)]} \qquad (5.1)$$

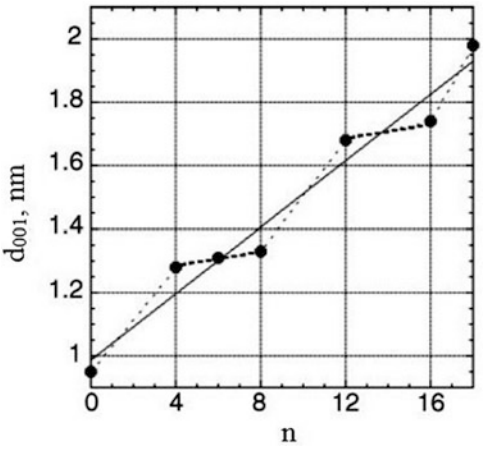

Fig. 5.4 The dependence of the interlayer spacing on the number of carbon atoms (n) in the amine intercalated into a layered silicate [43]

Table 5.3 Characteristics of organic silicate

Designation[a]	Interlayer distance, d_{001}, nm
1.40C	3.47
1.25C	2.36
0.95C	1.89

[a]The values are cation exchange capacity in the organic silicate, mg-eq/g

Fig. 5.5 Orientation of the modifying agent in silicate layers

The interplanar distance also depends on a modifying degree of a silicate (its cation exchange capacity), and on orientation of a modifying ammonium cation (Table 5.3).

The modifying agent can be parallel to the silicate layers, normal to them or placed in other way (Fig. 5.5).

Exchange mainly occurs in the layers containing solvated potassium cations. Taking into account the fact that hydrogen bonds form between layers, the character of small polar molecules inserted directly between them is limited and includes such ones as dimethylformamide, dimethyl sulfoxide, glycerol. Adsorption, its constant, and ΔH increase as a length of hydrocarbon radical increases. Interplanar distance also depends on orientation of cations in a layer, on how the layers are close-packed. These parameters, in turn, are defined by a surface charge: in low-charged silicates alkyl chains are between layers, in high-charged they are vertical to the surface [44]; for this type of substitution organic silicates gain hydrophobic properties due to blocking of absorption centers, and ability to swell

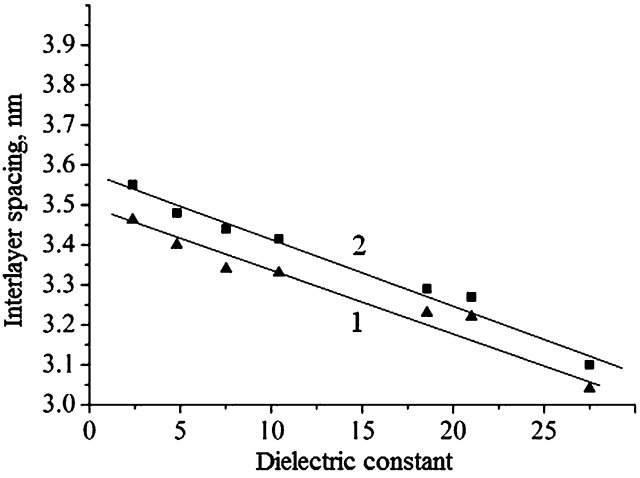

Fig. 5.6 Interlayer spacing of the MMT modified by 30 % (*1*) and 35 % (*2*) stearylbenzyldimethylammonium as a function of the dielectric constant of the solvent [44]

in organic solvents reaches maximum in the case of alkyl ammonium modifiers with a number of carbon atoms in a chain 12–18 (Fig. 5.6).

Molecular mobility of a modifying surfactant (taking for example tributylhexadecyl phosphonium bromide or dodecyl trimethyl ammonium bromide) in layers of synthetic magadiite [39]. In this case tributylhexadecyl phosphonium bromide was bound to imineoxyl radical to obtain spin-labeled surfactants such as

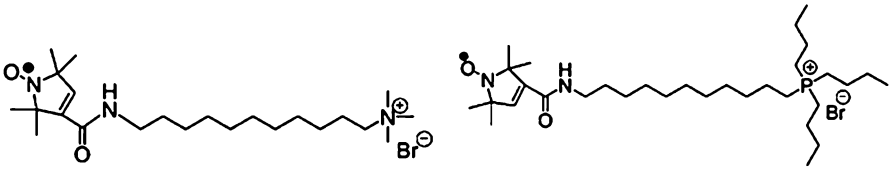

which made it possible to use EPR, NMR ^{31}P, and other techniques. Existence of two types of modifiers was found, bound to magadiite and individual, just one type of ligand was found as the temperature increased. Amine modifier enhances intercalation more efficiently than P-containing, due to smaller volume of its functional group. Behavior of these spin labels (rotation activation energy is 6–60 kJ/mol) resembles polymer-immobilized ones. The layered silicates modified with quarter amines with two long aliphatic chains have mixed layered structure consisting of packages with different interplanar distances. In their interplanar spaces ordered adsorption layers of a modifier are formed, which substantially draw apart plates of the layered silicate [45].

As a rule, mechanical properties of intercalated nanocomposites, such as ultimate tension strength, relative elongation in tension, elastic modulus and fracture energy are improved. Ultimate strength for tensile increases as a length of amine

chain increases depending on character of a clay: Na-MMT > bentonite > K-MMT, which corresponds with an increase in interplanar distance. Thus, an amine defines organophilic properties of a silicate, this, in turn, improves interaction between polymer and filler and properties of a composite [46]. Improvement of compatibility is proved by different methods, including solving and mechanical mixing. A tendency to improvement of properties is followed in the range: organophilic clay > Na hectorite > K bentonite > deposited SiO_2, which reflects their intercalation and organophilic abilities. It should be noted that not only ammonium but also alkylphosphonic salts [47], including tributylhexadecyl phosphonium bromide are suggested as organic exchanging cations, intercalating agents. Phosphor containing surfactants have higher thermal stability, than their nitrogen containing analogues, especially, in compositions on the basis of layered materials [48, 49]. Modifiers can be ranged in order of their intercalation, and finally, exfoliation activity: aqua-soluble sulfonates, sulfates, carboxylites. Modification of MMT by intercalation with various polyhydrocomplexes and other additives makes it possible to significantly increase its adsorption-structural characteristics and thermal stability.

Synthetic phyllosilicate clays, silicic acids, acid potassium phyllosilicate, magadiite, layered double hydroxides (LDHs) (Fig. 5.7), bilayered ($HLaNb_2O_7$) and trilayered ($HLa_2Nb_3O_{10}$) perovskites, zirconium phosphates (ZrPs), dichalcogenides are obtained by different, relatively simple ways [50]. Their main advantage is in chemical purity (absence of amorphous sand contaminators, arsenic, iron, heavy metals), they are transparent, which provides glossy color of a product, they have a wide rang of the aspect ratio from 20 to 6,000 [51]. The most widely applied is hydrothermal technique with usage of templates [52–57].

Coprecipitation of the respective cursors is used to obtain $Zn_{0.67}Al_{0.33}(OH)_2Cl_{0.33} \cdot 0.75H_2O$ or $Cu_{0.68}Cr_{0.32}(OH)_2Cl_{0.33} \cdot 0.92\ H_2O$, and magadiite is obtained via hydrothermal synthesis from two components: silica oxide, potassium hydroxide, and water in the ratio 3:1:200, its calculated formula is $Na_2Si_{14}O_{29} \cdot 11H_2O$, the exchange capacity is 1.82 mg-eq/g two potassium ions are substituted by one molecule, the total absorption of the modifier – long chained amine is 0.85 mmol/g. Layered nanohybrid materials are synthesized via interaction

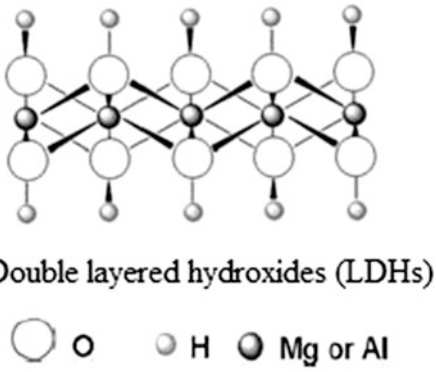

Fig. 5.7 The schematic illustration of LDH layers (The interlayer space is 0.50–0.60 nm) [50]

of $Zn(OH)_2$, ZnO or Zn/Al with carboxylic acids or with oxychlorides; the *guest*/*host* ratio in these composites is from 1.5:0.5 to 1.8:0.2. Depending on a character of the reacting components, morphology of the particles changes from fibers to plates, interlayer distance increases from 1.61 to 2.01 nm. Hydrotalcite materials[3] ($[AlMg_2(OH)_2(OH)_4]^+[0{,}5CO_3, OH, Cl]^-$) LDH [9] consist of layers of positively charged $[Mg_6Al_2(OH)_{16}]^{2+}$ cations neutralized by CO_3^{2-} ions in the interlayer area [4, 43, 58–61].

For modifying of LDH the following four approaches can be taken: anion exchange, in LDH, direct synthesis via precipitation, rehydration and calcinations of LDH, and thermal reactions. Styrene sulfonate RSO_3^-, alkyl benzene sulfates, dodecyl benzene sulfate are relatively stable modifiers of LDH, break of the tail-head bond in a surfactant happens at the temperatures 100–200 °C. However, these modifiers has not been widely applied for nanocomposites.

It should be especially noted that some metal oxides prepared by "wet" chemical synthesis (hydrothermal, solvothermal [62, 63]) have anisotropic structure, which should cause variation in their properties along different crystallographic directions. It relates, for example, to α-MoO_3, which is one-dimensional rod [64] to layered double hydroxides (LDHs) $M^{2+}_{(1-x)}M^{3+}_x(OH)_2]^{y+}(A^{n-y/n})m\ H_2O$, for example, $Mg_6Al_{3-4}(OH)_{18-8}(CO_3)_{1-7}H_2O$ or $Zn_6Al_2(OH)_{16}CO_3nH_2O$. Materials with layered-columnar structure made on the basis of montmorillonite clays are widely used in various areas, including sorption technique and catalytic processes. This is especially related to widely used in catalysis Ti(IV) columnar montmorillonite materials (see for example [65–70]). They include centers of acid and Lewis types (three-coordinate Al^{3+}cations substituting Si^{4+} in tetrahedral layers), as well as Brőnsted centers (containing Si-OH-Al- groups). Residual water has a significant effect on their acid capacity; they inflate when filled with organic solvents, monomers, or polymers. Inflation of interior crystalline cavities, which is sometimes called characteristic basis of clay swelling, depends on a nature of cations in layers and also on density of negative charge on them. Moreover, inorganic acids have surface hydroxyl groups, which develop strongly polar surface active in bonding of various metal ions. However, main properties of these materials are governed by characteristics of porous open systems and especially by pore sizes. In the compounds of insertion *guest*-molecules are in crystallographic hollow sites of the *host*-matter. The layered "sandwich" structures and one-dimensional channel structures mostly belong to these compounds. Metal ions included in these structures can easily reduce under action of various chemical reducers, or thermally, less often by photochemical process, and form nanoparticles [71].

[3] Synthetic hydrotalcite $Ex_{0.66}[Li_{0\cdot66}\ Mg_{5.34}Si_8O_{20}(OH, F)_4]$ (Ex = Li, R) is obtained, from the precursor of the composite 0.32 R, 1.0 LiF, 5.3 $Mg(OH)_2$, 8 $SiO_2 \cdot nH_2O$, in which R is organic salt of univalent metal and Ex is substituted cation. The process begins from solution of 0.72 mmol of organic salt in water and addition of 4.8 mmol of LiF during stirring. Separately 24 mmol of $MgCl_2 \cdot 6H_2O$ is solved in water and mixed with 32 ml 2 N NH_4OH to formation of fresh Mg $(OH)_2$.

The layered materials are distinguished as two types by their architecture and properties. First of them is characterized by stiff pores with a constant volume, parallel insulation of the lattice channels and communicating channels of the network. Localization, concentration and spatial distribution of *guests* are defined by the topology, chemical origin, and reaction ability of the inner surface of the *host*, whose matrix can additionally be subjected to functionalization. Moreover, *guests* types are limited by minimal conjugated channels, which causes selected intercalation behavior of *guests* in matrices (like molecular "sieves"). The second type is presented by low-dimensional lattice of a *host*, i.e. layered or chained structure. This provides "flexible" pores, whose dimensionality can adapt to dimensionality of a *guest*. Matrix lattice of a *host* can have no effect on intercalation-deintercalation (in the case of lattices of insulators, zeolites, layered aluminum silicates, metal phosphates, etc.). For them intercalation behavior is predominantly characterized by acid-base and exchange properties.

Host lattices with electron conductivity (semiconductors based on layered metals, their chalcogenides, etc.), undergoing redox reactions during intercalation with electron or ion transport accompanied by significant change in physical properties of a host matrix take a special place. Thus, a great intercalation capacity of xerogel on the base of V^{5+} oxide is known: this is $H_2V_{12}O_{31} \cdot nH_2O$ polyvanadium acid, in which negative charge of vanadium-oxygen layers is distributed along V_2O_5 fibres [72]. The fibers are plane ribbons up to 100 mm in length and 10 nm in width (Fig. 5.8) and include water molecules, chemically bound with vanadium atoms via different types of bonds. Intercalation can develop by dipole absorption, ion exchange or oxidation-reduction processes. Vanadyl phosphates are relatives to intercalation gels. Insertion of quite large $VOPO_4 \cdot H_2O \cdot EtOH$ molecules in $VOPO_4 \cdot 2H_2O$ layered structure, interlayer distance can increase from 0.75 to 1.03 nm.

Other phosphates such as: α-$Zr(HPO_4)_2 \cdot H_2O$, $HUO_2PO_4 \cdot 4H_2O$, layered aluminum phosphates, such as, for example, $AlPO_4$, berlinite, $Al_4(PO_4)_3(OH)_3.9H_2O$,

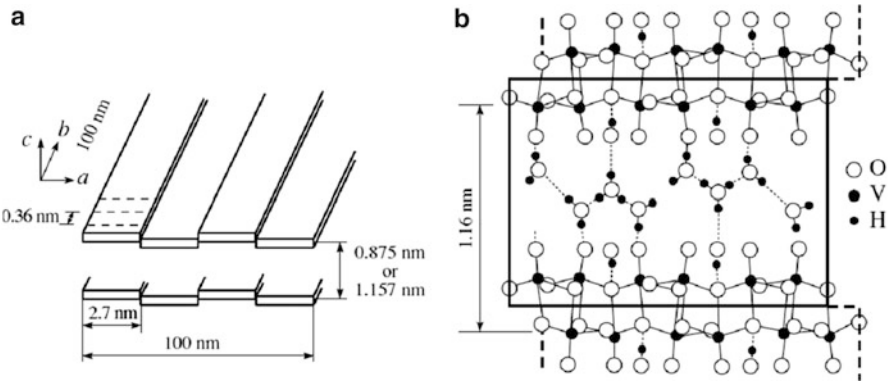

Fig. 5.8 (**a**) Schematic of the layered microstructure of V_2O_5 nH_2O xerogel and (**b**) a model for its crystal structure [72]

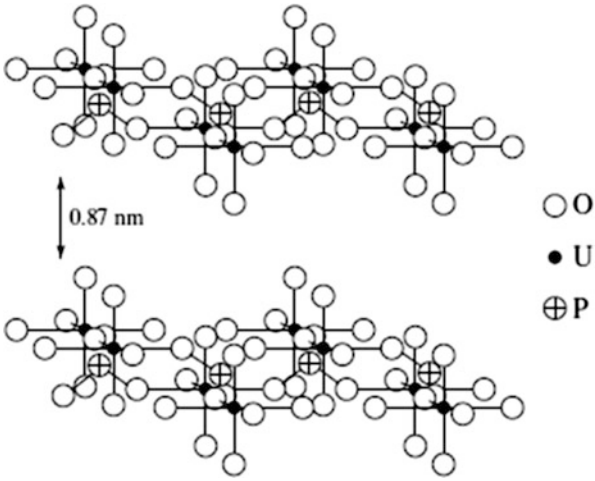

Fig. 5.9 Structure of $HUO_2PO_4\ 4H_2O$ [34]

vantasselite, produced by hydrothermal synthesis from H_3PO_4 and $Al(OH)_3$ with structural-governing agent (template), M^{4+} phosphates or phosphonates ($M^{4+} = Ti$, Zr, Sn), for example, α-form $Zr(HPO_4)_2 \cdot 2H_2O$, γ-form $ZrPO_4O_2P(OH)_2 \cdot 2H_2O$, λ-form $ZrPO_4XY$ (where X, Y is anion or neutral ligand), phosphorus-molybdenum acid $H_3PMo_{12}O_{40}$, etc. For example, uranyl hydrophosphate is layered bright yellow material with interplanar distance 0.87 nm. The layers include dumbbell shaped UO_2^+-ions with additional coordination of uranium with four equatorial oxygen atoms of PO_4^{3-} tetrahedrons forming 2D sheets (referred by [34]) (Fig. 5.9).

An important place in intercalation processes have cerium(IV)hydrophosphates, belonging to acid salts of tetravalent metals, in which inorganic network is built from $M^{4+}O_6$ conjugated octahedrons (M = Zr, Ti, Ce, Sn, etc.) and XO_4 tetrahedrons (X = P or As), structured as 2D and 3D structures [73]. Some layered acids, such as kanenite, makatite, octasilylsilicate, magadiite, kenyaite have interesting intercalating properties.

Among the materials, which are obtained by sol-gel synthesis [74] we shall note once again TiO_2 (anatase) pillared clays. They consist of saponite, natural purified montmorillonites (MMT-TiO_2), mica (mica-TiO_2). Nanoparticles TiO_2 intercalated into silicate clays widen their interlayer distance, while crystal structure and sizes of anatase remain almost identical for various types of clays [75]. Intercalation of TiO_2 in MMT or in hectorite can go in two ways [76]: preabsorption of precursors, titanium alkoxides, on mineral plates with the following hydrolysis and calcinations or heterocoagulation of titanium dioxide and the mineral [77, 78]. It is especially typical of SiO_2 intercalation, which depends on the character of alkoxysilane and initial clay, modified by longchained amines; most efficient is tetramethoxysilane (TMOS) with varied (from 1:0.5 to 1:5 mass.%) ratio clay/silane. A different ability of silanes to penetrate interlayer space is caused by facilitated diffusion, steric hindrances, which are weaker for TMOS than for $Si(OC_2H_5)_4$, etc.

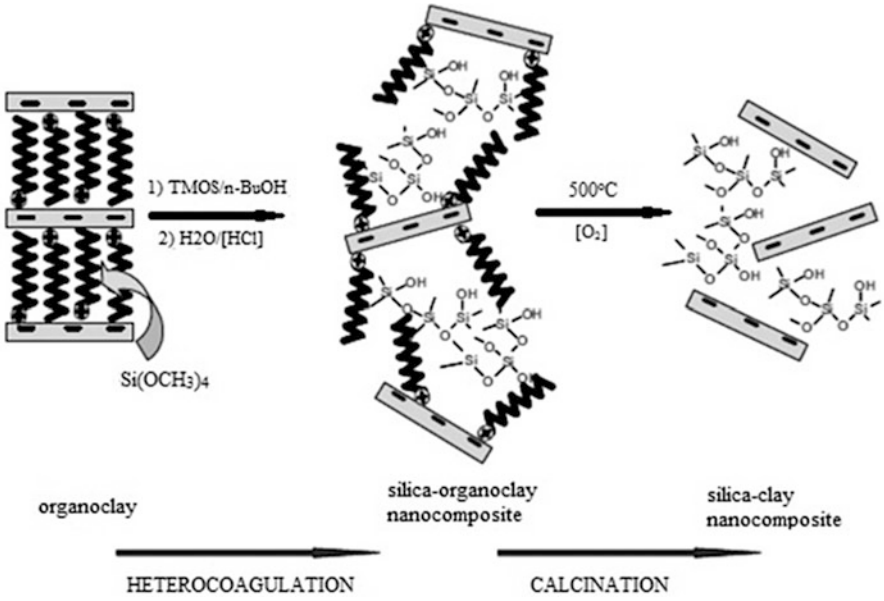

Fig. 5.10 Combined sol-gel-intercalation synthesis using a modified silicate [395]

General scheme of this combined sol-gel-intercalation process can be briefly described as follows [39, 79] (Fig. 5.10).

This process may be influenced by different density of electric charges in silicate, which is defined by a number of alkyl ammonium cations per unit area of its interlayer distance. After annealing at 500 °C SiO_2^- inorganic composite forms. For alkoxides of various metals (Ti, Al, Zr, Sn) this way can be used to obtain layered titanites, zirconites, etc.

An interesting field is production of vanadium oxide nanotubes, nanotubular forms of intercalating compounds. The case in point is sol-gel synthesis with participation of $VO(OPr^i)_3$ in presence of primary or α,ω-diamines followed by hydrothermal reaction in autoclave at 180 °C for 2–7 days. After washing and drying vanadium oxide of mixed valence had a nanorod shape with the composition $V_2O_5 \cdot 0.3\ H_2O$, diameter from 15 to 150 nm (inner diameter from 5 to 50 nm), its length reached 15 μm [80]. The tubes consisted of 2–30 layers of crystal oxides of vanadium and amine molecules, intercalated between them. A distance between layers is 1.7–3.8 nm proportional to the amine length, which acted as structure governing template. In contrast to mesoporous oxides of metals with lamellar structure these nanocomposites are characterized by tubular morphology and well-structured walls. "Curls" of vanadium-oxygen layers are very flexible, they can be stretched in line and take part in many exchange reactions. Structural flexibility provides possibilities of further formation of nanotubular structure and modifying of mechanical, electrical, and chemical properties of this material. Vanadium oxides, as will be shown below, are perfect *hosts* for obtaining of composites on the basis of conjugated polymers. For intercalation far rarely are used layered

minerals, oxides and hydroxides, such as brucite $Mg(OH)_2$; gibbsite $Al(OH)_3$; also $LiMn_2O_4$; $LiCoO_2$; $LiNiO_2$; $H_2Si_2O_3$; V_6O_{13}; $HTiNbO_3$; potassium titanate whiskers $K_2Ti_6O_{13}$; $W_{0.2}$ $V_{2.8}O_7$; Cr_3O_8; $MoO_3(OH)_2$; $CaPO_4CH_3 \cdot H_2O$; $MnHAs \cdot H_2O$; $Ag_6Mo_{10}O_{33}$; monoclinic structures (type *m*-WO_3), etc. [62–64].

Last advances in this field are described in recent reviews, concerning exfoliation of layered oxides [81, 82], etc.

As the methods of obtaining of nanocomposites will be analyzed, some other inorganic materials will be also discussed, among them the abovementioned phosphorus-molybdenum acid $H_3PMo_{12}O_{40}$, and layered compounds like graphite, graphene, chlorides $FeCl_3$, FeOCl, some chalcogenides TiS_2, MoS_2, MoS_3, $Cr_{0.5}$ $V_{0.5}S_2$, $(PbS)_{1.8}(TiS_2)_2$. Thus, layered MoS_2 structure consists of quite thin packs less than 5 nm in size (several layers) with a distance between layers (periodicity) 3.4 nm. Presence of negative charges in monolayer dispersions of MoS_2 separated by solvent molecules (which is ionic system $(MoS_2)^{x-}$ – alkali metal-hydroxide-anion [83] give a possibility of their modifying by various cations, including formation of layered compounds with the cations of quarter alkyl ammonium, etc. [84].

At the same time layered halogenides and thiophosphates of transition metals, oppositely to the abovementioned layered metal oxides (and considered below metal chalcogenides) did not attract much attention for intercalation. Maybe, a reason for this is low stability of majority of them that undergo various chemical transitions, hydrolysis, solution, decomposition, etc. one of exceptions is α-$RuCl_3$, which has a lamellar structure (Fig. 5.11).

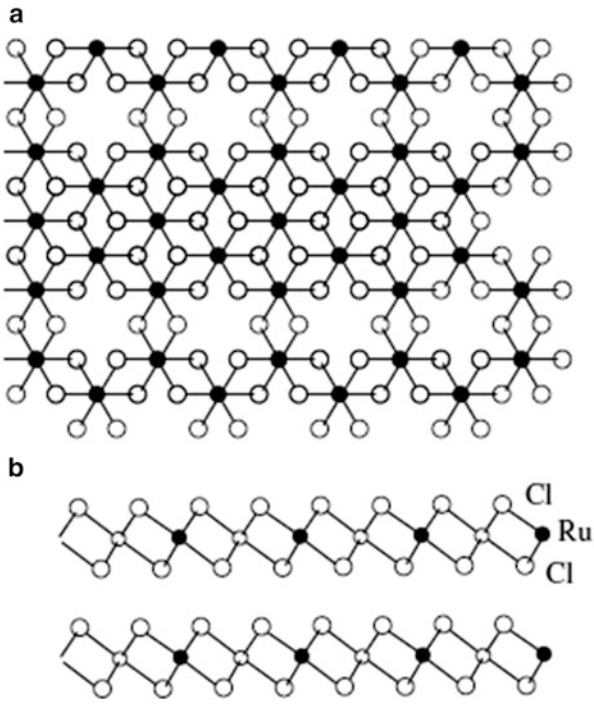

Fig. 5.11 Layered structure of α-$RuCl_3$: (**a**) octahedral coordination of Ru atoms; (**b**) projection along the *c* axis [34]

5.2 General Characteristics of Intercalated Systems

As it has already been noted, layered materials interesting for usage in technology of polymer composites, should form flakes 0.7–2.5 nm in thickness and having a definite size of interspace distance [85–87].

Nanocomposites are usually products, which consist of at least two different materials with a clear interphase boundary between them, at least one of them should have nano- (1–100 nm) sizes in no less than at least one direction. The same relates to the distances between networks and layers formed by polymer and inorganic gradients [71]. The last type includes materials in which monomeric or polymeric molecules are inserted as guests in a host structure, which possesses intercalation properties. Under effect of the forming polymer particles of this "host" disperse into individual layers which results in formation of exfoliated nanocomposite (Fig. 5.12). The "peeling" technique is quite well developed. Peeling lamellas of MMT can act on polymeric chains as nanosized "hosts" and effect structure and orientation of intercalated macromolecules.

The driving force of intercalation process is a decrease in free energy in the system: a change in enthalpy is due to intermolecular interactions, and change is entropy is due to configuration interactions. Enthalpy is a dominant factor, which governs intercalation process, at least because the liquid-plate interaction characterizes behavior of liquid molecules with respect to surface of a solid and is crucial in this case.

Analysis of thermodynamic parameters [88, 89] shows that nanostructures are formed if free energy of a change in interlayer volume (ΔF_v) is negative, it can be written as follows

$$\Delta F_v = \Delta E_v - T\Delta S_v \tag{5.2}$$

where ΔE_v, ΔS_v are enthalpy and entropy of a change in volume during intercalation, T is temperature.

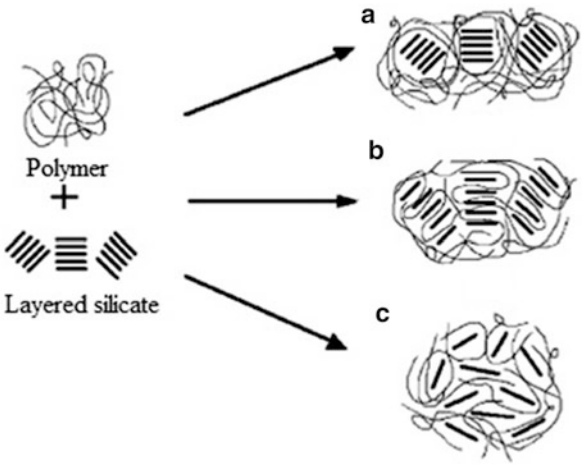

Fig. 5.12 Morphology structure of layered silicates in (**a**) conventional composites, (**b**) intercalated nanocomposites and (**c**) exfoliated nanocomposites [85]

Taking into account the fact that a small increase in gallery space has insignificant effect on a total change in entropy, the driving force of the process is a change in total enthalpy, which is expressed as follows:

$$\Delta E_v = \varphi_1 \varphi_2 \frac{1}{Q}\left(\frac{2}{h_0}\left(\varepsilon_{sp} - \varepsilon_{sa}\right) + \frac{2}{r}\varepsilon_{ap}\right) \tag{5.3}$$

where φ_1 and φ_2 are volumes of the intercalated polymer and bonded chains of a surfactant, Q is a number of links, h_o is initial size of organosilicate gallery, r is radius of intercalation surface of the chains of the bonded surfactant, ε_{sp}, ε_{sa} and ε_{ap} is intercalation energy of interaction between a layered silicate and polymer, layered silicate and intercalating (modifying) agent and intercalating agent and polymer, respectively.

Exfoliation can appear only for positive value of Flory-Huggins parameter between polymers and thin discs modeling silicate layers, though a mixture of polymers and clay can delaminate, while intercalation is expected if the interaction parameter is negative. Thus a polymer diffuses through energetically preferable gallery, which enhances its contact with two limiting silicate layers. The diffusing polymer molecule sticks two neighbor surfaces, making them kinetically captured. Therefore, even though interaction energy is required for diffusion of the polymer into the gallery of silicate layers, its increase would cause predominant intercalation, despite predominant exfoliation [90–92]. Adhesion behaviors of polar polymers and hydrophilic silicate layers is sometimes called sticking effect [93].

This effective way of obtaining of various types of nanocomposites, for example, based on PS, PE, PP [94], polyamide (PA) [95, 96], polyethylene terephthalate (PETP) [97–99] and others [100, 101]. As was already mentioned, exfoliation is accompanied by formation of monolayers of nanometer thickness with highly anisotropic shape, uniformly distributed in a polymeric matrix [9, 12, 85, 88, 102–109].

Thus, in this process three main hybrid-phase composites can form (taking for example dispersion of OMMT particles in polymer matrices): microcomposite with separated phases (traditional material), intercalated (including folliculated material) and exfoliated nanocomposites. Traditional microcomposites with separated phases include a clay tactoid with layers aggregated in non-intercalated state. A silicate is finely dispersed as a separate phase, these composites are often called delaminated (delaminated suspension). Depending on nature of the reacting components and conditions, a mixed composite can form, which contains the described structures in various proportions. Intercalation state is less stressed, its morphology is characterized by preserved order in the silicate layers, including one or more polymer chains intercalated in gallery space with a certain structure, which are tend to increased basal space of a layered silicate. Exfoliation of the silicate in a nanocomposite is a result of homogenous dispersion of nanoplates of delaminated silicate in a continuous phase. In other words, exfoliated or delaminated nanocomposites are materials in which packed silicate layers are absolutely fractured and single layers are uniformly distributed in polymeric matrix. In this case a collapsed structure consisting of elongated silicate plates can be absolutely random

or can have some order. In other words exfoliated nanocomposites can be formed as a result of ordered (by topography of silicate nanoplates) and disordered exfoliation [110]. Ratio between depends on such factors as capacity of the layers to swelling under conditions of the process, maximum separation, depending on volume fraction of exfoliated layers. Moreover, intermediate morphologies appear owing to rotation of partly exfoliated associates dispersed in layers in combination with small thickness of their bunches [111]. Widening, a distance between the separated layers is, as a rule, 10 nm and more and depends on a nature of inorganic component, its aspect ratio, concentration of a polymer in a composite [1, 110, 112, 113].

Exfoliated nanocomposite contains low concentrations of a silicate (which plays a role of nanorods), which does not cause a significant increase in density and deterioration in recycling ability of a material, which is a solid structure, its properties are defined by a nanoconfined polymer. One of the aspects of delamination is a possibility of introduction of polymers by the mechanism *guest-host* with intermediate reaction time and following precipitation of the intercalated systems after removal of a solvent. Taking into account directions of modified agents between layers of a silicate (Fig. 5.13) localized macromolecules between these layers can be presented as follows:

Moreover, morphology of the nanocomposites depends on polarity of the silicate, way of its modification, polarity of intercalated polymer, interaction between components, OH-groups in the silicate. The effect of these factors is schematically shown in Fig. 5.14 [114]. In a non-modified silicate non-polar polymer is localized, mainly, on side surfaces of the silicate, in a modified intercalated structures form, while polar polymers have mostly exfoliated morphology.

A significant difference in characteristics of these materials is shown, for example, for their barrier properties.

One more moment should be highlighted. The matter is about obtaining of concentrates of the composites (the method of dosed introduction of components, masterbatch). As a rule, they are obtained at the stage of polymerization or from a melt of polymer, taking high (higher than 21 mass.%) concentrations of a silicate with the following extrusion (including introduction of additional ingredients at this stage) for production of a necessary homogenous nanoconcentrate, which is then

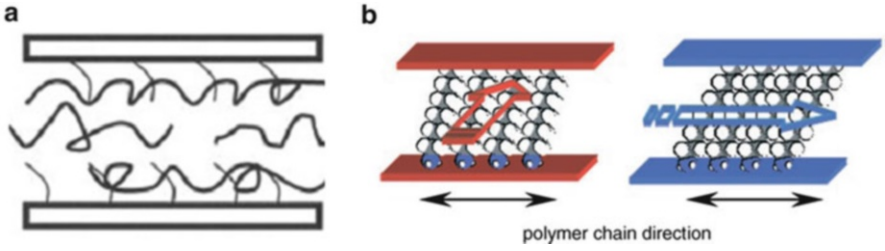

Fig. 5.13 Model of oriented structure of long-chain alkylamine (**a**) and polymer chain (**b**) in an interlayer space of MMT [42]

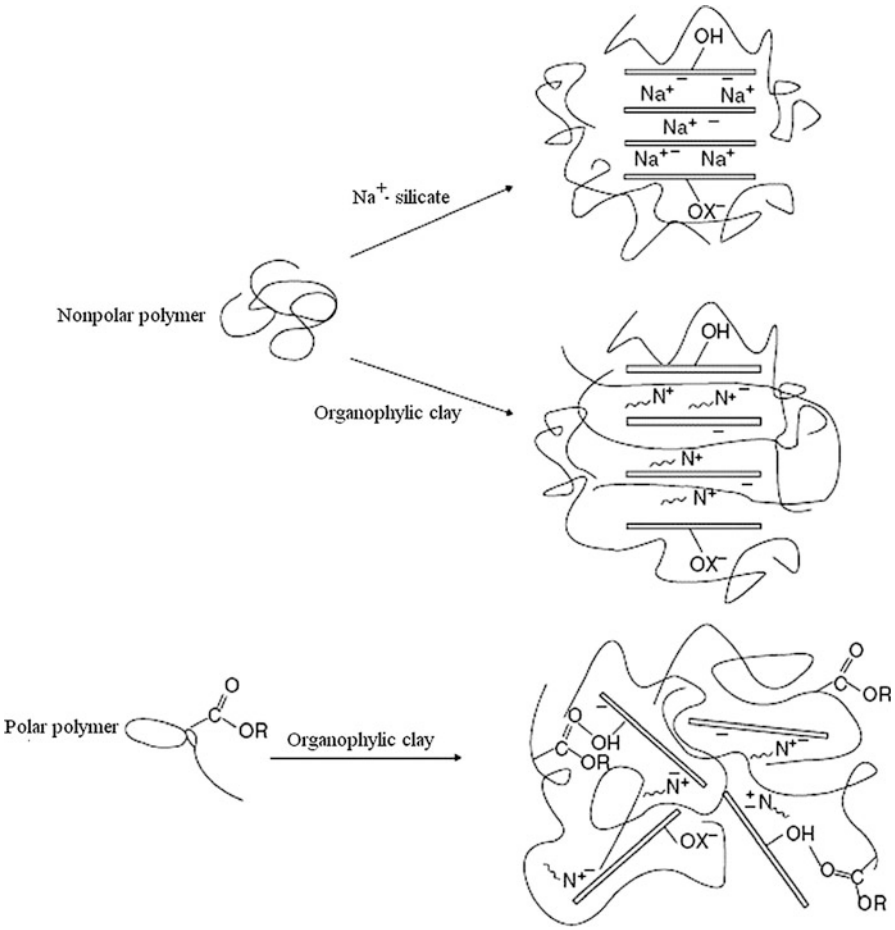

Fig. 5.14 Effect of organophilic and polar interactions on the morphologies of composites [114]

used for production of nanocomposites of a requires content. Other types of silicates are less active in intercalation of polymers due to their low intercalation ability. This relates, for example, to a family of crystal alkaline-earth polysilicates, whose oxygen ions are neutralized by sodium cations, such as kanemite, makatite, ortosilicate, magadiite, kenyaite, and hollandite, though for these purposes sometimes MnO_2 (KMn_8O_{16} type) nanocrystals are used with hollandite or mica structure.

The field of physical chemistry of intercalated systems and its lines are relatively often and in detail generalized, for example, composites based on intercalated polyolefins [115] and functionalized thermoplastic materials were considered in the informative review: [116] main data on PE intercalation, including linear low-density polyethylene (LLDPE), syndiotactic polypropylene, polybutadiene, copolymers poly(ethylene-co-propylene), poly(ethylene-co-vinyl acetate), their

preparation, thermal, mechanical, rheological, barrier and plasma-retarding properties, intercalated polyvinyl chlorides, polyamides, organic-inorganic materials for energy-efficient technologies in [15, 33, 34, 106, 117], etc.

Typical methods of production of intercalated composites, which are here analyzed, can be confined to following:

- in-situ polymerization (solution mixing)
- mixing in suspension
- latex compounding
- direct intercalation in a polymer melt (reactor mixing).

5.3 Special Features of Polymerization of Monomers in Interlayer Space

Probably, this is one of the most interesting types of intercrystalline chemical reactions, inserting of monomer molecules and initializing particles in pores of a *host* with the following interior transformation into polymer, oligomer, or hybrid sandwich products (postintercalation transitions). Often this method is called "ship-in-the-bottle" polymerizing approach or in situ polymerization of pre-intercalated monomers. A layered silicate in this process plays a role of nanoreactor. This is rather exhaustively investigated field, many studies of this way performed nanocomposite formation may be referred to [11, 118].

A special attention is drawn to monomers and polymer links synthesized via topotactic in-situ process [119, 120] characterized by low activation energy of diffusion controlled by structural organization of insertion compounds. The obtained nanocomposites are, as a rule, metastable, and cannot be synthesized in other ways, for example, by thermal synthesis or mixture of components (because of exfoliation of a polymer from inorganic component).

From thermodynamic point of view *in situ* intercalation polymerization has an advantage in formation of finer dispersion. Formation of hybrid systems takes place if free energy of a chain ΔG caused by separation of silicate layers and insertion of a polymer chain from a block is negative. Entropy to enthalpy ratio defines intercalation of a monomer molecule and its yield: the greater decrease in internal energy, the higher tendency to formation of intercalated/exfoliated hybrids. Since a great amount of heat is emitted during in situ intercalation polymerization, it is efficiently compensated by loss in entropy of the hybrid and promotes penetration of polymer in silicate layers.

Intercalation was modeled by molecular dynamics (MD) [121]. The calculations confirm non-equilibrium process of intercalation in layers with low aspect ratio at low concentration of the component stronger bound to the layers. As the latter increases, initial stages of exfoliated structures are generated [122]. Also intercalation of a solvent and polymer in the silicate gallery were modeled by Monte-Carlo technique [123].

A matrix polymer in interlayer space of aluminum silicate is synthesized almost by any known mechanism; polymerization in the interlayer space can be initialized by conventional methods. Since polymerization goes in presence of an incentive, various additives, a necessity appears to study intercalation processes of a monomer, incentive substance and additives modifying a silicate surface.

5.3.1 Emulsion Polymerization in Interlayer Space

The simplest method of intercalation of polymers in inorganic structures, one staged methods of emulsion or suspension polymerization of traditional monomers (most often styrene, methyl methacrylate, acrylonitrile, vinyl acetate, etc.) in presence of various organophilic minerals.

Though detailed mechanism of the process is not completely studied, say nothing about topochemistry of elemental stages, physical picture of intercalation can be considered as follows. Characteristic basis of a clay swelling in aqua systems containing 2–10-nm monomer micelles allows their deep penetration in inflated OMMT layers. At the same time, large monomer drops (10^2–10^4 nm) form during polymerization in a solution, therefore they usually easily absorb or are connected to exterior surface of silicate particles. A typical emulsion polymerization of latex particles takes place in ordered 2D colloid ensembles. This principle is used to produce PMMA/MMT, PVC/MMT, PS/MMT and others, their copolymers [124–129].

PS-organosilicate composites are obtained by suspension polymerization of intercalated styrene, an effect of a length of alkyl chain of ammonium modifier and its concentration on properties of the composite is found [130]. Non-extracted nanocomposites, styrene-acrylonitrile SAN/MMT is formed in two ways by intercalation technique: one staged emulsion co-polymerization in water or from a copolymer solution in cyclohexane and OMMT. Interlayer distance of the emulsion substance increases dramatically, by 0.76 nm, whereas in the solute substance it widens only by 0.39 nm. Emulsion polymerization of aniline in situ in presence of TiO_2 causes incapsulation of the nanocomposite, the process is interesting because of use of functionalized protonic acid, dodecylbenzene sulfonic acid, which is simultaneously surfactant for water emulsion polymerization and a doping agent for a forming polymer [131]. Emulsion polymerization has ecological advantages before the solution techniques, because it does not require organic solutions.

5.3.2 Interlayer Blocked Radical Polymerization and Copolymerization

Often during polymerization in situ intercalation of monomers in layered double hydroxides is used (see, for example, [132–134]). Thus, in LDH of the $Zn_{0.67}Al_{0.33}(OH)_2Cl_{0.33}$ $0.75H_2O$ or $Cu_{0.68}Cr_{0.32}(OH)_2Cl_{0.33} \cdot 0.92\ H_2O$ composition

chlorine is substituted by acid monomer during interaction with vinylbenzenesulfonate (VBS) sodium salt or aminobenzenesulfonate (ABS) before in situ polymerization. Interstitial monomers increase interlayer distance from 0.776 to 1.80 nm (VBS) or 1.54 nm (ABS) [132].

Lamellar aluminum silicates are often used as *hosts* for polymerization of acryl monomers [1, 113]. The type of forming nanocomposites polymer/clay is determined by a character of a monomer, conditions of its formation.

During radical polymerization of vinyl monomers a significant functional groups of long-chained amines-modifiers of layered silicates taking part in complex formation with polar monomers can play an important role. One of most obvious examples is synthesis of the functional nanocomposites via copolymerization of pre-intercalated itaconic acid with cations of N,N-(dimethyl)dodecyl ammonium (DMDA) modifying MMT surface, and n-butyl methacrylate (used as interior plasticizing comonomer) in the MEC solution [135–138]. In fact, they deal with a new type of radical polymerization, interlamellar complex-radical copolymerization (Fig. 5.15). Comparative analysis of various parameters points to formation of interlayer hydrogen bond with oxygen atom of flexible n-butyl methacrylate ether link (BMA) and its crucial role in interlamellar copolymerization and intercalation/exfoliation in presence of radical initiators (AIBN):

In future this approach was broadened, details of its mechanism were studied [139].

A special place in this problem should be assigned to orientation control of a *guest* molecule in intercalation systems of a *host* and, as a result, to formation of stereo-regular polymers: during intercalation the *host* identifies the *guest* type and reversibly accepts it in 2D layered structure [12] (Fig. 5.16).

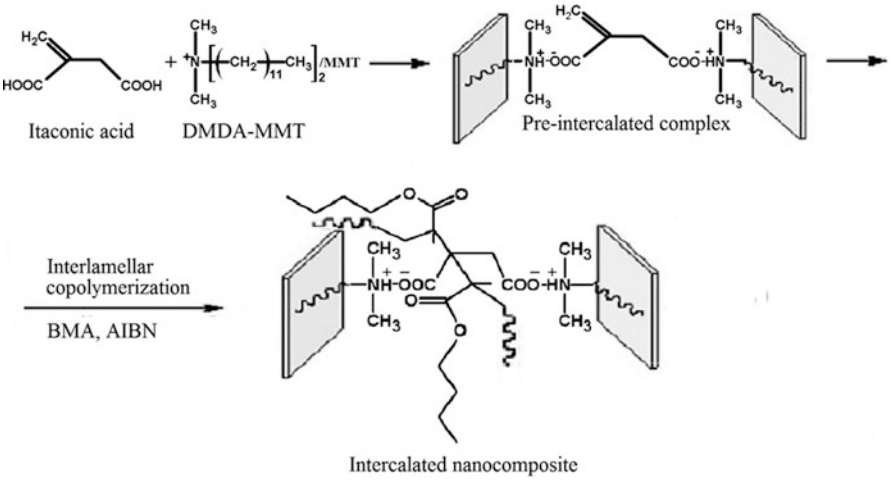

Fig. 5.15 Interlamellar complex-radical copolymerization of pre-intercalated itaconic complex with n-butyl methacrylate [135]

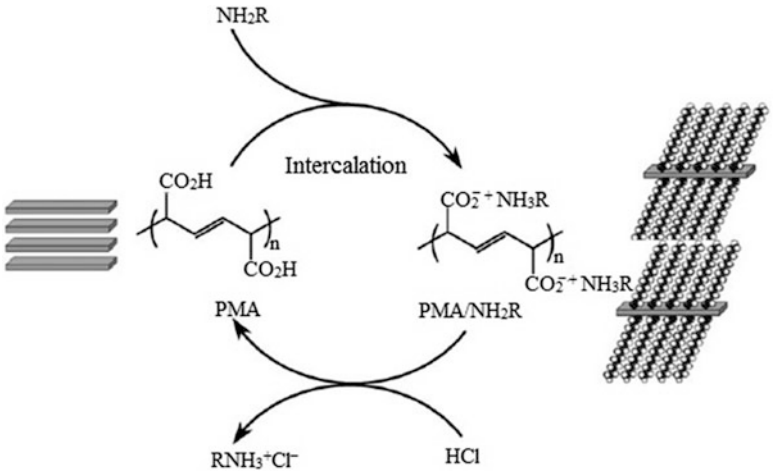

Fig. 5.16 Intercalation polymerization of muconic acid and orientational control of guest molecule

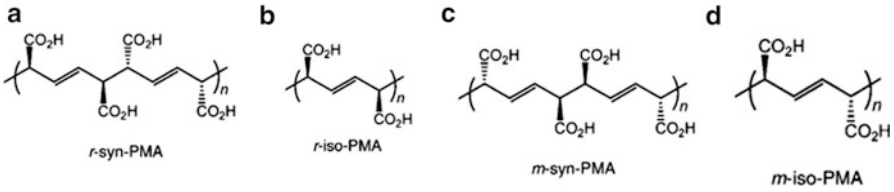

Fig. 5.17 Stereostructures of polymuconic acids obtained via intercalation polymerization of muconic acid: r-syn-tactic (**a**), r-iso-tactic (**b**), m-syn-tactic (**c**), and m-iso-tactic (**d**)

Stereo-regular polymers are produced via topochemical polymerization (Z, Z)- or (E, E)-derivatives of muconic acid *m*-iso-tactic, *r-syn*-tactic, *m-syn*-tactic, *r-iso*-tactic (Fig. 5.17) having translation and alternative stacked structure, respectively, in a solid state under UV-radiation of acid salt crystals and amines with different length of hydrocarbon chain in silicate layers [140–148]. Hydrolysis (HCl или H_2SO_4) converts them into stereo-regular polymuconic acids (PMA) in silicate layers.

Both *m-iso*-PMA and *r-iso*-PMA crystals show inclined line of the dependence of interlayer distance on a number of carbon atoms in alkylamine, *d* increases by 1Å with each carbon atom (Fig. 5.18). Most probably, *m- r-syn*-PMA (A, C, straight line 2) have different structures, as is also true for *iso*-PMA (B, D – straight line 1), which differ by a layer structure and by different packages of alkyl ammonium groups. Alkyl chain of a *guest* has a regular structure, corresponding to a *trans*-planar conformation with a partial *gauche*-conformation with different positions of carboxylic groups in the plane of polymer and by 2D structure of intercalated ammonium complex.

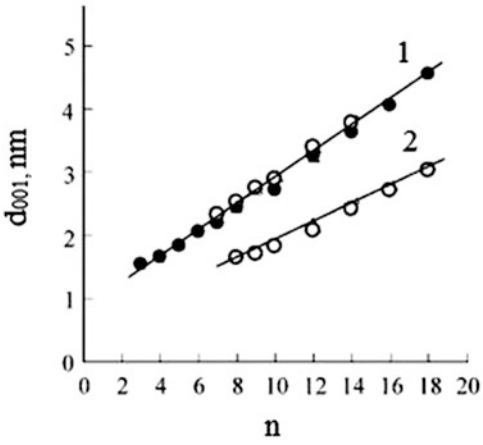

Fig. 5.18 Change in basal space value (d) as a function of the carbon number of n-alkylamines (n). Closed and open symbols indicate isotactic and syndiotactic polymers, respectively: *m-r-iso*-PMA (*1*), *m-r-syn*-PMA (*2*) [142]

The *host* provides control over variation of the *guest* orientation (tactics) and direction, normal or parallel to a polymer chain in isotactic or syndiotactic polymer sheets, respectively. Orientation control of the *host*-molecule (alkylamine in a polymeric crystal) opens a way to design of finely regulated layered materials with modern functions.

5.3.3 *Interlamellar Catalytic Polymerization*

An important stage in increase in intensity of intercalation processes and exfoliation of a layered silicate is intercalation of Ziegler-Natta catalyst with the following polymerization and co-polymerization of olefin monomers. Reviews of anion-coordination polymerization of olefins in presence of mineral fillers are referred to [33, 149, 150]. Then metallocenes catalysis was studied: after protection of the inner surface of a silicate with aluminum organic compound (most often methylaluminoxane) and introduction of zirconocene, the formed system causes catalytic polymerization of ethylene its copolymerization with higher olefins (for production of low-density polyethylene, LDPE), intercalated stereo-regular or oligomer polypropylene. More convenient approach is usage of single-component catalysts of olefins polymerization. In particular, this concerns the Pd^{2+} chelate complex [[(dppp)Pd(OTs)(H_2O)]OT[(dppp)Pd(OTs)(H_2O)]OT]

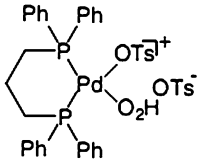

(where dppp = 1.3 Bis(diphenylphosphino)propane, OTs – *n*-toluene sulfonate) which is intercalated in synthetic hectorite modified by tetra(decyl)ammonium cations and performs gas phase polymerization of ethylene at 295 K with formation of high molecular polyethylene (PE extracted with toluene, $M_n = 159{,}000$, $M_w = 262{,}000$). After 2-h absorption of ethylene a dramatic increase in the silicate/catalyst size was observed followed by its collapse: in the composite produced after 24 h of polymerization there are absolutely no diffraction peaks of the silicate. Thus, at the initial stage of in situ formation of hybrid nanocomposites intercalated polymer forms, while at later stages exfoliation of a silicate takes place.

As it was mentioned in Sect. 5.2, almost all natural silicates contain as impurity constitutionally bound compounds of transition metals, components of metal complex catalysts (copper, titanium, vanadium chromium, zirconium, molybdenum, etc.) In this connection those are of a special interest that include impurity ions of metals initiating polymerization of an intercalated monomer. Thus, hectorite, whose sodium ions are substituted by Cu^{2+}, initializes styrene polymerization, in pores as well as on the surface. The polymer has a "brush" structure, which points to orientating effect of inorganic surface, which decreases as the chain growth distances from the surface. Compulsory neighboring in limited basal space has an effect on higher ordering of the polymer, its optical and mechanical properties. Intercalated PS exists in two forms, first of which is similar to blocked polystyrene on the surface, and another one is stiffer, maybe because of high ordering of the polymer. Redox-properties also have Fe^{2+} and Ru^{3+} cations exchanging in clay minerals: many monomers in their coordination sphere have a trend to intercalation radical polymerization. In the already mentioned review [35] crystal chemistry of the frame-forming silicate materials, in which impurity atoms of some transit metals, such as Ti, Nb, Ta, W, Fe, Mn (naturally immobilized metal ions) and others with coordination numbers 5, 6, as well as tetrahedral coordination atoms, are analyzed. Probably, they may serve as starting elements for hybrid materials, however, presently these data are limited, in the systems where naturally immobilized clays activated by aluminum organic compounds are used, activity of these elements in polymerization of olefins is low.

It should be noted that there is a possibility of obtaining molecular polymer-polymer nanocomposites [151] using spatial limitations which arise during catalytic formation of various chains in mesoporous systems [152]. Experimentally this approach is realized by treatment of silicates by methylalumoxane followed by bonding of two catalysts Cp_2TiCl_2 (Cp- cyclopentadienyl ligand) – the catalyst of ethylene polymerization and $CpmTi(OMe)_3$ (Cpm-pentamethylcyclopentadienyl ligand) – the catalyst of syndiotactic styrene polymerization. As a result, a composite forms with improved properties due to uniform (at nanometric level) distribution of polymers in a reactor mixture.

Oppositely to polar polymer matrices, in the case of polyolefin nanocomposites it is impossible to reach significant improvements of a complex of properties at low filling factor owing to, on the one hand, limited compatibility of non-polar polymers with layered silicates, and, on the other hand, difficulties in reaching exfoliation of a layered ingredient in single nanolayers in polyolefin matrix.

We shall especially highlight catalytic polymerization of MMA and formation of a stereo complex syndiotactic/isotactic PMMA in the layered silicate [153]. To do this, methyl-bis(2-hydroxyethyl)alkyl of fatty acids [$Me(T)N(C_2H_4OH)_2^+$/MMT] modified by ammonium salt is activated by toluene adduct *tris*-(pentafluoride phenyl)alane $Al(C_6F_5)_3(C_7H_8)_{0.5}$ (A activator) or $Al(CH_3)_3$ with the following treatment $B(C_6F_5)_3$ (B activator) and then combine with zirconium containing catalyst for production of iso- and syndiotactic PMMA [154]. Combination of thus activated (A and B) OMMT with decyl metallocene complexes of various symmetry, including achiral C_{2v}-symmetric Cp_2ZrMe_2, chiral C_2-symmetric *ras*-(EBI)$ZrMe_2$ (EBI = $C_2H_4(Ind)_2$, Ind- indenyl), pro-chiral Cs-symmetric $CGCTiMe_2$ (CGC = $Me_2Si(Me_4C_5(t\text{-BuN})$, with in situ MMA polymerization brings to formation with high yield of PMMA/OMMT nanocomposite with intercalated morphology (Fig. 5.19). In this case the forming polymer chain is subjected to stoichiometric control, realized as *atactic*, *iso-* or *syndiotactic* polymer from *iso-syndio-stereoblock* governed by metallocene symmetry (like polymerization of abovementioned muconic acid).

A range of stereo regulated systems of the considered type is significantly widened, see for example [155–157].

5.3.4 Intercalation Assembling

Molecules of a monomer intersticed by displacement form hydrogen and other bonds with a host, because kaolin-methanol intercalated compounds are comfortable intermediates for substitution by *guests* such as *n*-nitroaniline, ε-caprolactam, alkylamines, vinylpyrrolidone and others by relatively large molecules. This is a convenient way for formation of clays and nanocomposites based on condensation type of polymers, for example, ω- amino acids with a short carbon chain, β-alanine [$H_2N\text{-}(CH_2)_2COOH$], 6-aminocaproic acid [$H_2N\text{-}(CH_2)_5COOH$]. Taking into account that direct formation of compounds of 6-aminocaproic acid insertion is hindered by its relatively large dimensions and low intercalation ability it is more often intercalated in vermiculite or indirect way is used, *guest*-substitution reaction, when kaolin-methanol intercalate is used for intermediate [27]. Polymerization is performed via heating during 1 h at 250 °C in nitrogen flow. As is seen from Fig. 5.20, basal space of the matter of acid intercalation is 1.23 nm (intensive peak at 10.6° (0.84 nm)) corresponds to crystal structure of 6-aminocaproic acid absorbed on surface), it is greater than for kaolin (0.72 nm) or for the intercalated compound kaolin/methanol (1.11 nm). It is interesting that the basal space of thermally treated substance is 1.16 nm, which is shorter than the initial one (1.23 nm).

Probably, the reason for this decrease is reaction of polycondensation accompanied by spontaneous reorganizing of hydrogen bonds between OH-groups of *guest* molecules.

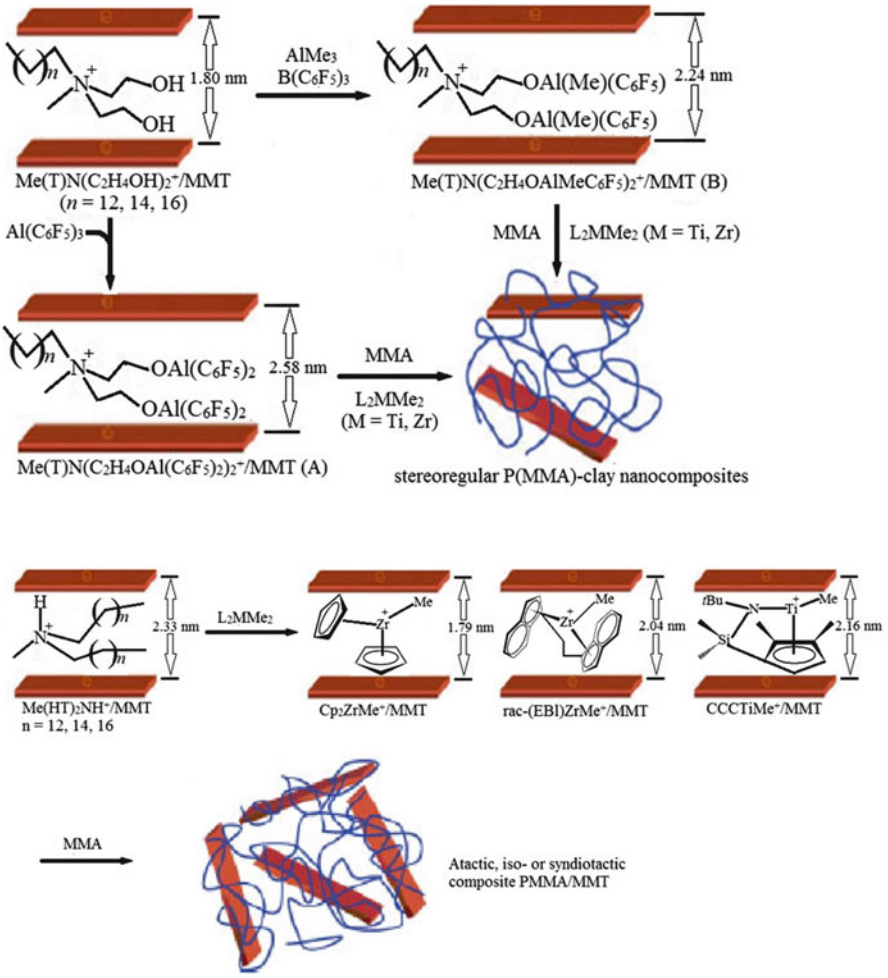

Fig. 5.19 Intercalated zirconocene cations for stereochemical control of PMMA chain growth [153]

Formation of aramid composite [158] can be presented schematically (Fig. 5.21), from which it is seen that interstitial co-monomer is simultaneously MMT modifier:

Intercalation technique [159] is applied to produce PA by polymerization in N,N (dimethylacetate amide) using 4,4(oxydianiline) (ODA) and isophthaloyl chloride (IPC) by the scheme (Fig. 5.22).

However, more widely used for formation of this type of composites are melt-intercalation techniques (see Sect. 5.4.4).

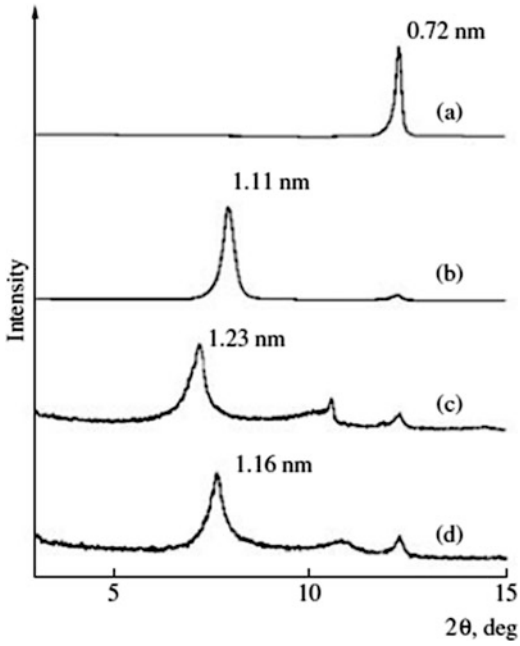

Fig. 5.20 X-ray diffraction patterns of (**a**) kaolinite, (**b**) a kaolinite–methanol intercalation compound prepared wetchemically, and (**c**, **d**) a kaolinite-6-aminohexanoic acid intercalation compound before and after heat treatment at 520 K, respectively [27]

5.3.5 Polymerization with a Ring Opening

This is a limited group of nanocomposites, only few examples of their synthesis are known. Hybrid polybenzoxazine/MMT nanocomposites are obtained via OMMT polymerization with a precursor ring opening (270–280 °C). The surface of OMMT has catalytic properties in this reaction [160]. In nanocomposites containing up to 10 mass.% OMMT there is distortion and breakage of its layered structure. In other words, nanocomposites with high content of organo-modified MMT have a mixed morphology, exfoliated in addition to intercalated one. The mechanism of the composite formation via ring-opening polymerization has much in common with intercalating polymerization of vinyl type of monomers [161, 162].

5.3.6 Redox-Intercalation Polymerization

Apart from vinyl monomers in mineral matrices also acetylene monomers are polymerized, for example, 2-ethylpyridine (EPy), implanted in MMT galleries [163, 164].

Probably, it is possible to realize photochemical polymerization of diacetylene-3,5-octadiine in the layers of metal phosphates (M = Mg, Mn or Zn). It can be assumed that under respective conditions monomers fill almost all volume of pores or interlayer distance. The next oxidizing polymerization is governed by molecular

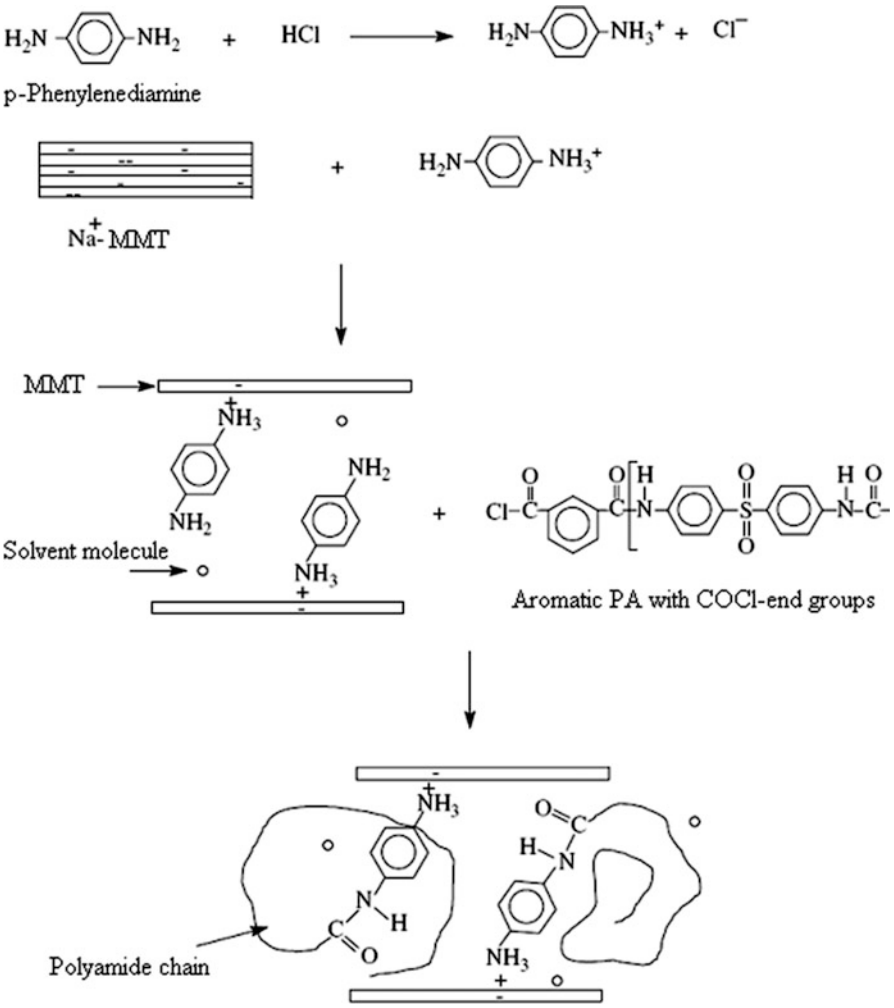

Fig. 5.21 Schematic representation for formation of aromatic PA/MMT nanocomposite [158]

oxygen acting as electron acceptor in presence of redox-active *host*, catalyst of electron transport, for example, Fe^{3+}, Cu^{2+}. Widely known are hybrid nanocomposites based on polyconjugated conductive polymers, such as polyaniline (PAn), poly(2-ethylaniline), poly-n-phenylene, polythiophene, polypyrrole (PPy) and polyacrylonitrile (followed by pyrolysis), and on various mineral matrices. Thus, interchannel reactions of polymerization of preadsorbed acrylonitrile in a confined volume result in formation of a fiber polymer. As a result of this pyrolysis, carbonized conductive material forms in channels of a *host*. Postintercalation polymerization of aniline (associated, as a rule, with amino groups proton treatment) is performed in air at 130 °C in phosphate layers: $Zr(HPO_4)_2$ zirconium

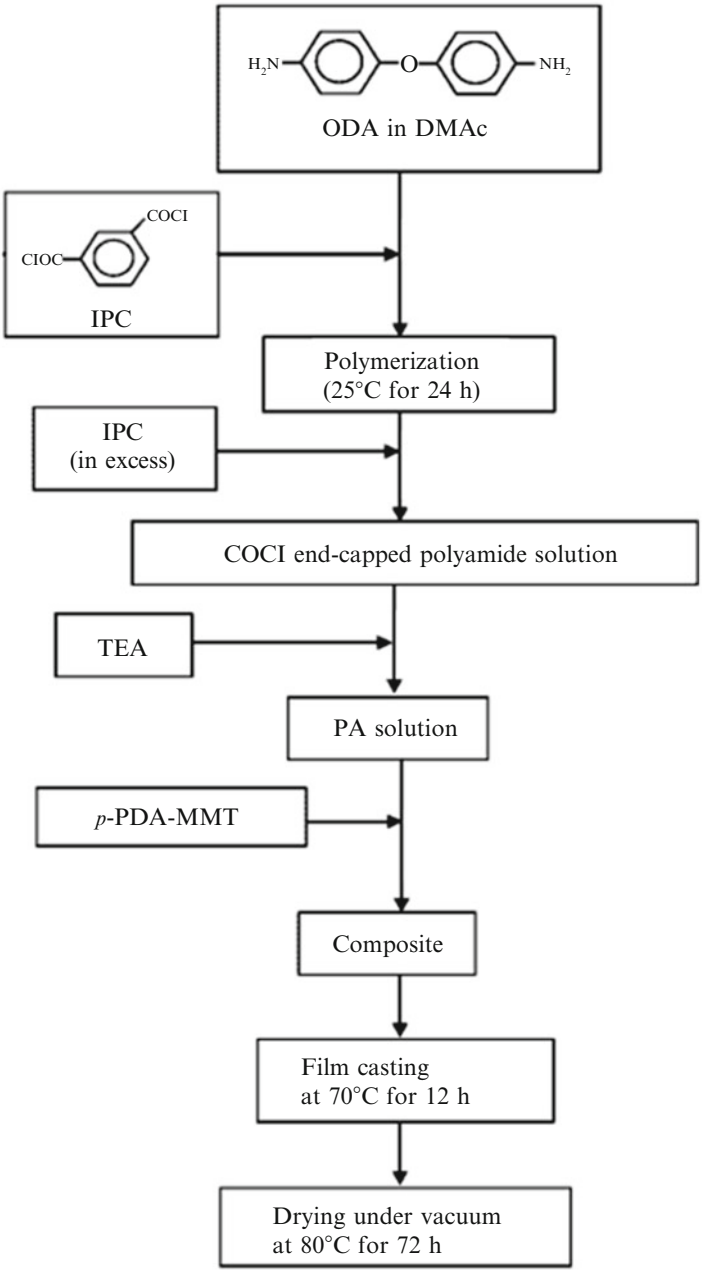

Fig. 5.22 Flow chart diagram for the synthesis of aramid/p-PDA-MMT nanocomposites [159]

phosphate, $VOPO_4$ vanadium phosphate, uranium HUO_2PO_4 hydrophosphate, Mg-Al layered binary hydroxides, $HMWO_6 \cdot H_2O$ (M = Nb, Ta), in layered acid zirconium-copper phosphates, etc. (see, for example [73, 165–167]).

Redox-intercalation aniline (An) polymerization proceeds with loss of two electrons and two protons for each monomer link:

$$n C_6H_5NH_2 \rightarrow (-C_6H_4NH-)_n + 2nH^+ + 2ne \tag{5.4}$$

It is important that oxidation polymerization of aniline, pyrrole, dithiophene monomers, intercalated in layered aluminum silicates leads to formation of highly oriented *host-guest* layers [117].[4]

Oxidation polymerization of pyrrole, dithiophene, tetrahydrofuran, acrylonitrile in FeOCl lattice has been known fairly long. Intercalated aniline forms hydrogen bonds with chlorine atoms of a lattice, polymerization proceeds along its diagonal (Fig. 5.23).

This lattice proves to be convenient for oxidation polymerization of An introduced from aprotonic solution. Gross content of the obtained substance is expressed by the formula $(An)_{0,28}FeOCl$, single crystal was grown from this. Zigzag polymer chains with $M_w = 6{,}100$, commensurable with FeOCl lattice are directed along the *host* crystal and hydrogen bonds of NH-groups with chlorine atoms of the lattice layers. In this case the ratio Fe^{2+}/Fe^{3+} is ~1:9, and polymer intercalate behaves as *p*-type semiconductor (specific conductivity of a single crystal is $1{,}5 \cdot 10^{-2}$ S/cm); during its long oxidation in air a mixture forms consisting of PAn and *β*-FeOOH. Other layered chlorides $FeCl_3$, CdI_2, $CdCl_2$ are seldom used in intercalation practice. At the same α-$RuCl_3$/PAn nanocomposites were obtained in situ via oxidation

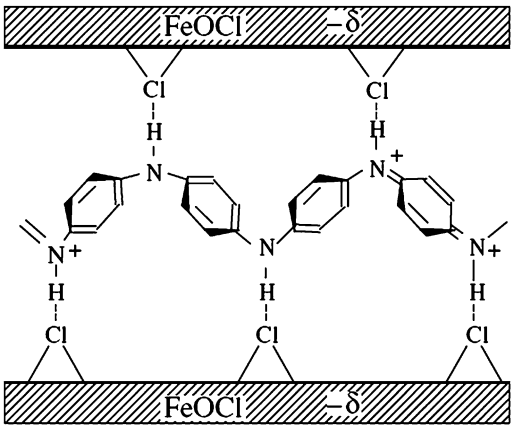

Fig. 5.23 Schematic representation of polyaniline intercalation into FeOCl lattice

[4] Very interesting is a title of one of the recent reviews [117], which considers energy efficient hybrid materials *Hybrid organic–inorganic materials: from child's play to energy applications.*

intercalation polymerization [168]. Moreover, α-$RuCl_3$ behaves as a perfect intercalation *host* polymer.

We should also notice that the materials obtained in polymerizing systems from N-vinylcarbazole and iron chloride impregnant with MMT (referred to [33]).

Hybrid nanocomposites based on PAn have special properties – variability of structures doping mechanisms, proper stability and recycling ability are widely used as materials for electronics. The most widely used variants are: PAn intercalations in V_2O_5, TiO_2, MoO_3, SnO_2, SiO_2, $BaSO_4$, HUO_2PO_4, Fe_2O_3, etc. [73, 131]. Thus, intercalation of aniline in $HMWO_6$ Bronsted layer acids proceeds at 130 °C in air and is accompanied by polymerization according to the scheme:

$$(C_6H_5NH_3)_xH_{1-x}MMoO_6 \times H_2O \xrightarrow{O_2} PAn \times H_{1-x}MMoO_6 + (1+x)H_2O \quad (5.5)$$

Lattice parameters of the monomer intercalate (x = 0.31) increase by ~0.69 nm as compared with non-aqueous $HMMoO_6$, while the corresponding polymeric only by 0.5 nm (Fig. 5.24). Probably, the polymer chain in PAn/$HMWO_6$ is so oriented that C_2 axis is parallel to inorganic lattice. Similar situation takes place in the V_2O_5-based nanocomposites.

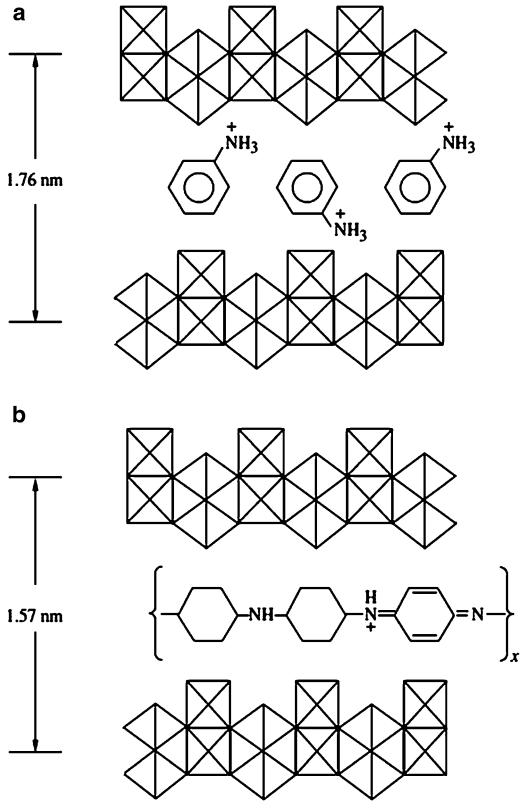

Fig. 5.24 Configurations of intercalated (**a**) aniline and (**b**) PAn in $HMMoO_6$. (M = Mg, Mn, Zn)

The hybrid material produced by polymerization of pyrrole in this fiber matrix is a solid conductive nanocomposite. Inorganic phase based on V_2O_5 xerogel is more expanded and is used for synthesis of hybrid materials with conductive polymers. Various intercalated types of conductive polymers, such as PAn, poly (2,2-dithiophen) or PPy are rather well investigated [169, 170]. Their redox-intercalation polymerization in V_2O_5 xerogel is an efficient method for obtaining of layered materials with a conductive polymer layer formed by polyconjugated anisotropic laminar microstructures [171, 172]. Their formation is based on oxidation-reduction reaction in which a monomer polymerizes after oxidation and V^{5+} is partially reduced to tetravalence. Intercalations (for example, in the case of aniline formation $(C_6H_4NH)_{0.44} \cdot V_2O_5 \cdot 0{,}5H_2O$) deep-blue complex with metal gloss is formed) are accompanied by polymerization. Growth of polymeric chains are realized first inside the xerogel, which is critical for formation of intercalation polymer, and are related to molecular oxygen transport, meanwhile, V_2O_5 xerogel also acts as a catalyst. Conductive polymer with different PAn/V_2O_5 ratios is formed with participance of mixed valence (V^{4+}/V^{5+}) lamellas of the *host* ordered in one direction. The material consists of altering vanadium oxide and polymer layers, its conductivity is by 4 orders of magnitude higher than the conductivity of initial $V_2O_5 \cdot nH_2O$ xerogel and is at room temperature ~$0.5\,\Omega^{-1} \cdot cm^{-1}$. Typically, depending on molar ratio of the components, two phases form with the composition $(C_6H_4NH)_{0.6} \cdot V_2O_5 \cdot nH_2O$ и $(C_6H_4NH)_{1.2} \cdot V_2O_5 \cdot nH_2O$. For the first one the interlayer distance is 1.4 nm, which corresponds to intercalation of one monolayer in the xerogel, for the second one (d = 2.0 nm), which corresponds to two monolayers. These structures allow doping of intercalated PAn accompanied by a small increase of electric conductivity of the produced materials, redox-active both in acid media and in aprotonic organic electrolytes. Physical chemical studies prove formation of a salted form of PAn. Aging of the material in air induces partial oxidation of inorganic frame and oxidizing binding of PAn in interlamellar space accompanied by further polymerization of aniline oligomers in xerogel layers. The formed polymer is as if frozen in them, which is caused by binding interaction organic and inorganic components due to formation of hydrogen bonds –N–H··· O–V–.

It is interesting that microstructure and properties of another conducting material, PPy/V_2O_5 aerogel composite depend on the synthesis method: it can be obtained as a result of combined polymerization of pyrrole and sol gel transformation of vanadyl alkoxide precursor ($VO(OPr)_3$ + pyrrole + water + acetone mixture) or mixturing of V_2O_5 gel with PPy). The best conductivity has a tablet nanocomposite synthesized by "post-gelatin" polymerization including consecutive polymerization of inorganic and organic phases. There is almost nothing known about co-intercalation of different types of monomers for synthesis of hybrid materials including two polymer components (by polymer-polymer type). Apart from the abovementioned catalytic way of formation of PE/PS composite, the method should be found based on mixing of methanol solution of 2,5-dimercapto-1, 3, 4-thiadiazole and aniline with $V_2O_5 \cdot nH_2O$ gel in molar ratio 1:2:2 [173]. Competitive polymerization and insertion of aniline takes place

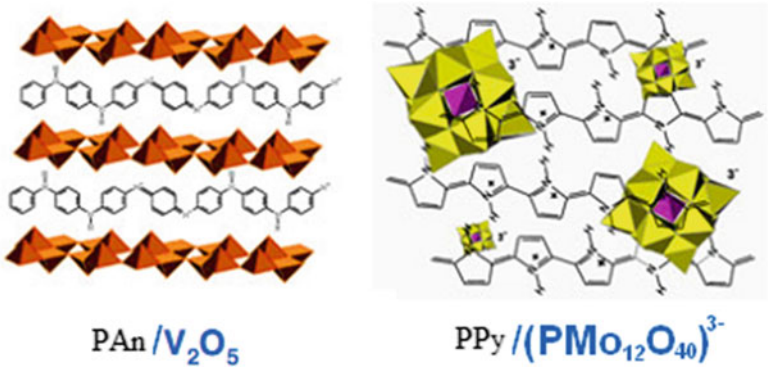

Fig. 5.25 Structure of conducting PAn/V_2O_5 and PPy/$(PMo_{12}O_{40})^{3-}$ composites [117]

also in the case of MoO_3 with formation of $(PAn)_{0,24} \cdot MoO_3$ nanostructures, including usage of low temperature intercalation technique. Polyaniline chains widen layers and change a potential surface, decreasing polarizing ability of the lattice. Further oxidation of polyaniline chains intercalated in MoO_3 is due to $(NH_4)_2S_2O_8$. Chemical synthesis of hybrid materials can realize via simple addition of pure aniline to the solid fluorite-molybdenum acid $H_3PMo_{12}O_{40}$. Its gallery includes a water layer bound with hydrogen bonds. Cation H^+-galleries can be substituted not only by other compensating cations, but also by aniline molecules with its following polymerization.

Heteropolyanions compose redox-frame of PAn, PPy [174], poly(3, -4-ethylenedioxythiophene) [175, 176] (Fig. 5.25).

The structure of conducting composites, ranged from the nucleus-shell complex to nanostructures and 100-nm nanoparticles, intercalation hybrids or smaller than 1 nm molecular structures are distinguished by a type of layered structures. Various inorganic phases with developed surface such as RuO_2, MnO_2, etc. are used as components of components of conductive systems [177].

Integration of polyoxometalates in conductive polymers is unusual class of electrically active hybrids, the result of a new idea of application of these in electrochemical supercapacitors. Figure 5.26 shows electrochemical characteristics of $(PMo_{12}O_{40})^{3-}$/PAn hybrid-based solid phased symmetric supercapacitor gauges as active electrodes [178, 179], in this case electric capacity evolves with increase in cycling acts up to 300 cycles (up to 120 F/g).

Polyoxometalates, which are ideal model electrodes for molecular batteries, are also active intercalating elements. In the forming hybrid organo-inorganic nanomaterials the conductive phase is polyaniline matrix and fluorine-molybdate anion $(PMo_{12}O_{40})^{3-}$ is active inorganic redox-component. Advantages of hybrid electrodes can be described as follows. First of all, a possibility of synthesis of hybrid materials exclusively with doped centers is shown. Next, they show stable behavior in terms of cyclic anion/cation integration. Thirdly, they can be used as blocked solid materials with molecular centers of fluorine-molybdate-anion.

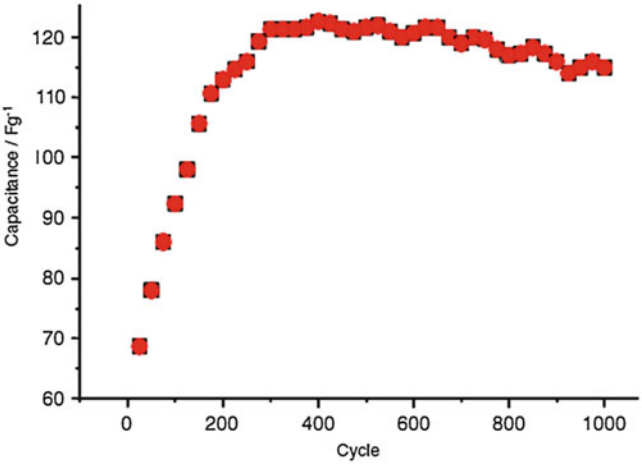

Fig. 5.26 Capacitance as a function of cycle number for a symmetrical supercapacitor cell with the hybrid $(PMo_{12}O_{40})^{3-}$/PAn as electrode material [117]

Very interesting intercalated agent for production of conductive materials is molybdenum disulfide (Fig. 5.27). X-ray diffraction patterns of MoS_2 and PPy intercalated in them show intense peaks at $2\theta = 7.63$ deg (Fig. 5.27b, 2) and 8.96 deg (Fig. 5.27b, 3) are associated with reflection (002, c axis) from the plane of layered molybdenum disulfide, interlayer distance in MoS_2 with intercalated polypyrrole 1.158 for PPy/MoS_2-1 and 0.986 nm for PPy/MoS_2-2, respectively [180].

Taking into account that the interlayer distance in the initial MoS_2 is estimated as 0.615 nm (Fig. 5.27b, 1) and it increases by 0.543 and 0.371 nm in two composites, which confirms intercalation of PPy between the layers of MoS_2. On the other hand, appearance of two different interplanar distances shows that the polypyrrole chains between MoS_2 layers are in two different conformations (orientations) (Fig. 5.27a). Most probably, smaller interplanar distance corresponds to a *guest* polymer molecule lying on a plane between layers of MoS_2, greater interplanar distance is responsible for the polymer molecules perpendicular to MoS_2. Intercalation of PPy in MoS_2 causes significant increase in electric conductivity of both conformations (PPy/MoS_2-2 far more than PPy/MoS_2-1). Probably, this molecule of the previous polymer lies in the plane of π-electrons parallel to layers of MoS_2, which facilitates electron transport between organic and inorganic components.

Despite great facilities of the intercalation method carried out via in situ polymerization, it has drawbacks. The main drawbacks of the intercalation polymerization method are the problems of specifying molecular – mass characteristics of produced polymers, which impedes investigation of kinetic parameters of intercalation polymerization and finding of its special features as compared to traditional processes. Applications of these methods are confined to thin films production, coats, etc.

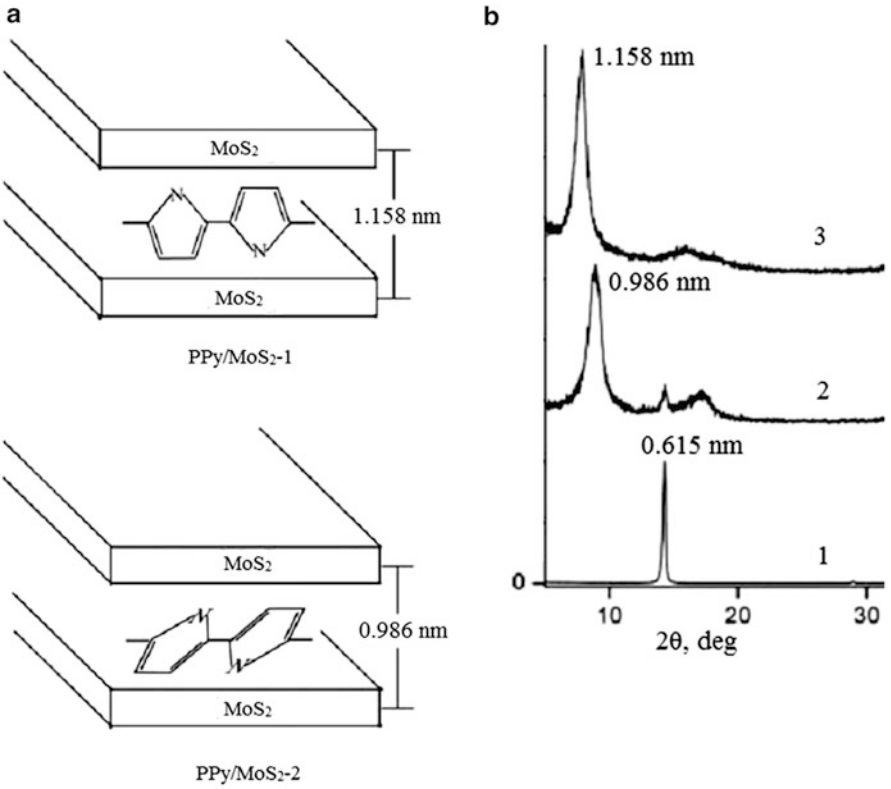

Fig. 5.27 (**a**) Schematic representation of PPy intercalation models into MoS_2 : PPy/MoS_2-1 и PPy/MoS_2-2 with perpendicular and flate orientation of polymer molecule, respectively (**b**) X-ray diffraction patterns of MoS_2 (*1*) and PPy/MoS_2 -1 (*2*), MoS_2-2 (*3*) intercalated nanocomposites [180]

5.4 Hybrid Nanocomposites Produced by Direct Intercalation of Macromolecules in *Host* Layers

Though intercalation from polymer solution of melt has being studied for rather long time, commercial applications have presently only composites on Nylon 6 and OMMT basis [39]. It seems promising to use polymer/silicate hybrids obtained this way in automotive industry, packing industry, and aerospace industry, as well as materials with high thermal, gas-separating, and mechanical properties.

Matrices are made of PS, polycaprolactam (PCL), PEO ($T_m = 328$ K) polyvinylidene fluoride ($T_m = 444$ K), polymethylmethacrylate (PMMA) ($T_m = 527$ K), poly-4-vinylpyridine ($T_m = 473$ K), etc. Degree of intercalation of a polymer does not correlate with its dielectric constant, most probably, presence of carbonyl group and low T_g of the polymer encourages its intercalation. Aminomodifier increases intensity of intercalation (as compared with a fluoride

containing one) due to smaller volume of its functional group and formation of stronger hydrogen bonds of surface hydroxyl groups of silicate with polycaprolactam. In this case mobility of spin-labeled modifier is increased in presence of polymer, which is probably caused by the fact that T_g of the polymer in the surfactant layer is lower than the order-disorder temperature in pure organo-magadiite. This phenomenon is similar to polymer plastification.

Direct methods (especially, melt technique) are of versatile interest. Firstly, they are relatively simple, as compared to polymerization in interlayer space, and are therefore, more practical for structuring of inorganic/organic polylayered composites [118]. Next, for this can be used well characterized polymer. And the last, the process is interesting due to its unusual intercalation physical chemistry. It displays in acquiring of electron conductivity by a system (in polyconjugated systems) for application, for example, in reversible electrodes, in improved physical-mechanical properties of many nanocomposites. Studying of these systems also can give important information on special features of absorption of a polymer on nanometer materials. Thus, absorption isotherms of polyvinylpyrrolidone in CeO_2 suspension (synthesized under hydrothermal conditions, particles size about 9 nm) for various pH is well studied (see, for example [33]. Most widely used are two types of direct intercalation of polymers: from solution or from melt.

In discussion main properties of nanocomposites obtained by comparative methods are analyzed, for example [181]. Nevertheless, still remain many problems as regards the effect of various parameters on properties of the forming nanocomposites.

5.4.1 Intercalation of Polymers from Their Solutions

Nanosilicate composite produced in this process includes three components: silicate layers, solvent and polymer. The controlling parameters are: composition, concentration and distribution of components, molecular mass of a polymer, temperature; distribution of the components plays important role in achievement of enhanced characteristics.

The most important factors are: the origin and polarity of a solvent, a silicate modifier, a character of interaction between the components, precipitation, etc. For example, precipitation is successfully used for formation of the systems based on ABS [182], polyvinylidene fluoride (PVdF) [183], PE [184], however, there is no intercalation from the copolymer solution of ethylene with acrylic acid into MMT, though it easily proceeds from the melt [185]. The effect of a solvent depends also on the origin of a modifier: when a modifier with one long alkyl chain is used, interlayer distance decreases linearly with increase in dielectric constant, while if a modifier with two long chains is applied, linear dependence of d on polarity of the solvent is observed under condition that the solvent has low (below 10) value of dielectric constant. Other listed parameters play less important role [44].

The experimental procedure is as follows. The layered silicates modified by organic cations are swelled in some solvent with the following intercalation of a polymer solved in the same solvent. Various approaches are possible to obtain these hybrids: mixing of a solution (for example, salt solutions of polyanilinehydrochloride in acid-methanol solution, sulfonic salt of poly-*n*-phenylelene soluble in many solvents, etc.), suspension, confinement of polymer in gel or xerogel, etc.

Layered silicates are dispersed to small aggregates (packs) consisting of several layers with high aspect ratio and intercalated between them and the polymer parallel to it consisting of one-two layers of macromolecules. The driving force of intercalation from the solution is an increase in entropy during desorption of a solvent made of active swelling polymer, which overpowers a decrease in entropy during sorption of swelled macromolecules. Though usage of great amounts of a solvent makes this process less attractive, the solution intercalation is applied in the fields where thin films are required, for example, in coatings [186], membranes [187], etc.

Most widely used are the following types of nanocomposites produced this way: PS thermoplastics [188], styrene-acrylonitrile copolymer, PMMA [189], thermoplastic elastomers [190–193], fluorine elastomers [194], PEO-MMT, nylon-layered silicates, composites based on hectorite and polyaniline, polythiophene or polypyrrole, TiO_2 and polyaniline shaped as nanotubes [195], etc. More rarely this method is used to form reactive plastics – poly(glycidyl methacrylate-co-methylmethacrylate) [196], epoxycomposites [197]. These hybrids can be used as nanofilms or nanocoatings formed in continuous (flow) regime during surface modification of various thermoplastic films, as reaction-capable compatibilizers, fillers for thermoplastic polymer compositions, especially based on acryl polymers, components of nanomaterials, made via extrusion, masterbatches, etc. [86, 195, 198–201].

Though intercalation of polyolefins is impeded by their solution, there are solutions adapted for this purpose, in particular, solutions of low density linear PE and PE-grafted-MA (PE-*gr*-MA) in xylene in combination with binary Zn_3Al-hydroxides for producing of exfoliated nanocomposites [202].

Generally, in this type of nanocomposites also hybrid structures of two types can form: intercalated, in which a polymer or a part of its links are implanted between silicate layers, or delaminated with dispersed individual silicate layers in organic matrix, and the composite structure is microscopically isotropic. Layered silicates are mostly used like in the case of polymerization, most often Na-MMT, including those modified by long chained amines.

To implant PEO from water solution, a convenient inorganic matrix is V_2O_5, in this case its interplanar distance increases to 1.32 nm, the same is observed in the case of PVP, PPO, etc. PEO is also implanted in lamellar networks of $V_2O_5 \cdot nH_2O$ and $CdPS_3$. Thus, PEO water solution (molar mass 10^5) with $V_2O_5 \cdot nH_2O$ gel (interplanar distance 1.155 nm) after water removal forms a nanocomposite of xerogel with the general formula $(PEO)_xV_2O_5 \cdot nH_2O$ (referred by [33]. Interplanar distances in the matrix increases from 1.32 to 1.68 nm at $x = 0.5$–1.0, while at $1 < x < 3$ it increases to 1.83 nm. It is interesting that the composites with $x < 1$ contain a monolayer, while at $x \geq 1$ bilayer of closely packed PEO molecules completely filling the interlayer distance of xerogel with fiber mono- and bilayers.

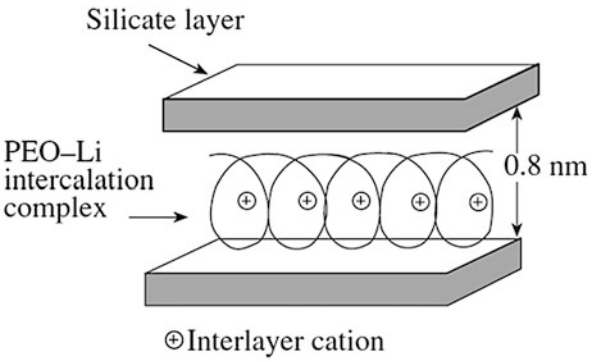

Fig. 5.28 Structure of PEO intercalated into a monoionic silicate layer [34]

The one-phased nanocomposite is formed at $x < 0.8$, it easily forms flexible thin film and can participate in oxidation-reduction intercalation. As a result of these processes solid electrolytes and materials with electrochromic properties form:

$$y\mathrm{LiI} + (\mathrm{PEO})_x\mathrm{V_2O_5} \times n\mathrm{H_2O} \rightarrow \mathrm{Li}_y(\mathrm{PEO})_x\mathrm{V_2O_5} \times n\mathrm{H_2O} + (y/2)\mathrm{I_2} \qquad (5.6)$$

Alkali metal ions and PEO form interstitial compounds that also can implant into silicate layers, for example, in MMT (Fig. 5.28). Intercalated salt complexes PEO/Li^+ – MMT are apart at 0.8 nm distance, in this case PEO chain has a little stressed helicoid conformation. To compare, we shall note that broadening in PEO-MMT nanocomposite is 0.81 nm, which is wider than in nylon-6-clay nanocomposite (0.6 nm).

The PEO-LiX (X – halogen, alkoxy-, aryloxy- groups, etc.) systems are widely used as flexible (soft) electrolytes, new ionic conductive materials. For these systems it is interesting to find the effect of value and number of charges on mesomorphic behavior and ion conducting properties [203]. Though lithium salts are used in majority of practical applications, other cations are also well studied. The most intensely studied during the last decade are PEO/Zn salt systems. The compounds containing different numbers of PEO links are considered and characterized: $(–CH_2–CH_2–O–)_nZnBr_2$ ($n = 6$, 8, 15). Local neighboring of macrocomplexes has a significant effect on properties of polymer electrolytes, which is demonstrated taking $(–CH_2–CH_2–O–)_n$ $[(ZnBr_2)_{1-x}(LiBr)_x]$ (n = 20–80, x = 0–0,5) systems for example [204].

As in other already analyzed cases, a cation can be intercalated by the ion exchanging and by reduction, while neutral polar molecules can be intercalated only via substitution by molecules of a solvent. For water-soluble polymers PEO, PVP, polyethylene imine (PEI) the method of incapsulated precipitation from solution is used. As it was already mentioned, α-$RuCl_3$, having lamellar structure, has high intercalation properties. In the inert atmosphere as a result of interaction between α-$RuCl_3$, and $LiBH_4$ Li_xRuCl_3 ($x \approx 0{,}2$) is obtained, which, in turn, forms intercalation compounds with $Li_x(PEO)_yRuCl_3$ type of polymer (Fig. 5.29).

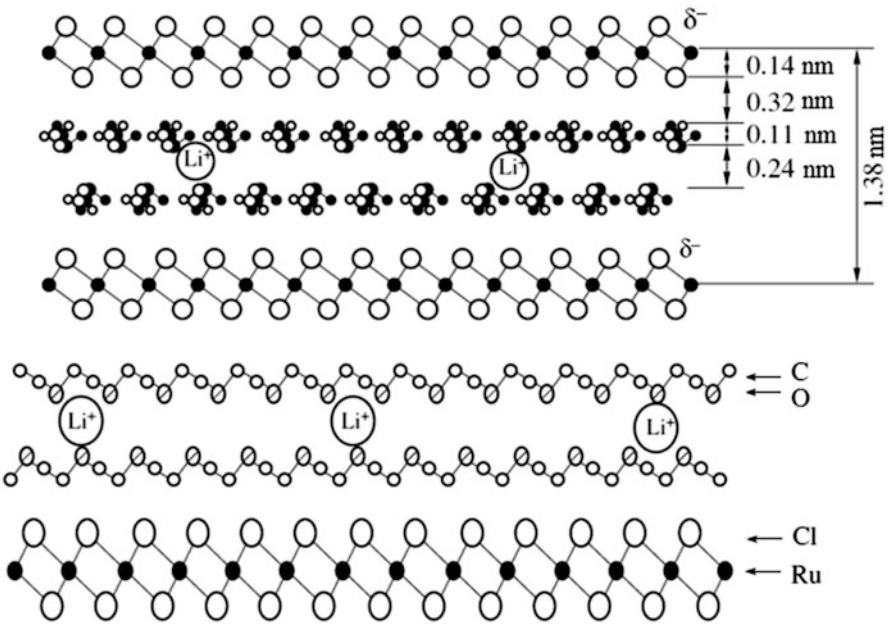

Fig. 5.29 Structural model for $Li_x(PEO)_yRuCl_3$ and schematic 1D electron-density map (projection along the *c* axis)

These products have ionic conductivity comparable with the best polymer electrolytes [168].

Comparative with the melt method, in situ intercalation polymerization causes homogenous dispersions and is accompanied by substantial improvements of properties [111]. However, taking into account the fact that intercalation of some polymers has special features (for example, requires their solubility) it has been studied for few polymers, in contrast to more conventional melt technique.

5.4.2 Intercalation Composites Produced from Polymer Melts

This method is a direct mixing of a polymer melt with organic silicate under action of shear loads at temperatures higher than the temperature of the matrix melt. Exfoliation of layered silicates or minerals caused by mixing with a polymer, when both components, polymer and inorganic material in the interphase layer, are exposed to thermomechanical stress under the treatment, combined with a filler dispersion into uniformly distributed nanoparticles forming a nanostructured system, significantly improve properties of the composites.

This preparation technique also called reactor mixing, is very convenient, it is used for various types of polymers (non-polar PE, PP, PS, natural resin; polar polyamides, polylactic acids, etc.), for its realization compaction, injection formation, extrusion can be used, which reduces production time and cost of materials, the process is ecological [205–216]. The experiments on the polymer/silicate hybrid materials show that intercalation of polymer chains causes 25 % increase in space between silicate layers. This increase corresponding to radius of inertia of the polymer melt assumes plane conformation of the chains in the galleries. Non-disturbed radius of inertia in the melt is calculated from the formula $R = u(N/6)^{1/2}$, where u is length of a segment of a polystyrene chain based on polymerization degree N, a u is valued 5 Å from the table data [217].

Theoretical studies of melt intercalation receive much attention. Thus, molecular dynamic techniques (elastic spheres method) is applied for promotion of intercalate and exfoliate formation in nanocomposite material. The effect of many factors is taken into account, among them the most important are temperature, structure of polymer and co-polymer chains, including functioning of end links, content and degree of interaction of polymer-silicate layers [218].

Commercial importance of this widely used versatile intercalation technique as ecologically preferable and technically easily realized has already been discussed. Lastly, it should be noted that intercalation is often enforced by stimulating power actions, for example, ultrasonic treatment (Fig. 5.30).

Intercalation of polystyrene from melt to organic clays is controlled by mass transport in primary particles and is not specifically controlled by diffusion of polymer chains in the space of a silicate gallery. Activation energy of hybrid

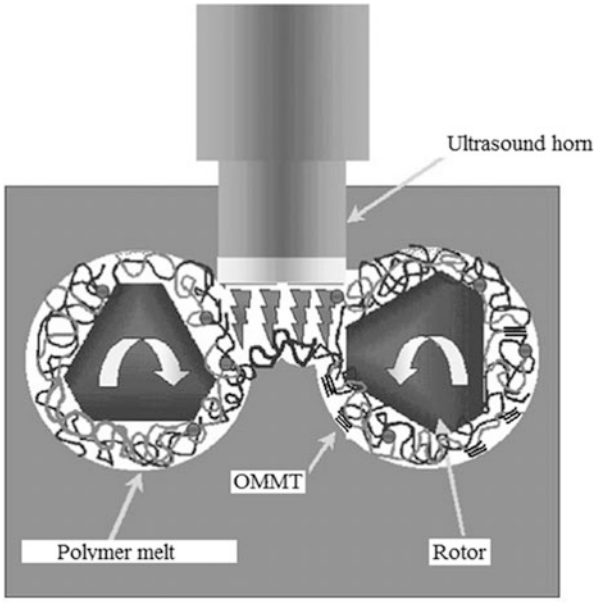

Fig. 5.30 Schematic diagram of mixing in melt activated by high intensive ultrasound irradiation (20 kHz)

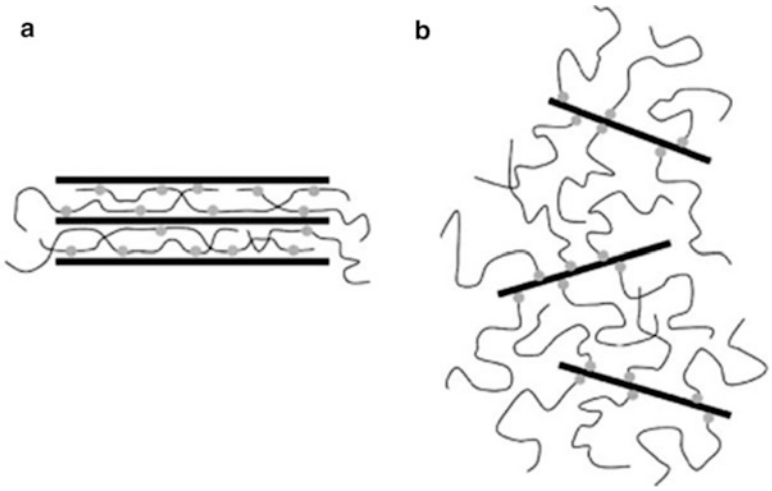

Fig. 5.31 Molecular structure of chain-end-functionalized polyolefin (**a**) and side-chain-functionalized polyolefin between the layers and related morphologies of nanocomposites (**b**) [219]

formation is analogue to activation energy of self-diffusion of polystyrene in blocked melt. Dynamic processes of hybrid formation on the basis of non-polar polymer/organic clay nanocomposites were studied using rheological techniques [97]. In contrast to this, PP functioned in the side chain or block-co-polymers have multiple contacts with each surface of the silicate, which provides not only equalizing of the polymer chains with respect to the silicate surface, but formation of sequent bridges between its plates to promote intercalation structures (Fig. 5.31) [219].

5.4.3 Nanocomposites Based on Non-polar Thermoplastics Produced by Reactor Mixing

Since this area of investigations develops very intensely, we will just briefly analyze here the most widely applied and typical, in our opinion, variants and laws. The polymer melts (PELD, PEHD, CEP, LPELD, PP, PS, etc.) are used to prepare polymer/clay composites, including screw, extruder, polymer fibers [184, 220–227].

In order to refine nanoclays, not only silicate chemical modification, but also those of polymers and implanted compatibilizer are used in the melt of non-polar polymer. In the case of PE with statistically distributed or end dimethyl-ammonium-chloride groups or PE-block-PMAA it is shown [228, 229] that one end ammonium group is, probably, not enough to change a structure of even organophilic clay, contrary to the results obtained for PP. The best results are

achieved for PE containing more than one ammonium group in a side chain, and due to increase in PE-block-PMMA concentration [122, 230].

Also various polymer-modifiers and increasing compatibility of ingredients additives are implanted into the melt, the most widely used is maleic anhydride (MA) applied as compatibilizer, however, it is more often introduced in PP melt in the composition PP-gr-MA, these composites are called PP-MA/OMMT or PP/PP-pr-MA-MMT. The silicate gallery (2–3-nm width) one or more stretched PP-MA chains are implanted. They simultaneously change rheology of the composition, interparticle structure, and chemistry of hybrid materials. Polyolefin-MA-MMT composites have improved mechanical properties, thermal stability, fire resistance, barrier properties, corrosion resistance, they favor non-isothermal crystallization, etc. [45, 231–244].

Properties of polyolefins induced by the intercalation technique are analyzed recently in the review [116]. Silicate layers of about 150 nm in length and 4 nm in thickness are fined in PP-MA-matrix, hierarchical structure of the intercalated PP-MA correlated with particle sizes of the clay (30–50 nm), which is comparable with the inertia rotational radius of macromolecules. The crystallized lamellas have thickness 7–15 nm; they can form a spherulite texture [245] with 10-μm diameter particles (Fig. 5.32). The clay particles are used as nuclei-agents for the PP-MA matrix (like in the case of PP crystallization in presence of carbon nanotubes) [246].

Crystallization of polymers is one of efficient methods of control over extension of an intercalated polymer chain in the silicate gallery. It is assumed that crystallization is impeded due to an interlayer space limited to 2-3-nm, however, one can expect that heat should accelerate diffusion and define orientation of a polymer in the silicate gallery [247]. The one-staged method of nanocomposite preparation is proposed using isotactic PP or its oligomer and organically modified (with dodecylamine) MMT with 0.15–1.22 mol% MA as compatibilizer (inoculated in double screw extruder initiated by dicumile peroxide): *iso*-PP was used a matrix polymer, oligo (*iso*-PP-*pr*-MA) as a reaction-capable compatibilizer and dodecylamine was used as MMT surface modifier. Under conditions of extrusion controlled destruction of *iso*-PP takes place and inoculation of MA links to *iso*-PP chains in the melt. In this case nanostructured morphology of PP/oligo(PP-gr-MA)/OMMT forms via creation of hydrogen bonds and the following reactions of

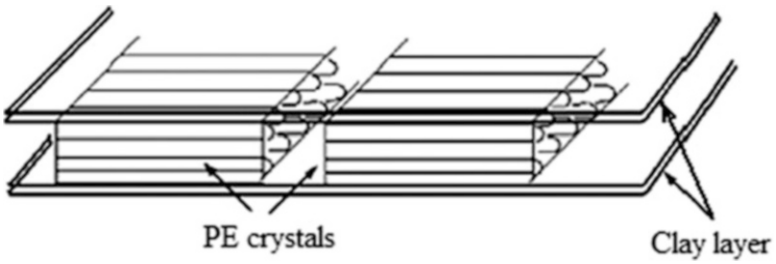

Fig. 5.32 Schematic of PE crystals intercalated between MMT layers [245]

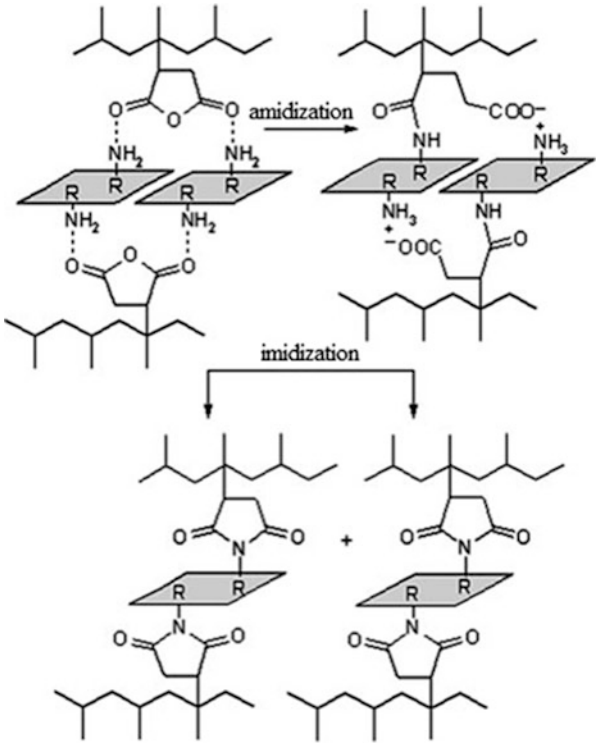

Fig. 5.33 Schematic representation of in situ reactions in the formation of nanostructural architectures in the PP/PP-gr-MA-OMMT system [198]

amidation/imidation with participation of anhydride cycles of exfoliated *iso*-PP and modifying OMMT alkylamine (Fig. 5.33).

It has been found that if intercalation is improved, the complete exfoliation of a composite may be not achieved [248–251]. Usage of inoculated MA as a compatibilizer and a modifying agent brought to good results as regards intercalation and exfoliation, however, high concentration of MA causes phase separation, which means a disadvantage in achievements of good mechanical properties of the composites [252]. Therefore numerous attempts are made to decrease MA concentration due to usage of other molecules favoring intercalation (secondary intercalated molecules) [253–255]. Relatively often PVA additives or its polymers are implanted [252, 256–260].

Fineness of a silicate depends on a matrix and an intercalation agent. MMT modified with octadecyl ammonium in the ethylene-vinyl acetate (EVA) matrices collapses owing to significant increase in the interlayer distance [260]. Good results are also achieved via intercalation of different components into basalt space of silicates (Fig. 5.34). Thus, mixing in a melt was used to obtain composites including PP, PP-pr-MA and a long chain amide, AM (docosanoic acid C_{21}, unsaturated erucic acid C_{22}) and OMMT in the ratios 95.5: 2: 0.5: 2 [261]. In fact, this amid increases interplanar distance, however, without PP-gr-MA it is difficult to reach homogenous dispersion of a silicate during exfoliation. Double system of PP-gr-

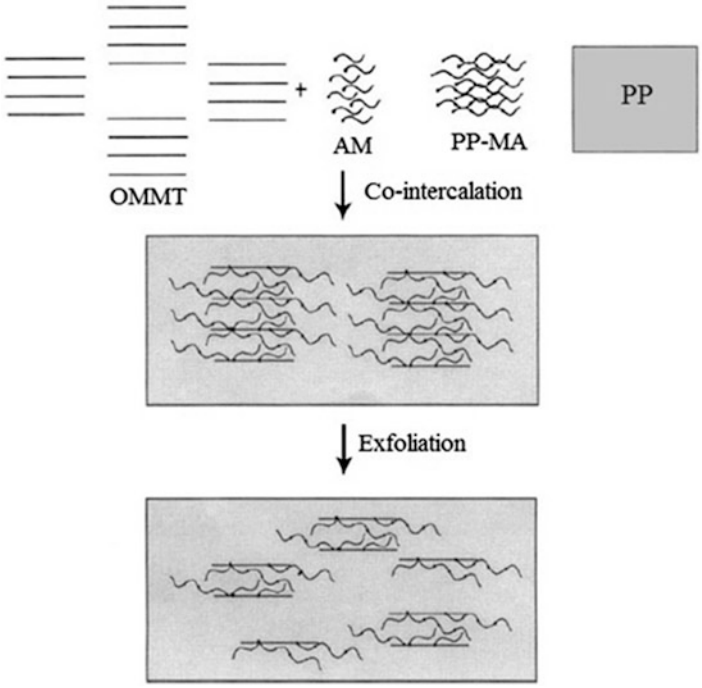

Fig. 5.34 Schematic illustration of preparation of polypropylene-clay nanocomposite by the co-intercalation of 13-*cis*-docosenamide (AM) and maleic anhydride grafted polypropylene (PP–MA) [261]

MA and AM improves properties of the produced composites, in particular, their thermal stability. Meantime, MMT modified by ammonium cations including links of carboxylic acids is not suitable for formation of these composites [262].

Comparative analysis of properties of the nanocomposites PE/PE-gr-MA-OMMT obtained by the solution (dimethyl benzene, 130 °C) and the melt techniques has shown [191] that the intercalation effect is expressed in improvement of nanocomposite structure and its physical mechanical properties caused by an increase in PE-gr-MA concentration, increase in the chain length of the modifying ammonium cation. A degree of crystal order of a composite and thickness of formed crystallites decrease as concentration of PE-gr-MA increases [263], crystallites formed in the solution technique are far smaller than those obtained via direct intercalation from melt (Table 5.4). Therefore, it is concluded that OMMT and PE-gr-MA are heterogeneous nuclei of PE crystallization from melt, maximum ultimate tensile strength (23.3 MPa) is achieved at the PE-gr-MA concentration 6 wt%, strength increases as a fraction of PE-gr-MA increases to 9 wt% and reaches 122.2 J/m.

Third polar component is introduced to achieve better refining of MMT in the nanocomposites [250, 264–267].

Table 5.4 Comparative analysis of basal space during formation of MMT-organosilicate exfoliated nanocomposite by various techniques [263]

	In situ polymerization		Intercalation from melt		Method of dosed integration of components (masterbatch)	
OMMT, wt %	2θ°	d_{001}, nm	2θ°	d_{001}, nm	2θ°	d_{001}, nm
0.73	2.43	3.63	2.65	3.30	2.72	3.25
1.60	2.40	3.68	2.65	3.30	2.74	3.24
2.40	2.69	3.28	2.64	3.32	2.65	3.30
3.36	2.65	3.30	2.60	3.35	2.69	3.28

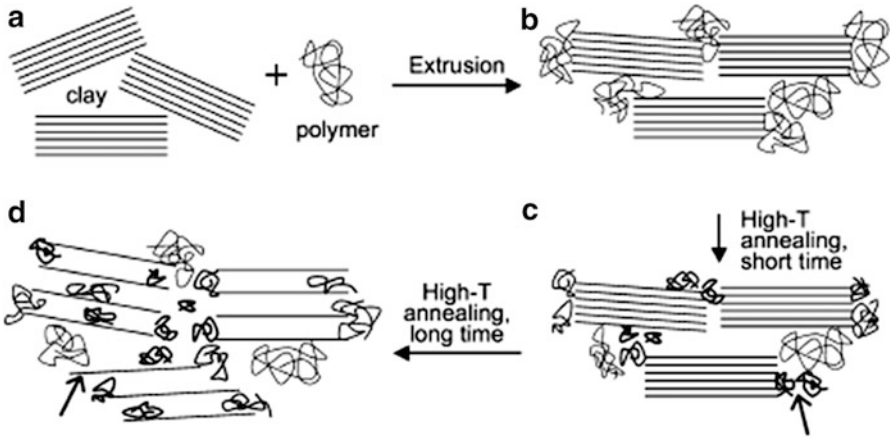

Fig. 5.35 A scheme depicting the evolution of nanocomposite morphology upon extrusion and subsequent annealing: **a**, **b**, **c**, **d** [268]

AIBN was introduced in organic-modified MMT, after which PS was intercalated from melt. Some increase in interplanar distance can be related with exothermal process of decomposition of the initiator and forming of free volume due to gas emission, which accelerates exfoliation [268]. Extrusion of a polymer with aggregated silicate (Fig. 5.35a) is accompanied by intermediate formation of agglomerate of polymer chains with potentially suitable intercalation places (Fig. 5.35b). Low temperature short-time annealing during t_1 interval or annealing in inert atmosphere change the structure insignificantly (Fig. 5.35c), whereas a long high temperature annealing during t_2 or annealing in presence of O_2 is associated with chains breakage and formation of bridge-structures with the following diffusion of short chains into layers (allow labeled). As the time increases, short PS chains generated by chains breaks insert into interlayer distance and cause fracture of the plates, the latter draw apart (Fig. 5.35d, pointed to by an arrow). The total molecular mass of this PS is up to 30,000 (initial mass is $M_w = 330{,}000$). The calculation are made and these processes are theoretically grounded (see for example, [269]).

These results confirm the well known fact that diffusion of long-chain PS to the silicate gallery is impeded more than that of short-chained. Double-screw extrusion of high-molecular PS and organically modified silicate with profile optimization of the screw compensates [270, 271] diffusion difficulties, which would otherwise need static annealing at high temperature [272, 273].

5.4.4 *Composites Formed in Melt of Polar Matrices*

A possibility of intercalation of polar polymers between the silicate layers is governed by total enthalpy of intercalation including adverse effect of interaction between the polymer and aliphatic chains of the modifying agent and favorable effect of polar interaction between a polymer and the silicate layers [274]. In other words, a decrease in entropy caused by integration of macromolecules into the interlayer space is compensated by increase in conformation freedom of alkyl radicals of the modifier at drawing apart the silicate layers or a polymer melt with a mineral. Drawing layers apart, especially exfoliation depends on their position, preferable interaction between the polymer and the surface of a silicate and further decrease in energy of the system.

An ethylene co-polymer with vinyl acetate (EVA) with various numbers of polar groups controlled by its composition is intercalated in the melt in OMMT. The intercalation/exfoliation behavior and properties are influenced by VA links content, concentration of MA inoculated to HDPE. Fineness of MMT and its exfoliation are improved as HDPE-MA content increases, inoculated MA amount decreases and vinyl acetate concentration increases, which, probably, is due to the synergetic effect of the polar groups. In this case PEVA-MA additive increases the elastic modulus (Fig. 5.36). One of remarkable and extensively studied

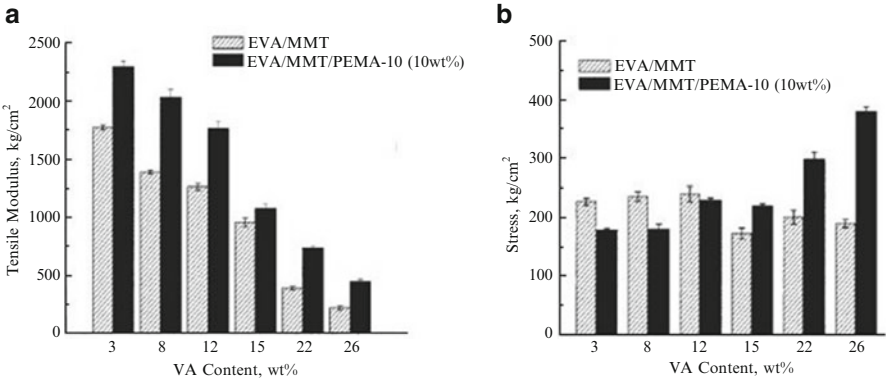

Fig. 5.36 Dependence of tensile modulus (**a**) and tensile stress at break (**b**) on the vinylacetate content in EVA/MMT/PEMA-10 (10 wt% maleic anhydride) composites [265]

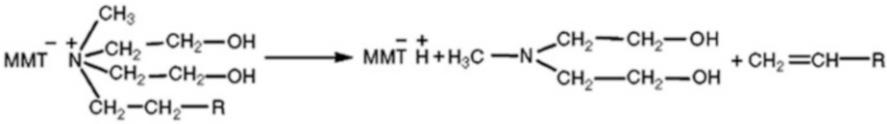

Fig. 5.37 Degradation of the OMMT ammonium salt with the formation of an olefin, an amine and a protonated silicate [277]

properties of the nanocomposites of this type is manifestation of flame-inhibiting ability[5] (see, for example, [243, 275, 276]).

Deacetylation of EVA polymer in the nanocomposite occurs at lower temperature, than in the initial polymer, which may be caused by catalytic effect of strongly acid centers on thermal decomposition of the modified silicate, for example, by Hoffman elimination or $S_{N\ 2}$ nucleophilic substitution at temperature below 155 @C, causing acid activation of OMMT [277, 278], which, in turn, has an effect on inflammability of the nanocomposite (Fig. 5.37).

The main part of decrease in permeability id owing to extension of real diffusive paths of gases, which flow in presence of a filler, layered silicates. Their sheet-like morphology causes maximization of this path length. The factor of convolution (τ) is defined as a ratio of a real distance (d'), which should be passed by a penetrant to the shortest distance (d), corresponding to a distance without a layered silicate (L, W, and Φ are length, width, and volume fraction of these plates, respectively, $W \sim 1$ nm, $L = 50$–$1{,}000$ nm and $\Phi = 0.05$):

$$\tau = \frac{d'}{d} = 1 + \left(\frac{L}{2W}\right)\Phi \tag{5.7}$$

As a rule, $W \sim 1$ nm, $L = 50$–$1{,}000$ nm and $\Phi = 0.05$.

The effect of convolution on permeability is expressed [279] as

$$\frac{P_s}{P_p} = (1 - \Phi)\tau, \tag{5.8}$$

in which P_s and P_p are permeability of the penetrant in the nanocomposite and in pure matrix, respectively. This idea is displayed in Fig. 5.38.

Actually, low flammability is caused by many factors, one of which is formation of barrier carbonated layer on the surface of a fractured composite during combustion [280].

[5] Often additives are introduced to decrease inflammability. In particular, 0.5 wt% cyclo [dineopentyl(diallyl)] pyrophosphate dineopentyl (diallyl) zirconate or Tamol 20011 (trade mark KZTPP1, Rohm and Haas Co, Philadelphia, PA, USA), hydrophobic highly efficient pigment, acid copolymer based on acrylic acid (un-neutralized acrylic-based acid copolymer) is used to prevent agglomeration of silicates.

Fig. 5.38 Schematic representation of the gas path in a nanocomposite (path of the penetrant = d') and in a pure polymer (path of the penetrant = d)

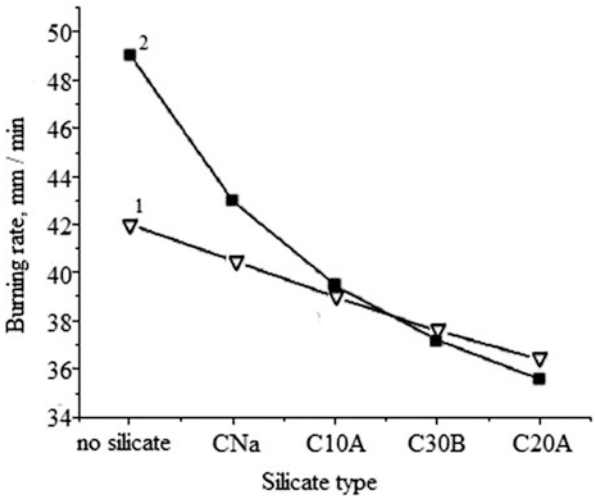

Fig. 5.39 Variation of the burning rate of the ABS with lower (*1*) and higher (*2*) acrylonitrile content and the corresponding ABS/Clay nanocomposites with the different Cloisite Clays, all nanocomposites at 4 wt% loading [281]

Under industrial conditions modified concentrated clays are also used (masterbatches), with their help it is easier to control dispersing of organosilicates in melt of components. Moreover, in combination with nanoclays as enforcing agents for a polymer composite, containing nanofillers such as carbon nanotubes, multifunctional materials with improved mechanic, thermal, and electric properties can be obtained.

The best characteristic of thermal stability and inflammability have Cloisites20A [281] (a decrease in a burning rate of plastic is 27 and 13 % with high and low concentration of AN, respectively) and 30B (24 and 11 %, respectively) (Fig. 5.39).

We shall highlight some more moments.

Intercalation of syndiotactic and isotactic PMMA from melt into organomodified bentonite [42] increase d-basalt space by 25 % and leads to improvement of physical mechanical properties: [161, 282, 283] polymer chains

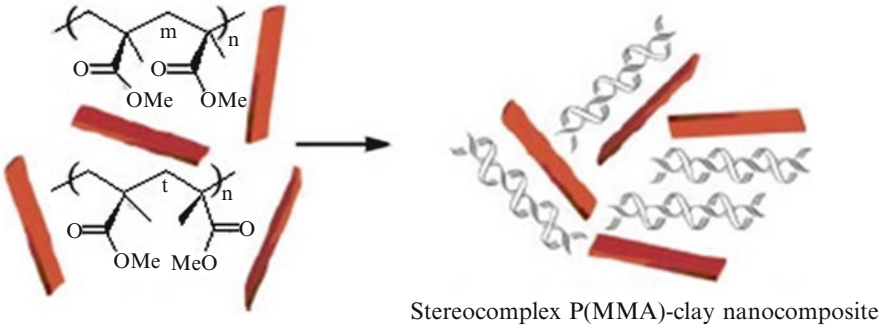

Fig. 5.40 Schematic illustration for the formation of isotactic/syndiotactic stereocomplex PMMA-clay nanocomposites. Modifying agent is methyl bis(2-hydroxyethyl)tallow alkyl ammonium [153]

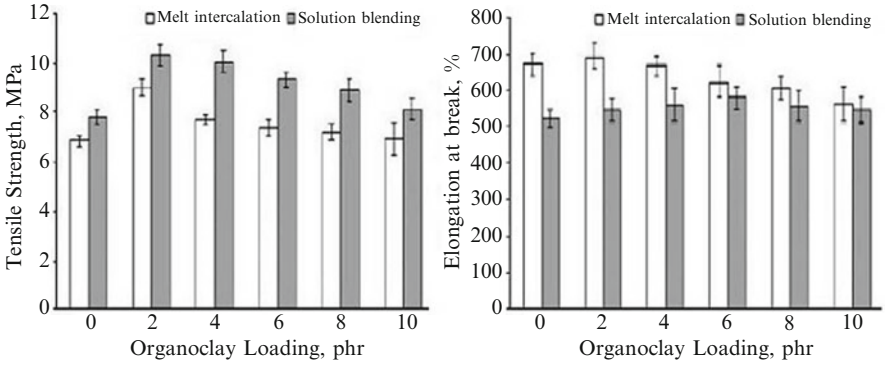

Fig. 5.41 Tensile strength and elongation at break for neat poly(ethylene-co-vinylacetate)/natural rubber and its nanocomposites obtained by solution blending (*dark column*) and melt intercalation (*white column*) [284]

with modified cation are associated (Fig. 5.40), thermal stability of the composite as compared to the initial polymer is increased, T_g of polymers increases [157, 284].

The solution (from toluene) and the melt methods of production and properties of intercalated composites based on poly(ethylene-co-vinyl acetate) mixtures (15 % VA)/natural rubber (0–10 mass parts per 100 parts of the mixture)/OMMT are compared.

The composites obtained via solution mixing show higher ultimate tensile stress (Fig. 5.41) and thermal stability due to better fineness of OMMT in the polymer matrix, than the respective value of the composites obtained from melt. At the same time the way of preparation of a nanocomposite has no effect on its flammability. Though relative elongation during tension of the composite produced by reactor mixing is higher than that of the one produced by solution method, it decreases as OMMT content increases [285].

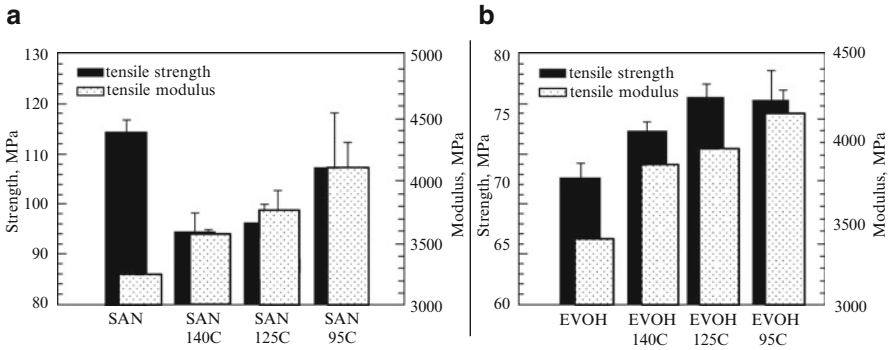

Fig. 5.42 The tensile properties of the intercalated poly(St-*co*-AN/OMMT and poly(E-*co*-VA)/OMMT nanocomposites prepared by dynamic melt intercalation [285]

Interphase interaction in the silicate-polymer systems appears in different ways for polar, copolymer of ethylene with vinyl alcohol (poly(E-*co*-VA), EVOH) forming strong hydrogen bonds with the surface of silicate and less polar bonds with lower interaction energy in the copolymer of styrene with acrylonitrile (poly (St-*co*-AN, SAN). Though poly(E-*co*-VA) more efficiently penetrates into a silicate gallery due to its hydrophilic nature, exfoliation is easier in the poly(St-co-AN) based system (with weaker polar interaction). However, mechanical properties of the poly(St-*co*-VA) based systems have higher values, probably, due to stronger interaction between nanoparticles and interphase layer of the polymer matrix (Fig. 5.42).

Intercalated poly(St-co-AN)/OMMT reveals lower ultimate tensile strength than the initial poly(St-*co*-AN); poly(E-*co*-VA)/OMMT shows a significant increase in ultimate strength and modulus of elasticity, probably, due to increase in interphase adhesion.

It should be specially noted that the functioned nanocomposites, for example, hydrogels [286] based on N-isopropylacrylamide, acrylic acid, neutralized by sodium hydroxide and MMT, modified by (3-acrylamidopropyl) trimethylammonium chloride have exfoliation properties both in dry and swelled states, in the latter case the products are potential agents of purposeful delivery of drugs.

5.4.5 Melt Intercalation of PVC

The method of intercalation from melt is widely used for production of PVC-based nanocomposites (see, for example, [287–294]).

In practice, apart from a polymer and a modified silicate also necessary amounts of the ingredients are introduced into the melt, including stabilizers (calcium stearate, tin-organic compounds, for example, di-n-octyl bis(isoctylthioglycolate)

tin), plasticizers (dioctyl phthalate), etc. Two method of production of hybrid nanocomposites are used: intercalation from PVC solution and in situ intercalation polymerization of vinyl chloride. In case of polymerization in interlayer distance neither type of a silicate, nor nature of the used ammonium cation has an effect of morphology of the formed nanocomposite, in contrast to that prepared by melt method. When the values polarity of the silicate and the polymer are almost equal, silicate layers are well dispersed in the matrix. The nanocomposites based on PVC and layered silicate (5 wt% of bentonite) are prepared using extrusion followed by roll milling [295]. KZTPP1 (cyclo[dineopentyl(diallyl)] pyrophosphate dineopentyl (diallyl) zirconate) or Tamol 2001 (un-neutralized acrylic-based acid copolymer) (0.5 wt%) introduced into the composites as inflammatory agents prevent agglomeration of silicates. The PVC-bentonite-KZTPP1 is anisotropic composite, which assumes compelled flow of nanoparticles with orientation in 001 direction, in other words, macromolecules are intercalated in silicate particles. In the PVC-bentonite-Tamol 2001 composite just insignificant isotropy was observed, which pointed to exfoliation of the silicate. The glass transition temperature of PVC and nanocomposites based on it increased in the range of PVC (1) <KZTPP (2) <Tamol 2001(3) (Fig. 5.43). The changes in mechanical modulus and activation energy obeyed the same relations.

These results confirm the fact that even small additives of nanosilicate have a significant effect on microstructure of the extruded composite and on relaxation of polymer chains.

5.4.6 *Nanocomposites PEO-Silicate Obtained by Melt Technique*

One of the most well studied polymers of direct intercalation is integration of PEO in layers of plane silicates, such as mica, by interaction between a melted polymer with Na^+- or NH_4^+-substitutional *host* lattice [78, 296–299].

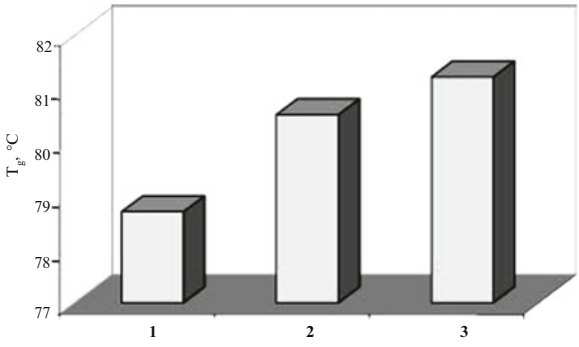

Fig. 5.43 Dependence of glass transition temperatures of PVC composites on their compositions (see the text) [295]

Intercalation of PEO melt into the layered silicates is one-staged process in the case when interlayer distance in them is smaller than 0.8 nm (according to spiral structure of a molecule, diameter of PEO molecule is 0.8 nm in normal to the axis direction) and low concentration of PEO is used. In the PEO/MMT-B34 system interlayer space increases by 0.68 nm, and, most probably, the intercalated molecule has slightly distorted elongated spiral shape.

This doped hybrid nanocomposite has ionic electric conductivity: specific conductivity of PEO/Li^+-MMT (40 wt% PEO) $1.6 \cdot 10^{-6}$ S/m at 30 °C, activation energy 2.8 kcal/mol. Stability of polymer electrolyte depends on ceramic additives, grain sizes, polymer/lithium ratio, conductivity between the silicate and the polymer is synergetic. The general formula of PEO intercalate in the layered silicate magadiite obtained from solution in aprotonic solvent and in the polymer melt at 155 °C corresponds to the composition $H_2Si_{14}O_{29}(–OCH_2CH_2–)_3$ [300]. This agrees with a structure in which one unit cell of magadiite correlates with three oxyethylene links. In other words, interplanar distance is not completely saturated with oxyethylene links.

In the general case intercalation in MMT-B34 is influenced by saturation with the polymer (PEO/MMT-B34 21:79, 10:90), the temperature and annealing time, molecular mass of PEO. Though there are data on polymer extraction from layered nanocomposites, there are no data on degree of extraction and it is unknown whether only a polymer is extracted (there is no confidence about presence of the polymer in the nanocomposite, i.e. it is not clear whether the process is accompanied with destruction). In this connection we shall highlight information [301] on a rapid and quantitative method of PEO extraction from $K_x(C_2H_4O)_4$ $M_{1-x/2}PS_2$ (M = Mn, Cd) composite. The polymer is quantitatively extracted using aqua salt of tetra-ethyl-ammonium under conventional conditions. This process is analyzed in detail, its kinetic effects are found, etc. [302]. Intensity of the peak responsible for PEO intercalation increases with its concentration (Fig. 5.44).

As it was already mentioned during PS intercalation, kinetics of a hybrid formation straightly depends on molecular mass of PEO: lower molecular polymer faster penetrates interlayer space, which is advanced by lower viscosity of the melt and higher diffusion coefficient. This confirms that melt-intercalation is mass transport and depends on mobility and diffusion rate of polymer chains. Theoretical models and developments predict that an increase in length of a polymer chain causes a decrease in compatibility between a layered silicate and a polymer and in a tendency of the system to intercalation. Studies of a structure of intercalated systems based on polymers with various molecular masses prove that intercalation has only kinetic nature and does not affect structure of a finite material.

Intercalation from melt in the PEO-clay system (MMT, hectorite, laponite) is induced not only by ultrasonic, but also by microwave radiation [303]. The intercalation process is influenced by radiation time (optimal 10 min), power (525 W), mass and ratio of regents, their moisture, and salt additions. It is also noted that polymer acts agglomerating agent, and severe control of the process is required, because high temperatures in localized polymer-silicate zone can cause destruction of PEO.

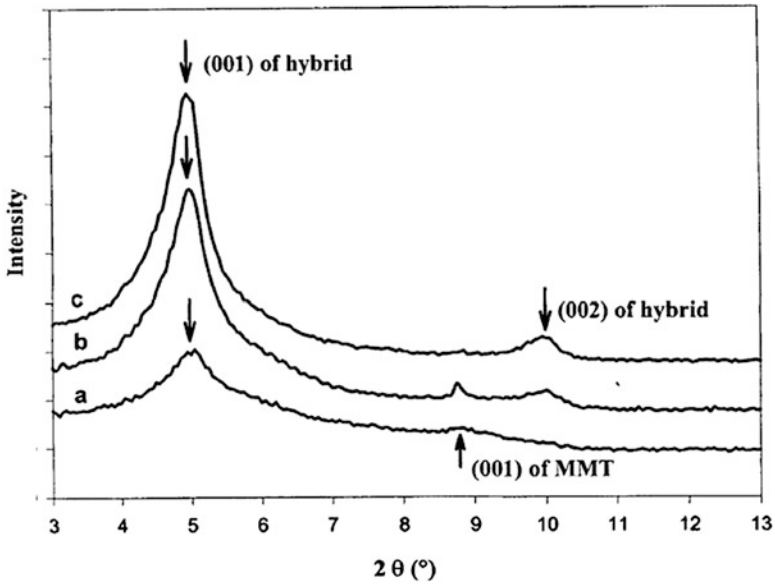

Fig. 5.44 XRD patterns of composites with PEO/MMT = 5:95, 10:90 and 15:85 [302]

We shall consider one more example of intercalated nanocomposites based on PEO or PPO as conducting materials. The obtained by sol-gel technique monoclinic structures (of *m*-WO_3 type) can be chemically composed with polypropylene glycol, end groups of which are modified by triethoxysilane [304] bringing to film formation with sensor properties. Often these systems are used in combination with ceramic fillers: $LiAlO_2$, Al_2O_3, TiO_2 (10 % TiO_2 with average grain size 13 nm or Al_2O_3 with the size 5.8 nm are dispersed in acetonitrile with $LiClO_4$ and PEO is implanted up to molar ratio $LiClO_4$: PEO links 1:8; conductivity of these polymer-inorganic composites is 10^{-4} S · cm^{-1} at 50 and 10^{-5} S · cm^{-1} at 30 °C).

5.4.7 *Intercalated Nanocomposites Formed in Polyamide Melts*

Polyamides and their aramid varieties are nanocomposites of intercalation type which are of great interest due to their special properties, such as various coatings, they are applied as structuring, inflammable and electronic materials [305–307], which caused not only research but also industrial interest [308, 309]. Properties of a traditional system containing poly-ε-caprolactam (PA-6)—MMT are quite completely studied [159, 310–315] and some of them represented in Table 5.5 [316].

Table 5.5 Some properties of PA/MMT compositions

MMT concentration, %	Maximum stress, MPa	Maximum strain, %	Initial modulus, MPa	Impact toughness, MPa	T_g, °C	Equilibrium water absorption, %
0.0	35.6	0.131	578.8	3.76	78.0	9.4[a]
2.0	47.5	0.095	943.4	3.23	83.7	8.6
4.0	50.4	0.085	950.9	2.96	89.1	8.1
6.0	50.5	0.066	1.240.7	2.31	90.3	7.6
8.0	48.8	0.064	1.125.7	2.04	92.1	7.1
10.0	48.3	0.062	1.117.3	2.03	94.9	6.7
12.0	48.1	0.061	1.113.1	1.94	97.4	6.1
14.0	47.7	0.059	1.082.7	1.71	99.2	5.7
16.0	47.5	0.056	995.4	1.63	105.0	2.1
20.0	47.4	0.051	977.6	1.34	100.0	0.0

[a]For 168 h

For such composites the mechanism of formation has been studied in detail as well as the dependencies of their properties and structure on the nature of polymer and silicate components [317–332].

Many properties of polyamides deteriorate because of water absorption (the initial polymer absorbs 9.4 % of water for 168 h): interaction between organic and inorganic phase decreases ability of polar groups to bind water, therefore, water absorption of these composites decreases as silicate concentration increases. Moreover, impenetrable clay layers make a trajectory convoluted for water penetration, as was in the case of gas penetration (see Fig. 5.38).

I.e. increased barrier characteristics, chemical resistance, low permeability of solvents, fire protection – all is a consequence of difficulties and complicated diffusion ways of gases through a layered nanocomposite.

5.4.8 Intercalated Polymer Mixtures

Mixtures of polymers with complementary properties are widely used [151]. Some of them have high compatibility, especially those formed in presence of compatibilizers. Composites based on polymer mixtures of PPO/PA-6 type formed in presence of intercalating agents are of interest [333]. Dispersed silicate plates play important role in control over morphology of the formed PPO/PA compositions, which is confirmed by selective localization of clay in PA phase. An example of LDPE/PA-66 composition reveals role of the silicate as nuclei agent, which causes a decrease in crystallite sizes [334], as a result compatibility between components is improved and morphology of the composite changes. It should be noted for comparison the tin composite of polybutylene terephthalate (PBT)/PE/Silicate silicate localizes in the PBT matrix and this has an effect on new morphology of the composite [218].

PBT is a typical engineering plastic with good mechanical properties and used, especially, for fiber formation or cast mould articles formation. Architecture of intercalated PBT/PE nanocomposites is similar to liquid crystal phase structure [218]. Studies of intercalation kinetics of PBT/PE (rheological technique) into organosilicate proves [218] that intercalation does not carry on during preparation of the sample, instead of it multilayered product forms with two PBT molecules and one PE/MMT layer, which alternately impose on each other and are compressed in a layered sheet. The entire characteristic of relative volume fraction of intercalated tactoid can be obtained from parameters of viscosity and accumulation modulus at lower frequencies, which could be used for definition of apparent diffusion coefficient for mass transport in primary particles at different temperatures. The data on calculated activation energy show that formation of PBT/clay composite depends on molecular mass, which can be conditioned by an increase in interaction of polar groups in PBT chains and on the surface of a silicate.

The coefficients of effective (s^{-1}) and observed ($cm^2 \cdot s^{-1}$) diffusion at temperatures 230, 240 and 250 °C are: [218] 0.0007 and $0.7 \cdot 10^{-13}$; 0.0013 and $1.3 \cdot 10^{-12}$; 0.0017 and $1.7 \cdot 10^{-12}$.

5.4.9 Intercalated Network Composites

Multicomponent nanocomposites in layered gallery are actually composed of ingredients. In the melt triple copolymer of ethylene-propylene-diene is vulcanized in layered silicates, and CEPD/silicate nanohybrid forms using organophilic clays (MMT, modified by hexadecyl trimethyl amine, octadecyl trimethyl amine or distearyl dimethyl amine) and accelerators of vulcanization [335] (Fig. 5.45). There is several times increase in strength properties of these hybrid materials [336].

After extrusion CEPD/MMT composite is subjected to roll milling in presence of vulcanizing components, and are then vulcanized [181].

Intercalated nanocomposites based on nitrile rubbers is relatively new area in chemistry of polymer materials. It includes a range of various approaches, such as coagulation of rubber latex with water dispersion of silicate, mixing of rubber solution with dispersed clay [205, 337–339] intercalation from melt [340–343].

Properties of the nanocomposites based on nitrile rubber (content of acrylonitrile is 45 %) and two types of modifiers Cloisite 15A (cation exchange-capacity is 1.25 mg-eq/g) and Cloisite 30B (cation-exchange capacity 0.9 mg-eq/g) dispersed by various procedures (melt mixture at 130 °C or in chloroform solution or in THF). The nanocomposite is solidified by the system dicumile peroxide in presence of phenylene bismaleimide as co-agent of solidification (Table 5.6).

The solution intercalation process is more effective than the melt process. In all cases elastic properties, such as ultimate tensile strength, modulus of elasticity improve, which points to good reinforcing properties of silicates. The best quality is reached for "solution" material (especially for OS30B), which is explained by high

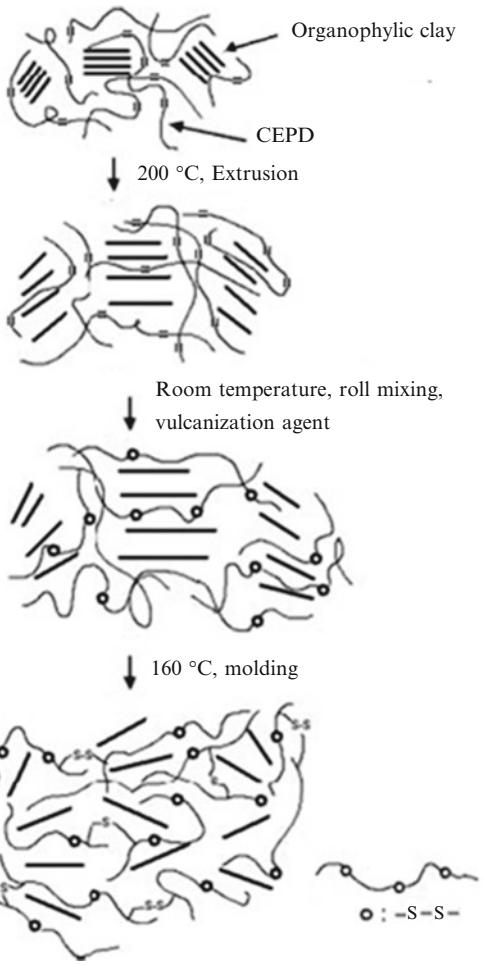

Fig. 5.45 A scheme of the vulcanization of CEPD and intercalation into clay gallery [336]

dispersion ability of the silicate as one of the most important characteristic for improvement of mechanical properties. These results confirm improvement of physical mechanical properties, including deformation, in the systems with high capacity of exfoliation/intercalation, which are reached during preliminary dispersion of the silicate in polymer solution.

At the same time, silicone rubbers (mixture of hydrated and containing end ethylene groups of siloxanes) in OMMT galleries modified with di(2-oxyethyl)-12-alkan-3-methyl-aminchloride are vulcanized at room temperature [344] with formation of intercalated or exfoliated structures (Fig. 5.46). This functioned silicon rubber has interesting physical chemical properties [345–350].

Nanocomposites based on unsaturated polyethers (glyptal resin), including the resin with styrene (up to 35 %) and modified in different ways silicates, solidified with cobalt octoate and peroxide are obtained by various methods: statistical,

Table 5.6 Some characteristics of intercalation systems and physical mechanical properties of intercalated CEPD

Organosilicate MMT-modifier	Intercalation procedure	Percentage of the modifier, %	d_{001}, nm	Total surface	Fraction of intercalated MMT, %	Ultimate tensile strength, MPa	Relative elongation in tension, %	Modulus at 10 % elongation, MPa
OS15A	From melt	2.5	4.2	1,676	43	4.1	730	2.8
OS15A	From melt	5.0	4.0	4,364	56	4.4	720	3.1
OS30B	From melt	2.5	>1.9	2,257	47	3.6	640	2.7
OS30B	From melt	5.0	>1.9	3,602	55	4.5	670	3.2
OS15A	From solution	2.5	4.0	1,450	15	4.3	750	3.0
OS15A	From solution	5.0	4.0	3,997	54	7.9	630	4.9
OS30B	From solution	2.5	>1.9	1.508	82	6.3	660	3.5
OS30B	From solution	5.0	>1.9	1,498	81	9.6	270	6.8
MMT-OS15A	–	100	3.0	2,526	–	–	–	–
MMT-OS30B	–	100	1.9	1,435	–	–	–	–
Initial CEPD	–	0	–	–	–	2.5	450	2.7

By the data [181]

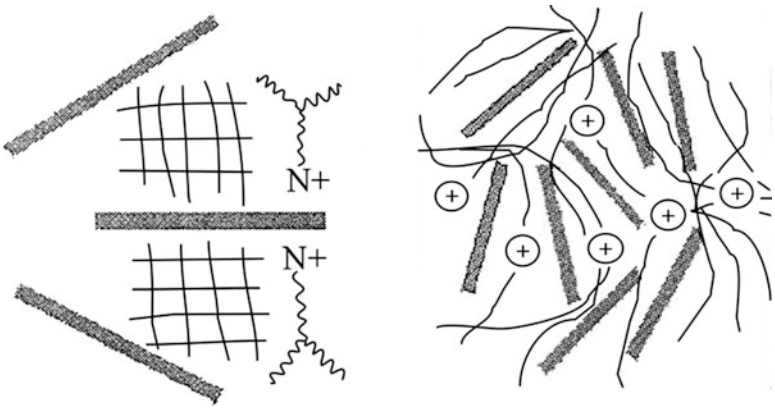

Fig. 5.46 Vulcanized silicone rubber in the gallery of the OMMT [344]

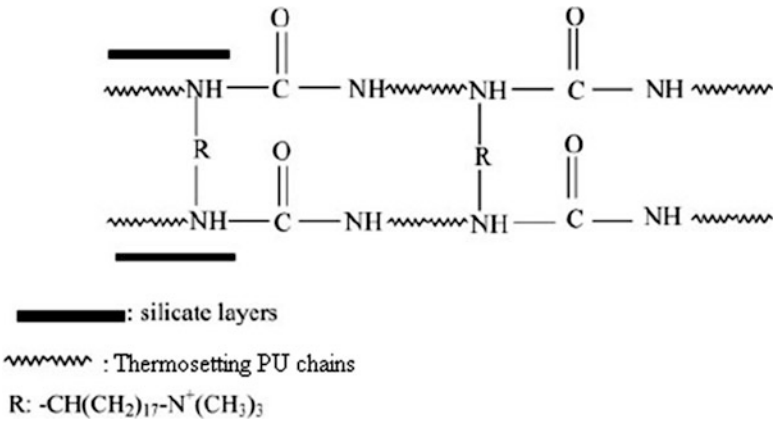

Fig. 5.47 A possible mechanism of the formation of layered PU/silicate composite [355]

mixing, and mixing with ultrasonic irradiation. Rheological properties of the composites correlate with temperature and time of mixing, intercalation space, delamination, and fineness of nanoparticles of exfoliated organic silicates [240, 306, 351–355].

Polyurethane (PU) composite is a polar polymer compatible with OMMT (modified with N-diamine octadecyl trimethyl ammonium chloride) is obtained in presence of 1, 2, 3, and 4.5 wt% OMMT and its treatment with PEG (MM 2000) at 80 °C and toluene diisocyanite, added by 3, 3′-dichloro-4,4′- 4 4′-diphenylmethane diamine (150 °C, 3 h). During mixing –NCO groups react not only with –OH, but also with $–NH_2$ groups of silicate modifying agent (Fig. 5.47). This effect is exothermal, it decreases Coulomb electrostatic attraction between the silicate and

Table 5.7 Elastic properties and temperature of thermal decomposition of SPU and SPU/OMMT composites [356]

Sample, silicate concentration, %	Ultimate tension strength, MPa	Relative elongation at fracture, %	T_{dec} (intense)	Carbon residue, %
SPU	6.85	500	299	3.5
SPU/OMMT-1	10.33	530	312	5.0
SPU/OMMT-2	15.68	570		
SPU/OMMT-3	20.19	590		
SPU/OMMT-4	24.79	630	320	6.7
SPU/OMMT-5	10.95	540	307	8.9

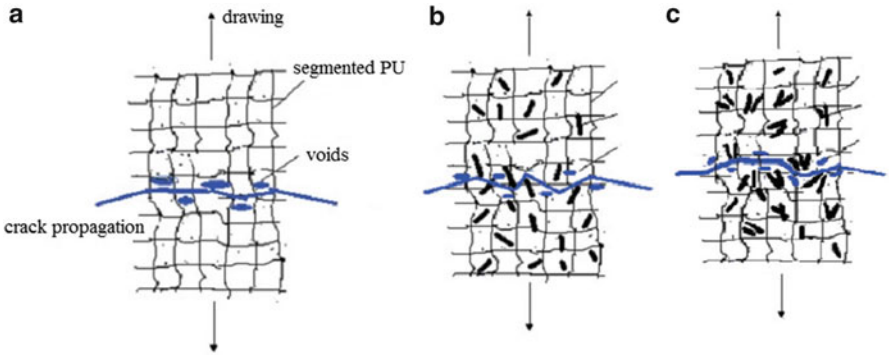

Fig. 5.48 Scheme of failure development during tensile drawing (**a**) thermosetting polyurethane TSPU; (**b**) TSPU/OMMT-4; (**c**) TSPU/OMMT-5 [355]

polymer chains, changing total enthalpy. This intercalate can be expressed as follows:

New nanocomposites have been synthesized, in particular, segmented SPU PU/clay based on PCL, methylene-diphenyl diisocyanite, butanediol and PCL-silicate-prepolymer [356]. This composite showed high elastic and thermostable properties as compared with pure PU matrix up to silicate/PCL concentration 4.2 wt %, however, when it was exceeded, properties of the composite deteriorated abruptly (Table 5.7), which confirmed transformation of PU/silicate from elastomer to thermoplastic material with increase in PCL/silicate portion.

Morphology of SPU/OMMT-4 nanocomposite displays presence of superfine mixture of intercalated and exfoliated silicate layers in the matrix. It is supposed to be the reason for the nanoenhancement effect in combination with a number and size of pores and increase in propagation paths of cracks (Fig. 5.48).

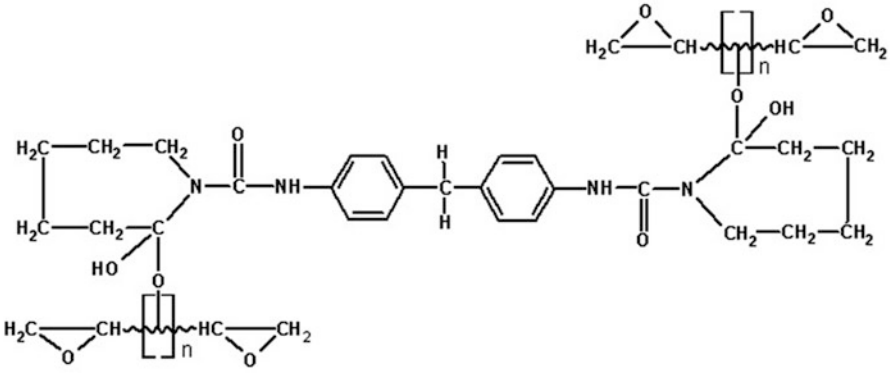

Fig. 5.49 A scheme of caprolactam-blocked methylenediphenyl diisocyanate-epoxy matrix [362]

The proposed mechanism of enhancement of mechanical properties on the example of SPU/OMMT-4 nanocomposites is associated with high dispersion ability of OMMT and an increase in crack widening in the nanocomposite. As OMMT portion increases, the character of crack development in material changes.

Far less comprehensively hybrid epoxy-silicate nanomaterials are studied [240, 357–359]. Interpenetrating networks based on enforced epoxy matrix with different content (5, 10, and 15 %) of caprolactam-blocked methylene diisocyanite (CDMI) are modified with 1, 3, 5 wt% of organophilic MMT (Fig. 5.49).

A decrease in T_g of epoxy systems filled with organic clay is registered as compared with initial epoxy resin, as well as a tendency to its thermal stability. Similarly, introduction of organic clay and CMDI into epoxy improves strength, elasticity and impact strength according to percentage of these additives [360–363].

Nanocomposites based on epoxy resins and layered silicates (ELS) are synthesized using pre-intercalated novolak resin layered silicate (NLS) nanocomposites. For this different approaches were used: melt, melt-US, solution (water, alcohol, toluene, o- xylene acetone, etc.) and solution-US methods of intercalation, various types of novolac epoxies, including benzene novolac, bis-phenol-A novolac, acryl phenol novolac, o-cresol-novolac, etc., and MMT modified with benzene octadecyl ammonium bis(2-hydroxyethyl)ethyl)methyl tallow ammonium (Cloisite 10A with exchanging capacity 1.25 mg-eq/g and Cloisite 30B – 0. 90 mg-eq/g).

NLS and ELS displayed stable structures at highly intense US irradiation, they intercalated and exfoliated. The material based on NLS and ELS showed far higher thermal and mechanical properties, for which chemical affinity between phenol epoxies and OMMT was very important.

To obtain exfoliated polymers of novolak epoxies hydroxyl modified MMT is more efficient than benzene-modified high efficiency in US dispersion and intercalation is observed in both melt and solution variants. Pre-intercalated NLS structures are very stable and do not fracture during solidification of epoxy resins, however, they have a trend to exfoliation during self-propagated intercalation and ELS solidification. Dramatic increase in mechanical properties, such as their

mechanic rigidity, thermal properties, including T_g decomposition temperature, which is assigned to different morphologies of intercalation and exfoliation, and with special features of solidification reaction between epoxy and phenol resins conducted in presence of layered silicates. Most probably, to obtain optimal composites from thermally reactive resins, especially in the case of self-propagating intercalation in the solidified systems, a balance is needed between the intercalation and solidification rates. However, many problems of intercalation chemistry of thermosetting plastic are not solved yet.

5.5 Supramolecular Assembling in Nanolayered Materials

Substantial development have hybrid self-assembling nanocomposites formed as multilayers with the general formula $(P/M)_n$, where M и P are nanometer oppositely charged of inorganic component and polymer (referred by [71]). Versatile approaches are made to assembling of layered systems, for example, polyelectrolytes and clays, flaked zirconium phosphates, colloid metal particles. Positively charged poly (diallyldimethylammonium chloride) (PDMAC) and glass, quarts, silver, gold, and even teflon nanoplates were used to consider in detail mechanism of formation of these materials. Subsequent immersion of these plates in P solution or M suspension cause increase in a number n of the layers, and each action is accompanied by increase in thickness by 1.6 nm in the case of P and by 2.5 nm in the case of M.

Similarly self-organized layers form from TiO_2 cation nanoparticles (~3 nm) obtained by acid hydrolysis of $TiCl_4$. They are organized in layered structures on the surface of superthin (~1 nm) films of cation polymers of poly(sodium 4-styrenesulfonite) (PSS) or already mentioned PDMAC. Optically transparent organized molecularly ordered films of up to 120 layers thick (60 bi-layers, each thickness is evaluated 3.6 nm) are gathered on the surface of substrate (metal, silicon, polymer) ((Fig. 5.50). This strategy makes it possible to obtain various

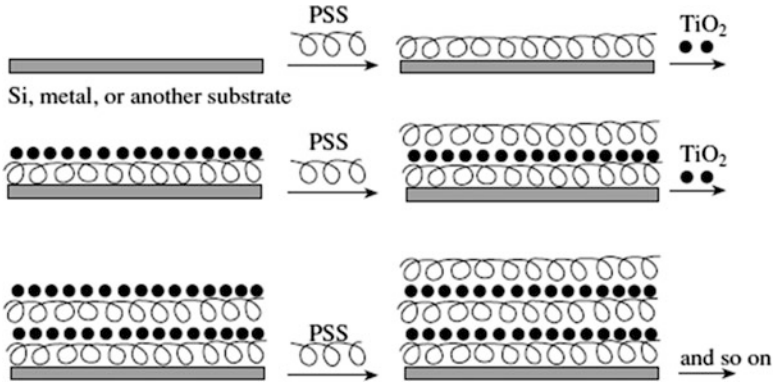

Fig. 5.50 Schematic representation of the fabrication of ultrathin TiO_2–polymer films [34]

combinations of semiconductor materials metal-insulator with nanometer sites *p-n, p-n-p, n-p-n* and others. Formation of multilayers includes the following stages. First, *P*-layer is absorbed at the surface of substrate via electrostatic and Van der Waals interactions. In this case structural hierarchy of *M* gives infinite possibilities of its usage as was used for a template for more versatility of molecules and clusters. They may be inserted between swelled layers and in *M* plates and on their surface, in planes of individual or coagulated @M. Secondly, @M-layer is strongly and irreversibly, which is confirmed by physical-chemical studies, adsorbed on the oppositely charged polymer electrolyte, displaying very dense plane orientation. Irregular *M*-layers cannot provide complete coating of intercalated *P*-layers, thus forming overlapped packs. Interphase roughness exceeds thickness of the *P*/*M* layer, they do not depend on nature of a substrate, control over this can be performed by applying external voltage during the self-assembling.

Polymers with inert surface (polyolefins, fluoropolymers, polyethers) "activate" PVC by spontaneous absorption and sewing with glutaric aldehyde [364]. Nanometer SiO_2 and TiO_2 layers are obtained by reaction of –OH groups (alcohol, silanol, or titanol) with $SiCl_4$ or $TiCl_4$ followed by hydrolysis (these cycles are repeated if necessary) by the scheme described below. In principle, this approach is similar to widely known and often used in practice "functional group lamination method" on inorganic surfaces.

We shall show some more typical samples. Particles TiO_2 form on the surface of photochemical electrode (from $TiCl_3$ solution at pH 2.5), size ~20 nm. Simultaneously, electrodeposition of PPy is registered, which is formed due to electrochemical polymerization of pyrrole (referred to by [71]). This is preceded by absorption in pores of an electrode coated by photosensitive ruthenium complex. These structurally controlled "templates" are analogue of self-assembling supramolecular aggregates. The supramolecular systems of molecular recognition, structured this way, including chromophores, semiconductors, cluster aggregates, and fulfilling specific optical and electronic functions, is a contemporary approach to modeling of ferments. If Al_2O_3-membranes are used as templates, matrix compounds, Au/PPy colloids with 1D morphology are synthesized. Fiber ZnO structures were obtained on the basis of zinc acetate and WO_3, electrode materials on V_2O_5 basis, MnO_2, Co_3O_4 oxide composites, and others. Fibrillate and tubular materials had a diameter corresponding with diameter of pores in Al_2O_3, however, their length was far more. In the case of TiO_2 metastable single crystals of anatase were observed. Tubular nanocomposites obtained via template sol gel synthesis in fibers or nanotubes, and in micro and nanoporous membranes are perfect photocatalysts [195].

At last, it should be noted that layered nanostructures are obtained using liquid-crystal polymers with ionic groups, and MMT or hydrotalcite are used as inorganic components. According to different estimations, average thickness of this pair *M*/*P* is 4.9 nm. It is assumed that such electrostatic assembly provides a close contact between components and strict molecular ordering, it can lead to formation of new types of liquid crystal structures with unusual properties.

A special place in the intercalation problem has layered interstitial compounds implanted in graphite (LGC) and graphite-like structures. Even though it seems that these problems are similar at first glance, graphite can be considered as a macromolecule of aromatic type with a number of aromatic rings about 1,000, period of identity (an interspace between neighbor planes) is 0.335 nm. Absence of chemical bonds between parallel carbon layers in graphite (energy of interlayer interaction is just 16.8 J/mol) makes possible insertion of monomolecular layers of various substances, including monomers, metal ions with formation of layered (laminated) graphite compounds. General methods of LGC production are confined to interaction between graphite and monomer vapors or solutions, metals in strongly ionizing solutions, volatile chlorides or cation metal complexes, accompanied by their implantation in interlayer distance of graphite lattice. Depending on a number of carbon layers, separating two neighbor layers of implanted matter, these compounds are classified as the products of the 1st, 2nd, etc. stages of implantation.

Nanocomposites PS/graphite are prepared as follows [365]. Graphite surface is modified by silane containing agent and subjected to ultrasonic treatment (for 0.5–1 h at 50 °C). Then PS/graphite nanocomposite is prepared by rolling, intercalation from THF solution, grinding of PS and graphite grains in a mill. The composite has high thermal conductivity at graphite concentration 34 vol.% (1.95 W/mK) (Fig. 5.51). In this case different methods of preparation of PS/graphite composites cause exfoliation, which increases in the range: intercalation via rolling < solution intercalation < combined grinding of PS and graphite grains. In the last case the structural chains of graphite are agglomerated, and the composite has high thermal conductivity and mechanical properties.

The origin of a bond between LGC and implanted metal depends on the latter. Thus, for Fe, Co, Ni, Mn, Cu the bond is provided by Van der Waals interactions, sometimes π-electron density is transported from graphite to the implanted metal layer. In this case carbon network of graphite is a kind of polymer ligand. For alkali metals this bond is formed due to transporting of electron from metal atoms to conducting zone of the neighboring graphite, i.e. due to electrostatic interaction of

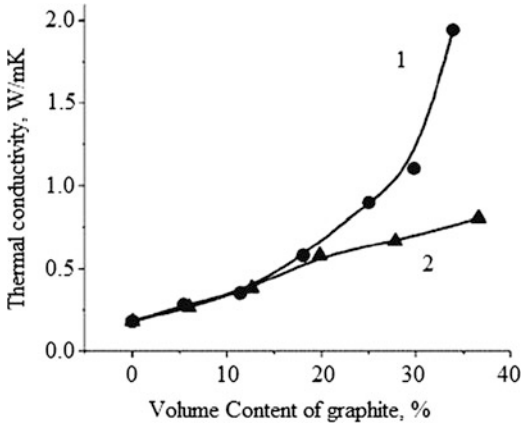

Fig. 5.51 Effect of the content of colloidal (*1*) and nano- (*2*) graphite on the thermal conductive properties of PS/graphite composites [365]

positive ions with free electrons of the conductive zone of graphite. The processes of reduction of interstitial metal ions can be accompanied by partial yield of them from layered packs and reduction on the exterior surface of graphite with formation of nanoparticles, for example, Ti included in its defective lattice. Under conditions of high pressure in combination with shear deformation many different atoms can be implanted in graphite. Due to interplanar distances being extremely constricted, as compared to silicates, there are very scarce data on intercalation of monomers and polymer links and exfoliated composites in graphite. Conducting properties of the PE-graphite nanoplates composite produced by in situ polymerization can be highlighted [366]. Nanographite plates are uniformly coated with the forming PE layer, the product is characterized by low (2.7 vol.%) percolation threshold and high dielectric permeability.

A special interest is drawn to graphemes, single layered carbon atoms [367] which attract increasing interest due to special conductive and transport properties and mass-less Fermi-Dirac interaction between graphene layers. Wide choice of intercalates with different physical properties allows achievement of high electric, thermal, and magnetic characteristics [368, 369]. Intercalation in few layer graphenes (FLG) is efficient method of their properties modification, for example, I_2, Br_2 intercalate in FLG [370, 371].

Intercalation distance increases dramatically in presence of intercalating agent, which abruptly changes properties of FLG. Thus, $FeCl_3$-FLG complex (Fig. 5.52) with homogeneous distribution of the intercalated agent is stable in environment [372]. Intercalation is easier than in blocked graphite (in chlorine atmosphere), $FeCl_3$ as a doping is completely intercalated in FLG. Fourier spectroscopy has shown that there is no electron interaction between adjusted graphene layers. These results confirm that FLG is a promising material not only modifying electron structure of graphene, but also changing electric, thermal, and magnetic properties during usage of different intercalating agents [368], for example, Ca-FLG is expected to display superconducting properties [373]. Most probably, this line of studies is expected to develop intensely.

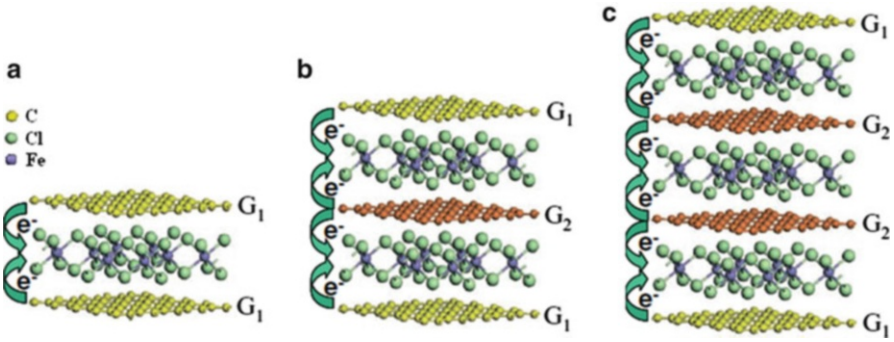

Fig. 5.52 Schematic crystal structures of FLG with two (**a**), three (**b**) and four (**c**) layers of grapheme. The model is constructed based on $FeCl_3 \cdot GIC$. The graphene layers flanked on one/both side(s) by $FeCl_3$ layer(s) [372]

5.6 Structure of Inclusion Nanocomposites Metal Chalcogenide-Polymer

Synthesis and characteristics of hybrid nanocomposites with periodic nanostructure of a superconductor arises a special interest due to their unusual optical, electrical, and other properties. Owing to this, they have great application prospects in microelectronics. Composites of this type are obtained, as a rule, by "aqueous" chemical methods, including sol gel method, in which CdS crystals are trapped in SiO_2 films with formation of Cd-S- SiO_2 systems, $Co_6S_8(PPh_3)_x$ intercalate in MoS_2, also CdS-Ag are described hybrids of self-assembling particles, semiconductors on Cd_3P_2 basis, etc.

A special feature of layered materials, dichalcogenides of metals, such as MoS_2 or TaS_2 with low density of a layer charge is ability to decompose into nanometer structural blocks under specific conditions and to form colloid solutions. If anion is easily polarized, and cation has strong polarizing properties, then MX_2 compound has a layered structure. This structure have molybdenum dichalcogenides, in which a layer of molybdenum is between two layers of chalcogen (X), as a result, triple-layered packages form. Bonds in them are far stronger than between two triple-layered packages, between them are Van der Waals cohesion forces. Monolayers of molybdenum disulfate display distorted octahedral configuration with (2×1) superlattice and coordination with unsaturated Mo-centers in prismatic sites of MoS_2. It is interesting that NbS_2 и TaS_2, and MoS_2 and WS_2, obtained in hydrogen flow during heating of MS_3, have multifaceted fullerene-like structure of nanotubes. For example, NbS_2 are individual nanotubes with hollow core of 4–15 nm in diameter [374]. Probably, the same structure have TiS_2, ZrS_2 и HfS_2 obtained in the same way. Exfoliation procedure in this case is well developed.

Interlayer distance of MoS_2 is small, $d_{001} = 0.615$ nm, the treatment in *n*-butyllithium in hexane leads to formation of $Li_{1.15}MoS_{2.216}$ complex, which is dispersed in aqua solution of PEO with exfoliation [375]. The purified dry product contains from 21 to 31 wt% PEG, $d_{001} = 1.45$ nm, which corresponds to double layer of polymer in the gallery. Thermal stability of the polymer increases as temperature increases to 255 °C, PEO intercalation increases conductivity of MoS_2 by 4–5 orders of magnitude [376]. However, this system is unstable: already at 90 °C MoS_2 catalyses decomposition of PEO, depending on its molecular mass and content of a composite causing a loss in conductivity of the system. A replacement of PEO by PAN causes formation of more stable $[Li_{0.6}MoS_2(PAN)_{1.2} \cdot 0.5H_2O]$ system [377] having mixed electronic conductivity [378, 379].

One of the best superconductors among layered chalcogenides is $NbSe_2$, its superconduction transition temperature is $T_c = 7.2$ K. The general scheme of PVP, PEO, and PPO from aqua solutions in monolayers of suspended $NbSe_2$ can be expressed [380] as:

$$NbSe_2 + xLiBH_4 \rightarrow Li_xNbSe_2 + xBH_3 + x/2H_2 \qquad (5.9)$$

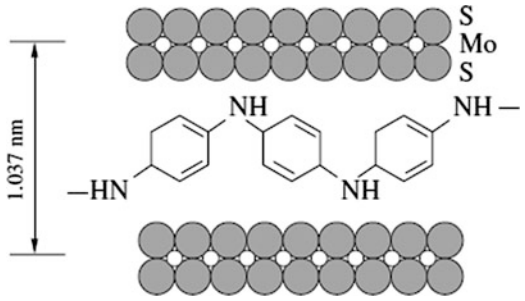

Fig. 5.53 Structure of a PAn–MoS_2 nanocomposite

$$Li_xNbSe_2 + xH_2O \rightarrow NbSe_2(\text{monolayer}) + x/2H_2 + LiOH \quad (5.10)$$

$$NbSe_2(\text{monolayer}) + \text{polymer} \rightarrow NbSe_2/\text{polymer} \quad (5.11)$$

Principal scheme for these nanocomposites is shown in Fig. 5.53.

Polymers are implanted in WS_2 phase by the same mechanism. The promising application of these nanocomposites may be plastic superconducting electromagnetic materials. In Sect. 5.4 direct intercalation of polyaniline in interlayer space of MoS_2 ($d = 1{,}037$ nm) through colloid suspensions was already mentioned. It is important that PPy/MoS_2 is a product of in situ oxidation polymerization, which under kinetically limited conditions is *p*-type conductor; its electronic conductivity is by three orders of magnitude higher than that of the initial MoS_2. Similarly PEO is intercalated in delaminated TiS_2, Ta_{S2} и MoS_2 suspensions.

Interesting results are obtained during studies of intercalated polymer electrolytes alkali metal-PEO in layered $MnPS_3$ and $CdPS_3$ synthesized by two-staged a solvent ion-exchanging mechanism [72]:

$$CdPS_3 + 2xA^+_{aq} \rightarrow Cd_{1-x}PS_3A_{2x}(H_2O)_y + xCd^{2+}_{aq}(A = Li, K, Na, Cs) \quad (5.12)$$

$$Cd_{1-x}PS_3A_{2x}(H_2O)_y + PEO \rightarrow Cd_{1-x}PS_3A_{2x}(PEO) + yH_2O \quad (5.13)$$

Widening of the *host* lattice due to intercalation is $\Delta = 0.8$ nm, some of PEO links have trans-*gauche* and *gauche*-slanted configurations, spiral conformation in intercalated PEO disappears. The experiment proves planar zig-zag structure of intercalated PEO, its likewise conformation in complex with $HgCl_2$. Under equal conditions oligo oxyethylene ethers intercalate in CdS, CdSe and ZnS by direct template mechanism, whereas it is not true for the case of Ag_2S, CuS and PbS [381] and from aqua solution of linear PEI with layered $MoSe_2$, TiS_2, MPS_3 (M = Mn, Cd) the respective nanocomposites are synthesized, from the same polymer or from poly(styrene-4-sulfonate) in TiO_2/PbS layers hybrid materials with semiconductor properties are obtained.

A keen interest is in the inverse problem, implantation of metal chalcogenides in polymers, especially, 1D, self-organized semiconductor nanoparticles. The abovementioned hydrothermal polymerization and spontaneous sulfidizing [382] bring to formation of 1D nanocomposites with finely dispersed self-collecting CdS

nanoparticles in polymer nanorods. These products are applied for plated semiconductor materials with superconducting properties and forms of superconductors such as wires, films with special properties, etc.

Nanocomposites of the considered type is a new class of hybrid organic-inorganic photoactive materials. The example of CdS/polyvinylcarbazole (PVC) is used to show photorefracting ability of nanocomposites in the visible spectrum. The composites including PbS or HgS nanocrystals (~50 nm) are photosensible at the wavelength 1.31 μm [383] nanocomposites PbS/polymer have high display properties. Different types of nanostructured systems based on PbS are studied including self-collecting layered lead sulfide ensembles in MMT and PbS nanocrystals dispersed in various polymer matrices. In ethanol (homogenous system) PbS nanoparticles are uniformly distributed in PVA matrix. In heterogeneous (aqua) mixture nanocomposites are structured as a nanocable with PbS core 30 nm in diameter and PVA shell with length from 80 nm to 10 μm [384].

Semiconductor properties have other layered materials, such as PbI_2, BiI_3, HgI_2, Bi_2S_3, Sb_2S_3. Thus, PbI_2 is an interesting material for X-ray digital visualization. Organic solution technique was used to synthesize CdS-wurtzite nanorods and nanowires.

Interesting approach is instabilizing of CdSe/CdS nanocrystals with the core/shell structure in dendrimers of third generation [385]. After removal of inorganic nanocrystal in the center of a dendrimer forms a nanometer cavity with very thin shell. These nanometer capsules are a new class of molecular containers, calibrated mesoporous structures.

Metal chalcogenides with a more complex structure $PbNb_2S_5$ or $SmNb_2S_4$ can also be exfoliated and intercalated. In polar solvents one-dimensional *host* phases with various chalcogenides like MMo_3Se_3 (M = Li, Na) form colloid systems with mono disperse negatively charged condensed cluster chains (Mo_3Se_3), they can also be of interest for intercalation.

A list of these examples and generalization require, of course, a special consideration.

As is seen from the performed analysis, the intercalation physical-chemical methods, chemistry of intercrystalline structures *guest-host* provide almost infinite possibilities for structuring of nanocomposites of hybrid type. Presently many processes accompanying formation of these materials are found, which are associated with formation of these materials, basically their structure and most important properties are studied. It becomes clear that intercalation of monomers and polymers in interlayer space of layered materials is the most important way for creation of hybrid phased nanocomposites, intensely and fruitfully developed line. At the same time, many problems, especially concerning implanting mechanism and *guest-host* interaction interphase processes, control for maximum intercalation, *guest-host* ratio followed by exfoliation – drawing layers apart, are not completely understood. In the intercalated nanocomposite inorganic layer preserves structural characteristics of matrix polysilicate (or other layered material), and organic polymer layer has a stressed structural organization, causing strong interaction with interlamellar surface of the host. Architecture of these formations can be very

versatile, not only layered, but depending on the nature of organic component, which governs formation of hybrid phases of different structures. For example, for zinc oxide and sulfide nanocrystals three molecular blocks form with rod-like, dendritic, and coil-like architecture [386].

This property is widely used in the *host-guest* chemistry and for selective recognition. Probably, in future this line incited by increasing demands in many fields of materials science to hybrid nanocomposites will intensely develop. Probably, new types of these materials with required hierarchic structure of intercalated systems will appear. The composites of this type can be used for formation in them of metal nanoparticles, and electrically active polymers (polyaniline, polypyrrole, etc.) with a silicate – for binding of metal ions (gold, platinum, palladium). As much as polymers, hydrazine reduces those forming immobilized particles, catalysts of different reactions. At last, it should be noted that hybrid composites form at the stage of polymer reprocessing. From numerous examples we shall highlight just production of hybrid composites polyamide – 6 "potassium-titanium wickers" ($K_2Ti_6O_{13}$) in double-screw extruder with the following injection and forming [387]. For commercial applications of most polymers of intercalation type an important role plays their ecology, usage of available materials and reagents, low flammability. The last characteristic is determined by ability of a fracturing composite to form a barrier carbonized layer on the surface during burning [280].

Thus, intercalation polymerization has a great potential for structuring of hybrid polymer-inorganic nanocomposites by different ways [352] which are still far from implementation, and this governs intense development of studies in this direction. For example, the considered methods can be used to obtain composite materials of not only polymer, but also of metal types. Thus, one of the methods [352] is based on application of double-layered aluminum and lithium hydroxide, containing in the interlayer distance Ni, Co and Cu complexes with organic ligand, $[LiAl_2(OH)_6]_2[M(Edta)] \cdot nH_2O$, ethylenediaminetetraacetic acid. During annealing in vacuum at 400–450 °C materials form including resistant to oxidizing nanometer mono- and bimetal particles (3–4 to 40–50 nm in diameter): carbonized matrix reliably protects them from oxidizing not only from air oxygen, but also during holding in nitric acid.

Whilst intercalation of polymers followed by exfoliation is one many types of topochemical reactions, it is not the most widely used (Fig. 5.54). Topochemical intercalation procedures can include other lines of development with structural characteristics including ion exchange, reduction or oxidization (while implanting cations or anions, respectively), substitution reactions in layers, especially, H_2O. Taking into account ability of layered perovskites to exfoliate into individual nanosheets, exfoliation can be considered as the edged case of intercalation. Among other reactions we shall single out reduction intercalation, inoculation (modification type), formation of layered structures between neighboring layers, including columnar interlayer structures (pillars), etc. Thus, formation of structural columns between the neighboring layers, layered-columnar materials (pillaring) having far more developed surface as compared to the initial silicates, are widely currently used for preparing catalyst carriers of different types.

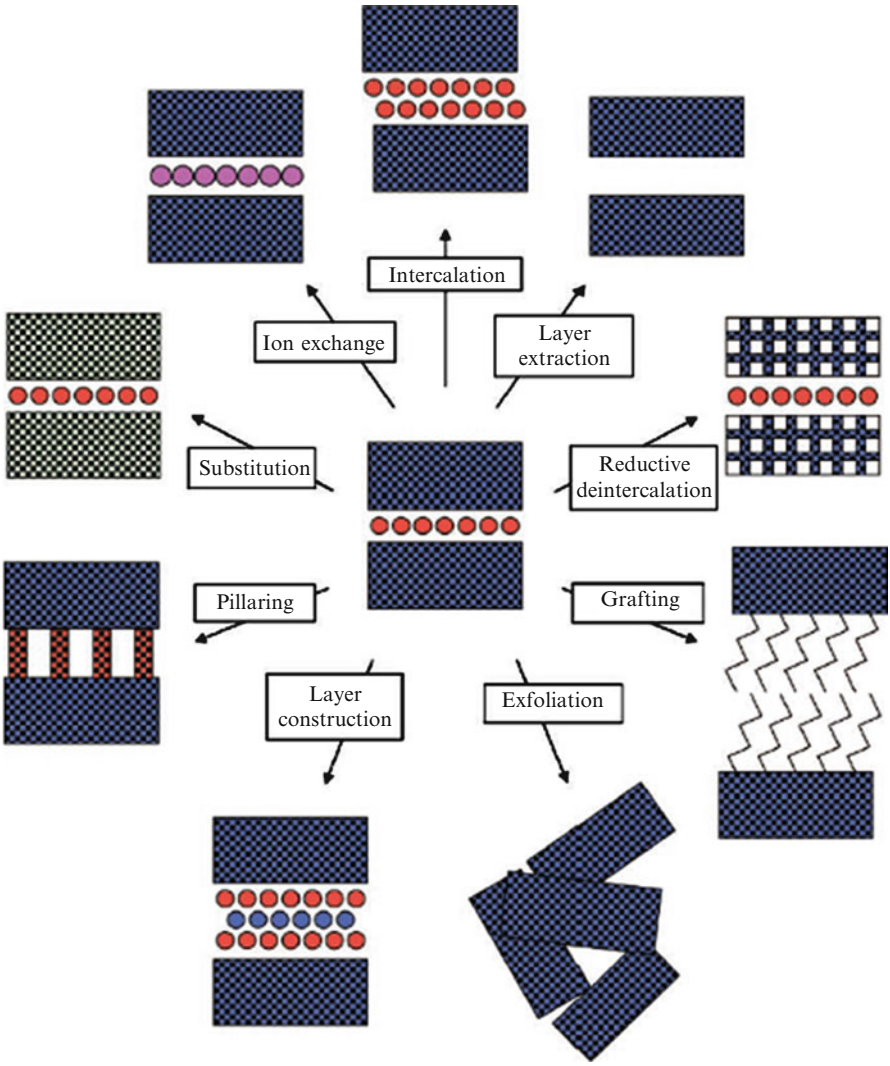

Fig. 5.54 Topochemical reactions in an interlayered space [388]

Topochemical syntheses are performed in a solid phase under relatively soft conditions (temperature below 500 °C), and the products are characterized by high stability. Many aspects of topochemical transformations in layers are very important (they are described in [388]), for example, ion or molecular stability, demands to redox-potential of intercalated compounds, thermal stability of reagents and products, etc. As was repeatedly mentioned, special demands are made to structuring of interlayer frame and its basal space. Topochemical methodology supposes steric control over the structure of intercalated component, which in the end brings to regulation of properties of the produced products. Ability to use this approach

should take into account structural perfection of components and knowledge about mechanisms of the processes, and tools for their realization, physics and chemistry of intercalated systems.

A possibility of purposeful usage of these approaches together with routine design and synthesis of new materials with specific properties can give a wide approach to important materials [389], such as superconductors, ferroelectrics, thermoelectric materials, optical materials, catalysts, ionic conductors, microwaves absorbing materials, components of batteries and solar cells, various types of nanocomposites, including structuring ones. Synthetic approaches used in topochemical procedures, although limited as compared to molecular chemistry, are still efficient. In matrices of layered silicates, in particular in pillared DHL, protected nanoparticles of transition metals (Co, Ni, Cu and others) can be obtained by reduction reactions [390]. Encapsulation does not cause a significant decrease in magnetic properties of cobalt or nickel nanoparticles in these dielectric matrices stabilizing them from oxidation by air oxygen, after storage in nitric acid conservation of the particles was found.

Here a diversity of problems related to usage of porphyrin, natural polymers, etc. as intercalating agents are not considered. The promising for producing of these intercalating agents are also water-resistant microcrystal cellulose and other polymers, which in contrast to synthetic ones are highly porous fiber systems and can be used as a matrix for intercalation of metal nanoparticles, in particular, silver [391] There are no data on intercalation of new class of monomers containing metal, potential candidates for metal composites and catalysts based on them. Finally, methods of intercalation physical chemistry in the recent years are widely used in structuring of pharmaceutical [392], biological [393], including cellular, objects, for example, [394] which rest out of limits of the present study.

References

1. P. Gomez-Romero, Adv. Mater. **13**, 163 (2001)
2. R.S. Sinha, M. Okamoto, Prog. Polym. Sci. **28**, 1539 (2003)
3. S. Yariv, H. Cross (eds.), *Organoclay Complexes and Interactions* (Marcel Dekker, New York, 2002)
4. K.A. Carrado, Appl. Clay Sci. **17**, 1 (2000)
5. E. Ruiz-Hitzky, in *Organic-Inorganic Materials*, ed. by P. Gómez-Romero, C. Sanchez (Wiley-VCH, Weinheim, 2004)
6. E. Ruiz-Hitzky, P. Aranda, J.M. Serratosa, in *Handbook of Layered Materials*, ed. by S. Aucherbach, K.A. Carrado, P. Dutta (Marcel Dekker, New York, 2004)
7. D. Gournis, A. Lappas, M.A. Karakassides, D. Tobbens, A. Moukarika, Phys. Chem. Miner. **35**, 49 (2008)
8. R.K. Bharadwaj, R.A. Vaia, B.L. Farmer, in *PolymerNanocomposites*, ed. by R. Krishnamoorti, R. Vaia. ACS Symposium Series, vol. 804 (American Chemistry Society, Washington, DC, 2002)
9. T.J. Pinnavaia, G.W. Beall (eds.), *Polymer-Clay Nanocomposites* (Wiley, West Sussex, 2000)

10. E. Ruiz-Hitzky, A. Van Meerbeeck, Polymer-clay nanocomposites, in *Handbook of Clay Science*, ed. by F. Bergaya, B.K.G. Theng, G. Lagaly (Elsevier, Amsterdam, 2006)
11. M. Biswas, S.S. Ray, Adv. Mater. Sci. **155**, 167 (2001)
12. M.A. Alexandre, P. Dubois, Mater. Sci. Eng. **28**, 1 (2000)
13. S. Letaïef, E. Ruiz-Hitzky, Chem. Commun. **2996** (2003)
14. S. Yoda, Y. Nagashima, A. Endo, T. Miyata, S. Yanagishita, K. Otake, T. Tsuchiya, Adv. Mater. **17**, 367 (2005)
15. P. Gomez-Romero, C. Sanchez, *Functional Hybrid Materials* (Wiley-VCH, Weinheim, 2004)
16. K. Vermogen, K. Masenelli-Varlot, R. Seguela, J. Duchet-Rumeau, S. Boucard, P. Prele, Macromolecules **38**, 9661 (2005)
17. J. Liu, W.-J. Boo, A. Clearfield, H.-J. Sue, Mater. Manuf. Process **21**, 143 (2006)
18. T.G. Gopalkumar, J.A. Lee, M. Kontopoulou, J.S. Parent, Polymer **43**, 5483 (2002)
19. L. Jiankun, K. Yucai, Q. Zongneng, Y.J. Xiao-Su, Polym. Sci. B. Polym. Phys. **39**, 115 (2000)
20. S. Horsch, G. Serhatkulu, E. Gulari, R.M. Kannan, Polymer **47**, 7485 (2006)
21. A.D. Pomogailo, Russ. Chem. Rev. **69**, 53 (2000)
22. B.K.G. Theng, *Formation and Properties of Clay-Polymer Complexes* (Elsevier, New York, 1979)
23. H.V. Olephen, *An Introduction to Clay Colloidal Chemistry* (Wiley, New York, 1977)
24. A. Okada, Y. Kojima, M. Kawasumi, Y. Fukushima, T. Kurauchi, O. Kamigaito, J. Mater. Chem. **8**, 1179 (1993)
25. Y. Kojima, A. Usuki, M. Kawasumi, A. Okada, T. Kurauchi, O. Kamigaito, K. Kaji, J. Polym. Sci. Polym. Phys. **32**, 625 (1994)
26. Y. Kojima, A. Usuki, M. Kawasumi, A. Okada, T. Kurauchi, O. Kamigaito, K. Kaji, J. Polym. Sci. Polym. Phys. **33**, 1039 (1995)
27. A. Matsumura, Y. Komori, T. Itagaki, Y. Sugahara, K. Kuroda, Bull. Chem. Soc. Jpn. **74**, 1153 (2001)
28. L.A. Goettler, K.Y. Lee, H. Thakkar, Polym. Rev. **47**, 291 (2007)
29. F. Gao, Mater. Today **7**, 50 (2004)
30. S.S. Varghese, J.J. Karger-Kocsis, Appl. Polym. Sci. **91**, 813 (2004)
31. S. Pavlidou, C.D. Papaspyrides, Prog. Polym. Sci. **33**, 1119 (2008)
32. V. Mehrotra, E.P. Giannelis, R.F. Ziolo, P. Rogalskyj, Chem. Mater. **4**, 20 (1992)
33. A.D. Pomogailo, Polym. Sci. Ser. C **48**, 85 (2006)
34. A.D. Pomogailo, Inorg. Mater. **41**, S47 (2005)
35. N.V. Chukanov, I.V. Pekov, R.K. Rastsvetaeva, Usp. Khim. **73**, 227 (2004)
36. K.A. Carrado, S. Petit, F. Bergaya, G. Lagaly, Synthetic clay minerals and purification of natural clays, in *Handbook of Clay Science*, ed. by F. Bergaya, B.K.G. Theng, G. Lagaly (Elsevier, Amsterdam, 2006)
37. H.G. Karge, J. Weitkamp (eds.), *Molecular Sieves – Science and Technology* (Springer, Berlin/Heidelberg/New York, 2002)
38. S. Letaïef, B. Casal, N. Kebir-Ariguib, M. Trabelsi-Ayadi, E. Ruiz-Hitzky, Clay Miner. **37**, 517 (2002)
39. Q. Mao, S. Schleidt, H. Zimmermann, G. Jeschke, Macromol. Chem. Phys. **208**, 2145 (2007)
40. L.A. Utracki, *Clay-Containing Polymeric Nanocomposites*, vol. 1 & 2 (RAPRA, Shawbury, 2004)
41. F. Leroux, J.P. Besse, Chem. Mater. **13**, 3507 (2001)
42. Z. Shen, G.P. Simon, Y.-B. Cheng, J. Appl. Polym. Sci. **92**, 2101 (2004)
43. P. Reichert, H. Nitz, S. Klinke, R. Brandsch, R. Thomann, R. M lhaupt, Macromol. Mater. Eng. **275**, 8 (2000)
44. M. Huskic, M. Zigon, J. Appl. Polym. Sci. **113**, 1182 (2009)
45. V.A. Gerasin, PhD thesis, Institute of Oil Chemistry. Synthesis RAS, Moscow, 2005
46. R. Magaraphan, W. Thaijaroen, R. Lim-Ochakun, Rubber. Chem. Technol. **76**, 406 (2003)

47. J.M. Yeh, S.J. Liou, C.Y. Lin, C.Y. Cheng, Y.W. Chang, K.R. Lee, Chem. Mater. **14**, 154 (2002)
48. W. Xie, R. Xie, W. Pan, D. Hunter, B. Keone, L. Tan, R. Vaia, Chem. Mater. **14**, 4837 (2002)
49. E.M. Moujahid, J.P. Besse, F. Leroux, J. Mater. Chem. **12**, 3324 (2002)
50. J.H. Shi, X. Shu, M. Li, A.I.Ch.E. J **56**, 1352 (2010)
51. L.A. Utracki, M. Sepehr, E. Boccaleri, Polym. Adv. Technol. **18**, 1 (2007)
52. X. Duan, D.G. Evans (eds.), *Layered Double Hydroxides* (Springer, Berlin, 2006)
53. J.M. Miehe-Brendle, L. Delmotte, R. Le Dred, Micropor. Mesopor. Mater. **66**, 155 (2003)
54. G. Alberti, M. Casciola, U. Costantino, R. Vivani, Adv. Mater. **84**, 291 (2004)
55. M. Reinholdt, J. Miehe-Brendle, L. Delmotte, R. Le Dred, Clay Miner. **40**, 177 (2005)
56. J.M. Miehe-Brendle, C.R. Chimie **8**(2), 229 (2005)
57. J.M. Miehe-Brendle, L. Delmotte, R. Le Dred, Solid State Sci. **7**, 610 (2005)
58. A.I. Khan, D. O'Hare, J. Mater. Chem. **12**, 3191 (2002)
59. F. Leroux, C. Taviot-Gueho, J. Mater. Chem. **15**, 3628 (2005)
60. D.G. Evans, X. Duan, Chem. Commun. **485** (2006)
61. P. Ding, W. Chen, Q.U. Baojun, Prog. Nat. Sci. **16**, 573 (2006)
62. C. Pcholski, A. Kornowski, H. Weller, Angew. Chem. Int. Ed. **41**, 1188 (2002)
63. G.R. Patzke, F. Krumeich, R. Nesper, Angew. Chem. Int. Ed. **41**, 2446 (2002)
64. X.W. Lou, H.C. Zeng, J. Am. Chem. Soc. **125**, 2697 (2003)
65. K. Ebitani, T. Kawabata, K. Nagashima, T. Mizugaki, K. Kaneda, Green. Chem. **2**, 157 (2000)
66. K.V. Bineesh, D.R. Cho, S.Y. Kim, B.R. Jermy, D.W. Park, Catal. Commun. **9**, 2040 (2008)
67. G.K. Zhang, X.M. Ding, F.S. He, X.Y. Yu, J. Zhou, Y.J. Hu, J.W. Xie, Langmuir **24**, 1026 (2008)
68. P. Yuan, X. Yin, H. He, D. Yang, L. Wang, J. Zhu, Micropor. Mesopor. Mater. **93**, 240 (2006)
69. A.L. Villa, D.E. DeVos, F. Verpoort, B.F. Sels, P.A. Jacobs, J. Catal. **198**, 223 (2001)
70. K. Motokura, N. Fujita, K. Mori, T. Mizugaki, K. Ebitani, K. Kaneda, J. Am. Chem. Soc. **127**, 9674 (2005)
71. A.D. Pomogailo, A.S. Rozenberg, I.E. Uflyand, *Metal Nanoparticles in Polymers* (Khimiya, Moscow, 2000)
72. G.S. Zakharova, V.L. Volkov, Usp. Khim. **72**, 346 (2003)
73. C. Verissimo, O.L. Alves, J. Mater. Chem. **13**, 378 (2003)
74. A.D. Pomogailo, Colloid J. **67**, 658 (2005)
75. C. Ooka, H. Yoshida, K. Suzuki, T. Hattori, Chem. Lett. **32**, 896 (2003)
76. K. Mogyorosi, I. Dekany, J.H. Fendler, Langmuir **19**, 2939 (2003)
77. J. Njuguna, K. Pielichowski, S. Desai, Polym. Adv. Technol. **19**, 947 (2008)
78. M. Pluta, M.A. Paul, M. Alexandre, P. Dubois, J. Polym. Sci. B. Polym. Phys. **44**, 299 (2006)
79. H.Y. Zhu, Z. Ding, C.Q. Lu, G.Q. Lu, Appl. Clay Sci. **20**, 165 (2002)
80. F. Krumeich, H.-J. Muhr, M. Niederberger, F. Bieri, R. Nesper, Z. Anorg, Allg. Chem. **326**, 2208 (2000)
81. M.A. Bizeto, A.L. Shiguihara, V.R.L. Constantino, J. Mater. Chem. **19**, 2512 (2009)
82. M. Osada, T. Sasaki, J. Mater. Chem. **19**, 2503 (2009)
83. A.S. Golub, Y.V. Zubyavichus, Y.L. Slovokhotov, Y.N. Novikov, Uspekhi Khim. **72**, 138 (2003)
84. A.S. Golub, D.P. Rupasov, N.D. Lenenko, Y.N. Novikov, Z. Neorg, Zh. Neorg. Khim. **55**, 1239 (2010)
85. R. Sengupta, S. Chakraborty, S. Bandyopadhyay, S. Dasgupta, R. Mukhopadhyay, K. Auddy, A.S. Deuri, Polym. Eng. Sci. **47**, 1956 (2007)
86. Q.T. Nguyen, D.G. Baird, Adv. Polym. Technol. **25**, 270 (2006)
87. F. Santiago, A.E. Mucientes, M. Osorio, C. Rivera, Eur. Polym. J. **43**, 1 (2007)
88. E. Manias, L. Touny, K. Wu, B. Strawhecher, Chem. Mater. **13**, 3516 (2001)
89. A. Mousa, J. Karger-Kocsis, Macromol. Mater. Eng. **286**, 260 (2001)

90. S.-S. Lee, C.S. Lee, M.-H. Kim, S.Y. Kwak, M. Park, S.H. Lim, C.R. Choe, J.J. Kim, Polym. Sci. B: Polym. Phys. **39**, 2430 (2001)
91. S.-S. Lee, J. Kim, J. Polym. Sci. B: Polym. Phys. **42**, 246 (2004)
92. S.-S. Lee, J. Kim, J. Polym. Sci. B: Polym. Phys. **42**, 2367 (2004)
93. S.S. Ray, K. Okamoto, M. Okamoto, Macromolecules **36**, 2355 (2003)
94. E. Manias, H. Chen, R. Krishnamoorrti, J. Genzer, E.J. Kramer, E.P. Giannelis, Macromolecules **33**, 7955 (2000)
95. Z.G. Wu, C.X. Zhou, R.R. Qi, H.B. Zhang, J. Appl. Polym. Sci. **83**, 2403 (2002)
96. Z.G. Wu, C.X. Zhou, Polym. Test. **21**, 479 (2002)
97. G. Galgali, C. Ramesh, A. Lele, Macromolecules **34**, 852 (2001)
98. J. Li, C.X. Zhou, G. Wang, J. Appl. Polym. Sci. **89**, 3609 (2003)
99. J. Li, C.X. Zhou, G. Wang, D. Zhao, J. Appl. Polym. Sci. **89**, 318 (2003)
100. D.F. Wu, C.X. Zhou, F. Xie, D.L. Mao, B. Zhang, Polym. Polym. Compos. **13**, 61 (2005)
101. D.F. Wu, C.X. Zhou, F. Xie, D.L. Mao, B. Zhang, Eur. Polym. J. **41**, 2199 (2005)
102. I. Matsubara, K. Hosono, N. Murayama, W. Shin, N. Izu, Bull. Chem. Soc. Jpn. **77**, 1231 (2004)
103. M.R. Bockstaller, R.A. Mickiewicz, E.L. Thomas, Adv. Mater. **17**, 1331 (2005)
104. M.J. Kawasumi, Polym. Sci. A Polym. Chem. **42**, 819 (2004)
105. R.A. Vaia (ed.), *ACS Symposium Series*, vol. 804 (American Chemical Society, Washington, DC, 2002)
106. S.S. Ray, M. Okamoto, Prog. Polym. Sci. **28**, 1539 (2003)
107. D.D. Schmidt, D. Shah, E.P. Giannelis, Curr. Opin. Solid. State. Mater. Sci. **6**, 205 (2002)
108. C. Zilg, F. Dietsche, B. Hoffmann, C. Dietrich, R. Mülhaupt, Macromol. Symp. **169**, 65 (2001)
109. M. Zanetti, S. Lomakin, G. Camino, Macromol. Mater. Eng. **279**, 1 (2000)
110. L.S. Schadler, Polymer-based and polymer-filled nanocomposites, in *Nanocomposite Science and Technology*, ed. by P.M. Ajayan, L.S. Schadlerand, P.V. Braun) (Wiley-VCH, Weinheim, 2003)
111. V.V. Ginzburg, C. Singh, A.C. Balazs, Macromolecules **33**, 1089 (2000)
112. R.A. Vaia, Structural characterization of polymer-layered silicate nanocomposites, in *Polymer–Clay Nanocomposites*, ed. by T.J. Pinnavaia, G.W. Beall (Wiley, Chichester, 2000), p. 229
113. D.W. Kim, A. Blumstein, S.K. Tripathy, Chem. Mater. **13**, 1916 (2001)
114. E. Passaglia, R. Sulcis, F. Ciardelli, M. Malvaldi, P. Narducci, Polym. Int. **54**, 1549 (2005)
115. A.C. Balazs, J. Bicerano, V.V. Ginzburg, in *Polyolefin Composites*, ed. by D. Nwabunma, T. Kyu (Wiley, Hoboken, 2008). Chapter 15
116. F. Chiardelli, S. Coiai, E. Passaglia, A. Pucci, G. Rugg, Polym. Int. **57**, 805 (2008)
117. P. Gómez-Romero, O. Ayyad, J. Suárez-Guevara, D. Muñoz-Rojas, J. Solid State Electrochem. **14**, 1939 (2010)
118. A. Leszczyńska, J. Njuguna, K. Pielichowski, J.R. Banerjee, Thermochim. Acta. **453,** 75 (2007); **454**, 1 (2007)
119. M. Wark, Porphyrins and phtalocyanines encapsulated in inorganic host material, in *The Porphyrin Handbook*, ed. by K.M. Kadish, K.M. Smith, R. Guilard. Phtalocyanines: Properties and materials, vol. 17 (Elsevier Science, Amsterdam, 2003), pp. 247–283
120. T. Ogoshi, H. Itoh, K.-M. Kim, Y. Chujo, Macromolecules **35**, 334 (2002)
121. K. Anderson, A. Sinsawat, R. Vaia, B.L. Farmer, J. Polym. Sci. B Polym. Phys. **43**, 1014 (2005)
122. A. Sinsawat, K.L. Anderson, R.A. Vaia, B.L. Farmer, J. Polym. Sci. B Polym. Phys. **41**, 3272 (2003)
123. R.B. Pandey, B.L. Farmer, J. Polym, Sci. B Polym. Phys. **47**, 2487 (2009)
124. H. Li, Y. Yu, Y. Yang, Eur. Polym. J. **41**, 2016 (2005)
125. Y.S. Choi, H.T. Ham, I.J. Chung, Chem. Mater. **16**, 2522 (2004)
126. Y.S. Choi, M. Xu, I.J. Chung, Polymer **44**, 6989 (2003)

127. M.R. Moghbeli, N. Mehdizadeh, J. Appl. Polym. Sci. **123**, 2064 (2012)
128. L.B. de Paiva, A.R. Morales, F.R.V. Díaz, Appl. Clay Sci. **42**, 8 (2008)
129. Y.K. Kim, Y.S. Choi, K.H. Wang, I. Chung, J. Chem. Mater. **14**, 4990 (2002)
130. W. Xie, J.M. Hwu, G.J. Jiang, T.M. Buthelezi, W. Pan, Polym. Eng. Sci. **43**, 214 (2003)
131. W. Feng, E. Sun, A. Fujii, H. Wu, K. Niihara, K. Yoshino, Bull. Chem. Soc. Jpn. **73**, 2627 (2000)
132. E.M. Moujahid, F. Leroux, M. Dubois, J.P. Besse, C. R. Chimie **62**, 259 (2003)
133. P. Ding, B. Qu, J. Appl. Polym. Sci. **101**, 3758 (2006)
134. L. Vieille, E.M. Moujahid, C. Taviot-Guého, J. Cellier, J.P. Besse, J. Phys. Chem. Solids **65**, 385 (2004)
135. Z.M.O. Rzayev, A. Güner, E.A. Soÿlemez, S. Kavlak, Polym. Adv. Technol. **22**, 1349 (2011)
136. J. Rzayev, Macromolecules **42**, 2135 (2009)
137. K. Huang, J. Rzayev, J. Am. Chem. Soc. **131**, 6880 (2009)
138. L. Zhao, M. Byun, J. Rzayev, Macromolecules **42**, 9027 (2009)
139. Z.M.O. Rzayev, E.A. Sôylemez, B. Davarcioğlu, Polym. Adv. Technol **23**, 278 (2011)
140. A. Matsumoto, T. Odani, Macromol. Rapid Commun. **22**, 1195 (2001)
141. A. Matsumoto, Polym. J. **35**, 93 (2003)
142. S. Oshita, A. Matsumoto, Chem. Eur. J. **12**, 2139 (2006)
143. A. Matsumoto, K. Sada, K. Tashiro, M. Miyata, T. Tsubouchi, T. Tanaka, T. Odani, S. Nagahama, T. Tanaka, K. Inoue, S. Saragai, S. Nakamoto, Angew. Chem. **114**, 2612 (2002)
144. A. Matsumoto, T. Odani, M. Chikada, K. Sada, M. Miyata, J. Am. Chem. Soc. **121**, 11122 (1999)
145. A. Matsumoto, S. Nagahama, T. Odani, J. Am. Chem. Soc. **122**, 9109 (2000)
146. T. Tanaka, A. Matsumoto, J. Am. Chem. Soc. **124**, 9676 (2002)
147. S. Nagahama, T. Tanaka, A. Matsumoto, Angew. Chem. **116**, 3899 (2004); Angew. Chem. Int. Ed., **43**, 3811 (2004)
148. S. Oshita, T. Tanaka, A. Matsumoto, Chem. Lett. **34**, 1442 (2005)
149. P. Sozzani, S. Bracco, A. Comotti, R. Simonutti, I. Camurati, J. Am. Chem. Soc. **125**, 12881 (2003)
150. P. Sozzani, S. Bracco, A. Comotti, M. Mauri, R. Simonutti, P. Valsesia, Chem. Commun. **1921** (2006)
151. A.D. Pomogailo, Russ. Chem. Rev. **71**, 1 (2002)
152. S.-H. Chan, Y.-Y. Lin, C. Ting, Macromolecules **36**, 8910 (2003)
153. W. Mariott, N. Escude, E.Y.-X. Chen, J. Polym. Sci. A Polym. Chem. **45**, 2581 (2007)
154. W.R. Mariott, E.Y.-X. Chen, J. Am. Chem. Soc. **125**, 15726 (2003)
155. Y.H. Jin, H.J. Park, S.S. Im, S.Y. Kwak, S. Kwak, Macromol. Rapid. Commun. **23**, 135 (2002)
156. S.-Y.A. Shin, L.C. Simon, J.B.P. Soares, G. Scholz, Polymer **44**, 5317 (2003)
157. A. He, L. Wang, J. Li, J. Dong, C.A. Han, Polymer **47**, 1767 (2006)
158. S. Zulfiqar, I. Lieberwirth, Z. Ahmad, M.I. Sarwar, Polym. Eng. Sci. **48**, 1624 (2008)
159. S. Zulfiqar, Z. Ahmad, M. Sarwar, Polym. Adv. Technol. **19**, 1720 (2008)
160. T. Agag, T. Takeichi, Polymer **41**, 7083 (2000)
161. M. Okamoto, S. Morita, H. Taguchi, Y.H. Kim, T. Kataka, H. Tateyama, Polymer **41**, 3887 (2000)
162. C. Zeng, L.J. Lee, Macromolecules **34**, 4098 (2001)
163. D.W. Kim, A. Blumstein, H. Liu, M.J. Downey, J. Kumar, S.K. Tripathy, J. Macromol. Sci. Pure Appl. Chem. **38**, 1405 (2001)
164. S.K. Sahoo, D.W. Kim, J. Kumar, A. Blumstein, A.L. Cholli, Macromolecules **36**, 2777 (2003)
165. M. Casciola, A. Donnadio, M. Pica, V. Valentini, P. Piaggio, Macromol. Symp. **230**, 95 (2005)
166. G.D. Gatta, S. Masci, R. Vivani, J. Mater. Chem. **13**, 1215 (2003)

167. R. Singhal, M. Datta, J. Appl. Polym. Sci. **103**, 3299 (2007)
168. L. Wang, M. Rocci-Lane, P. Brazis, C.R. Kannewurf, Y. Kim, W. Lee, J.-H. Choy, M.G. Kanatzidis, J. Am. Chem. Soc. **122**, 6629 (2000)
169. I. Boyano, M. Bengoechea, I. DeMeatza, O. Miguel, I. Cantero, E. Ochoteco, H. Grande, M. Lira-Cantu, P. Gomez-Romero, J. Power. Sources **174**(2), 1206 (2007)
170. I. Boyano, M. Bengoechea, I. de Meatza, O. Miguel, I. Cantero, E. Ochoteco, J. Rodriguez, M. Lira-Cantu, P. Gomez-Romero, J. Power. Sources **166**, 471 (2007)
171. D.R. Rolison, B. Dunn, J. Mater. Chem. **11**, 963 (2001)
172. A. Gapeev, C.N. Yang, S.J. Klippenstein, R.C. Dunbar, J. Phys. Chem. **104**, 3246 (2000)
173. E. Shouji, D.A. Buttry, Langmuir **15**, 669 (1999)
174. P.J. Kulesza, M. Chojak, K. Miecznikowski, A. Lewera, M.A. Malik, A. Kuhn, Electrochem. Commun. **4**, 510 (2002)
175. L. Adamczyk, P.J. Kulesza, K. Miecnikowski, B. Palys, M. Chojak, D. Krawczyk, J. Electrochem. Soc. **152**, E98 (2005)
176. J. Vaillant, M. Lira-Cantu, K. Cuentas-Gallegos, N. Casañ-Pastor, P. Gómez-Romero, Prog. Solid. State. Chem. **34**, 147 (2006)
177. V. Subramanian, H.W. Zhu, R. Vajtai, P.M. Ajayan, B.Q. Wei, J. Phys. Chem. B **109**, 20207 (2005)
178. P. Gomez-Romero, M. Chojak, A.K. Cuentas-Gallegos, J.A. Asensio, P.J. Kulesza, N. Casañ-Pastor, M. Lira-Cantu, Electrochem. Commun. **5**, 149 (2003)
179. A.K. Cuentas-Gallegos, M. Lira-Cantu, N. Casañ-Pastor, P. Gomez-Romero, Adv. Funct. Mater. **15**, 1125 (2005)
180. T. Wang, W. Liu, J. Tian, X. Shao, D. Sun, Polym. Compos. **25**, 111 (2004)
181. B.G. Soares, M. Oliveira, S. Zaioncz, A.C. Gomes, A.A. Silva, K.S. Santos, R.S. Mauler, J. Appl. Polym. Sci. **119**, 505 (2011)
182. B. Pourabas, V. Raeesi, Polymer **46**, 5533 (2005)
183. D.R. Dillon, K.K. Tenneti, C.Y. Li, F.K. Ko, I. Sics, B.S. Hsiao, Polymer **47**, 1678 (2006)
184. L. Qiu, W. Chen, B. Qu, Polymer **47**, 9 (2006)
185. S. Filippi, E. Mameli, C. Marazzato, P. Magagnini, Eur. Polym. J. **43**, 1645 (2007)
186. D. Burgentzle, J. Duchet, J.F. Gerard, A. Jupin, B. Fillon, J. Colloid Interface Sci. **278**, 26 (2004)
187. M.K. Song, Y.M. Kim, Y.T. Kim, H.W. Rhee, A. Smirnova, N.M. Sammes, J.M. Fenton, J. Electrochem. Soc. **153 A**, 2239 (2006)
188. A.K. Ghosh, E.M. Woo, Polymer **45**, 4749 (2004)
189. T.L. Wang, W.S. Hwang, M.H. Yeh, J. Appl. Polym. Sci. **104**, 4135 (2007)
190. V. Sridhar, D.K. Tripathy, J. Appl. Polym. Sci. **101**, 3630 (2006)
191. G. Liang, J. Xu, S. Bao, W. Xu, J. Appl. Polym. Sci. **91**, 3974 (2004)
192. H. Acharya, S.K. Srivastava, A.K. Bhowmick, Polym. Eng. Sci. **48**, 837 (2006)
193. M. Frounchi, S. Dadbin, Z. Salehpour, M. Noferesti, J. Membr. Sci **282**, 142 (2006)
194. R. Valsecchi, M. Vigano, M. Levi, S. Turri, J. Appl. Polym. Sci. **102**, 4484 (2006)
195. L. Zhang, M. Wan, J. Phys. Chem. **107**, 6748 (2003)
196. Y. Someya, M. Shibata, Polymer **46**, 4891 (2005)
197. I.M. Daniel, H. Miyagawa, E.E. Gdoutos, J.J. Luo, Exp. Mech. **43**, 348 (2003)
198. Z.M.O. Rzayev, A. Yilmazbayhan, E. Alper, Adv. Polym. Technol. **26**, 41 (2007)
199. E. Söylemez, N.C. Aylak, Z.M.O. Rzayev, eXPRESS Polym. Lett. **2**, 639 (2008)
200. S.C. Tjong, Mater. Sci. Eng. **53**, 73 (2006)
201. H.K. Can, Z.M.O. Rzayev, A. G ner, J. Appl. Polym. Sci. **90**, 4009 (2003)
202. W. Chen, L. Feng, B. Qu, Chem. Mater. **16**, 368 (2004)
203. T. Ohtake, Y. Takamitsu, K. Ito-Akita, K. Kanie, M. Yoshizawa, T. Mukai, H. Ohno, T. Kato, Macromolecules **33**, 8109 (2000)
204. B.P. Grady, C.P. Rhodes, S. York, R.E. Frech, Macromolecules **34**, 8523 (2001)
205. D. Choi, M.A. Kader, B.H. Cho, Y. Huh, Y. Nuh, C. Nah, J. Appl. Polym. Sci. **98**, 1688 (2005)

206. A. Kelarakis, E.P. Giannelis, K. Yoon, Polymer **48**, 7567 (2007)
207. S.D. Wanjale, J.P. Jog, J. Appl. Polym. Sci. **90**, 3233 (2003)
208. S. Sadhu, A.K. Bhowmick, Rubber Chem. Technol. **78**, 321 (2005)
209. Y.-R. Liang, W.-L. Cao, X.-B. Zhang, Y.-J. Tan, S.-J. He, L.-Q. Zhang, J. Appl. Polym. Sci. **112**, 3087 (2009)
210. J. Karger-Kocsis, C.-M. Wu, Polym. Eng. Sci. **44**, 1083 (2004)
211. K.S. Santos, S.A. Liberman, M.A.S. Ovieda, R.S. Mauler, J. Polym. Sci. B Polym. Phys. **46**, 2519 (2008)
212. J.H. Joo, J.H. Shim, J.H. Choi, C.-H. Choi, D.-S. Kim, J.-S. Yoon, J. Appl. Polym. Sci. **109**, 3645 (2008)
213. L. Liu, D. Jia, Y. Luo, B. Guo, J. Appl. Polym. Sci. **100**, 1905 (2006)
214. N. Ristolainen, U. Vainio, S. Paavola, M. Torkkeli, J. Appl. Polym. Sci. **43**, 1892 (2005)
215. S.H. Kim, J.W. Chung, T.J. Kang, S.Y. Kwak, T. Suzuki, Polymer **48**, 4271 (2007)
216. D. Kang, D. Kim, S.-H. Yoon, D. Kim, C. Barry, J. Mead, Macromol. Mater. Eng. **292**, 329 (2007)
217. M. Kurata, Y. Tsunashima, in *Polymer Handbook*, ed. by J. Brandrup, E.H. Immergut, vol. Section VII (Wiley-Interscience, New York, 1989), p. 381
218. D. Wu, C. Zhou, H. Zheng, J. Appl. Polym. Sci. **99**, 1865 (2006)
219. Z.M. Wang, H. Nakajimia, E. Manias, T.C. Chung, Macromolecules **36**, 8919 (2003)
220. P. Ding, B. Qu, Polym. Eng. Sci. **46**, 1153 (2006)
221. S. Zhang, T.R. Hull, A.R. Horrocks, G. Smart, B.K. Kandola, J. Ebdon, P. Joseph, B. Hunt, Polym. Degrad. Stab. **92**, 727 (2007)
222. Y. Ji, B. Li, S. Ge, J.C. Sokolov, M.H. Rafailovich, Langmuir **22**, 1321 (2006)
223. F.R. Costa, M.A. Goad, U. Wagenknecht, G. Heinrich, Polymer **46**, 4447 (2005)
224. F.R. Costa, U. Wagenknecht, D. Jehnichen, M.A. Goad, G. Heinrich, Polymer **47**, 1649 (2006)
225. U. Costantino, A. Gallipoli, M. Rocchetti, G. Camino, F. Bellucci, A. Frache, Polym. Degrad. Stab. **90**, 586 (2005)
226. D. Wang, J. Zhu, C.A. Wilkie, Polym. Degrad. Stab. **80**, 171 (2003)
227. W. Lertwimolnun, B. Vergnes, Polym. Eng. Sci. **46**, 315 (2006)
228. M. Mainil, M. Alexandre, F. Monteverde, P. Dubois, J. Nanosci. Nanotechnol. **6**, 337 (2006)
229. M.A. Osman, J.E.P. Rupp, U.W. Suter, Polymer **46**, 8202 (2005)
230. K. Chrissopoulou, I. Altintzi, S.H. Anastasiadis, E.P. Giannelis, M. Pitsikalis, N. Hadjichristidis, N. Theophilon, Polymer **46**, 12440 (2005)
231. S. Parija, S.K. Nayak, S.K. Verma, S.S. Tripathy, Polym. Compos. **25**, 646 (2004)
232. K.H. Chen, S.M. Yang, J. Appl. Polym. Sci. **86**, 414 (2002)
233. Y. Güldoğan, S. Eğri, Z.M.O. Rzaev, E. Pişkin, J. Appl. Polym. Sci. **92**, 3675 (2004)
234. J.M. Yeh, S.J. Liou, C.Y. Lai, P.C. Wu, T.Y. Tsai, Chem. Mater. **13**, 1131 (2001)
235. H. Nasegawa, M. Okamoto, A. Usuki, J. Appl. Polym. Sci. **93**, 758 (2004)
236. A. Tidjani, O. Wald, M.-M. Pohl, M.P. Henschel, B. Schartel, Polym. Degrad. Stab. **82**, 133 (2003)
237. C.M. Koo, M.J. Kim, S.M.N. Choi, O. Kim, I.J. Chung, J. Appl. Polym. Sci. **88**, 1526 (2003)
238. W. Xu, G. Liand, W. Wang, S. Tang, P. He, W.-P. Pan, J. Appl. Polym. Sci. **88**, 3093 (2003)
239. Z.M.O. Rzaev, A. Güner, H.K. Can, A. Asıcı, Polymer **42**, 5599 (2001)
240. X. Kornmann, H. Lindberg, L.A. Berglund, Polymer **42**, 1303 (2001)
241. J. Zhang, C.A. Wilkie, Polym. Degrad. Stab. **80**, 163 (2003)
242. Y. Tang, Y. Hu, S.F. Wang, Z. Gui, Z. Chen, W.C. Fan, Polym. Degrad. Stab. **78**, 555 (2002)
243. J.W. Gilman, C.J. Jackson, A.B. Morgan, J.R. Harris, E. Manias, E.P. Giannelis, M. Wuthenow, D. Hilton, S.H. Philips, Chem. Mater. **12**, 1866 (2000)
244. M. Böhning, H. Goering, A. Fritz, K.-W. Brzezinka, G. Turky, A. Schönhals, B. Schartel, Macromolecules **38**, 2764 (2005)
245. J.T. Xu, Q. Wang, Z.Q. Fan, Eur. Polym. J. **41**, 3011 (2005)

246. L. Valentini, J. Biagiotti, M.A. López-Manchado, S. Santucci, J.M. Kenny, Polym. Eng. Sci. **44**, 303 (2004)
247. Z.M.O. Rzaev, A. Yilmazbayhan, E. Alper, Adv. Polym. Techn. **26**, 41 (2007)
248. F. Perrin-Sarazin, M.T. Ton-That, M.N. Bureau, J. Denault, Polymer **46**, 11624 (2005)
249. D. Garicia-López, O. Picqazo, J.C. Merino, J.M. Pastor, Eur. Polym. J. **39**, 945 (2003)
250. C.H. Jeon, S.H. Ryu, Y.W. Chang, Polym. Int. **52**, 153 (2003)
251. Y. Wang, F. Chen, Y. Li, K. Wu, Soc. Plast. Eng. Ann. Tech. Conf. **61**, 3670 (2003)
252. K.A. Nara, Soc. Plast. Eng. Ann. Tech. Conf. Proc. **61**, 3717 (2003)
253. X. Liu, Q. Wu, Polymer **42**, 10013 (2001)
254. Y. Zang, J. Lee, J.M. Rhee, K.Y. Rhee, Compos. Sci. Technol. **64**, 1383 (2004)
255. Y. Zang, J. Lee, H. Jang, C. Nah, Compos. Eng. **35**, 133 (2004)
256. H.R. Dennis, D.L. Hunter, S.K.D. Chang, J.L. White, J.W. Cho, D.R. Paul, Polymer **41**, 9513 (2001)
257. M. Zanetti, G. Camino, R. Mülhaupt, Polym. Degrad. Stab. **74**, 413 (2001)
258. M. Zanetti, G. Camino, R. Thomann, R. Mülhaupt, Polymer **42**, 4501 (2001)
259. A. Riva, M. Zanetti, M. Braglia, G. Camino, L. Falqui, Polym. Degrad. Stab. **77**, 299 (2002)
260. F. Bellucci, G. Camino, A. Frache, V. Ristori, L. Sorrentino, S. Iannace, X. Bian, M. Guardasole, S. Vaccaro, e-Polym. **014**, (2006)
261. U.N. Ratnayake, B. Haworth, D.J. Hourston, J. Appl. Polym. Sci. **112**, 320 (2009)
262. M. Alexandre, G. Beyer, C. Henrist, R. Cloots, A. Rulmont, R. Jerome, P. Dubois, Macromol. Rapid Commun. **22**, 643 (2001)
263. U. Yilmazer, G. Ozden, Polym. Compos. **27**, 249 (2006)
264. K.H. Wang, M.H. Choi, C.M. Koo, Y.S. Choi, I.J. Chung, Polymer **42**, 9819 (2001)
265. I.S. Suh, S.H. Ryu, J.H. Bae, Y.W. Chang, J. Appl. Polym. Sci. **94**, 1057 (2004)
266. J.T. Yoon, W.H. Jo, M.S. Lee, M.B. Ko, Polymer **42**, 329 (2001)
267. Q. Zhang, Q. Fu, L. Jiang, Y. Lei, Polym. Int. **49**, 1561 (2000)
268. D.J. Frankowski, S.A. Khan, R.J. Spontak, Adv. Mater. **19**, 1286 (2007)
269. M. Vacatello, Macromolecules **34**, 1946 (2001)
270. S. Tanoue, L.A. Utracki, A. Garcia-Rejon, J. Tatibouët, K.C. Cole, M.R. Kamal, Polym. Eng. Sci. **44**, 1046 (2004)
271. D.Z. Chen, H.Y. Yang, P.S. He, W.A. Zhang, Compos. Sci. Technol. **65**, 1593 (2005)
272. Y.Q. Li, H. Ishida, Macromolecules **38**, 6513 (2005)
273. B. Hoffmann, C. Dietrich, R. Thomann, C. Friedrich, R. Mülhaupt, Macromol. Rapid Commun. **21**, 57 (2000)
274. R.A. Vaia, E.P. Giannelis, Polymer **42**, 1281 (2001)
275. A.B. Morgan, R.H. Harris Jr., T. Kashiwagi, L.J. Chyall, J.W. Gilman, Fire Mater. **26**, 247 (2002)
276. O. Monticelli, Z. Musina, A. Frache, F. Bellucci, G. Camino, S. Russo, Polym. Degrad. Stab. **92**, 370 (2007)
277. M. Zanetti, Polym. Nanocomposites **253** (2006)
278. M. Lewin, E.M. Pearce, K. Levon, A. Mey-Marom, M. Zammarano, C.A. Wilkie, B.N. Jang, Polym. Adv. Technol. **17**, 226 (2006)
279. R.K. Bharadwaj, Macromolecules **34**, 9189 (2001)
280. S.M. Lomakin, G.E. Zaikov, Vysokomol. Soed. Ser. B **47**, 105 (2005)
281. A.P. Patio-Soto, S. Sanchez-Valdes, L.F. Ramos-Devalle, J. Polym, Sci Part Polym. Phys. **46**, 190 (2008)
282. G. Chen, X. Chen, Z. Lin, W. Ye, J. Mater. Sci. Lett. **18**, 1761 (2002)
283. J.M. Hwu, G.J. Jiang, Z.M. Gao, W. Xie, W.P. Pan, J. Appl. Polym. Sci. **83**, 1702 (2002)
284. Y. Munusamy, H. Ismail, M. Mariatti, C.T. Ratnam, J. Vinyl Addit. Technol. **15**, 244 (2009)
285. S.-S. Lee, M.H. Hur, H. Yang, S. Lim, J. Kim, J. Appl. Polym. Sci. **101**, 2749 (2006)
286. W.-F. Lee, L.-L. Jou, J. Appl. Polym. Sci. **94**, 74 (2004)
287. T. Peprnicek, J. Duchet, L. Kovarova, J. Malac, J.F. Gerard, J. Simonik, Polym. Degrad. Stab. **91**, 1855 (2006)

288. M.A. Souza, L.A. Pessan, N. Rodolfo Jr., Polimeros **16**, 257 (2006)
289. Y. Yoo, S.-S. Kim, J.C. Won, K.-Y. Choi, J.H. Lee, Polym. Bull. **52**, 373 (2004)
290. B. Dietrich, J. Vinyl Addit. Tech. **7**, 168 (2001)
291. C. Wan, X. Qiao, Y. Zhang, Y. Zhang, Polym. Test. **22**, 453 (2003)
292. X.L. Xie, R.K.Y. Li, Q.X. Liu, Y.W. Mai, Polymer **45**, 2793 (2004)
293. L. Kovarova, A. Kalendova, J.F. Gerard, J. Malac, J. Simonik, Z. Weiss, Macromol. Symp. **221**, 105 (2005)
294. H. Hu, M. Pan, X. Li, X. Shi, L. Zhang, Polym. Int. **53**, 225 (2004)
295. M.E. Romero-Guzman, A. Romo-Uribe, E. Ovalle-Garcıa, R. Olayo, C.A. Cruz-Ramos, Polym. Adv. Technol. **19**, 1168 (2008)
296. P. Jawahar, M. Balasubramanian, J. Nanosci. Nanotechnol. **6**, 3973 (2006)
297. J. Chandradass, M.R. Kumar, R. Velmurugan, Mater. Lett. **61**, 4385 (2007)
298. J. Kwiatkowski, A.K. Whittaker, J. Polym. Sci. B Polym. Phys. **39**, 1678 (2001)
299. I. Mironi-Harpaz, M. Narkis, A. Siegmann, Polym. Eng. Sci. **45**, 174 (2005)
300. M.-J. Binette, C. Detellier, J. Chem. **80**, 1708 (2002)
301. C.O. Oriakhi, M. Lerner, Chem. Mater. **8**, 2016 (1996)
302. Z. Shen, G.P. Simon, Y.-B. Cheng, Polym. Eng. Sci. **42**, 2369 (2002)
303. P. Aranda, Y. Mosqueda, E. Perez-Cappe, E. Ruiz-Hitzky, J. Polym. Sci. B Polym. Phys. **41**, 3249 (2003)
304. U. Opara-Krasovec, R. Jese, B. Orel, G. Drazic, Monat. Chem. **133**, 1115 (2002)
305. N. Hasegawa, H. Okamoto, M. Kato, A. Usuki, N. Sato, Polymer **44**, 2933 (2003)
306. T.D. Fornes, P.J. Yoon, H. Keskkula, D.R. Paul, Polymer **42**, 9929 (2001)
307. T.D. Fornes, P.J. Yoon, D.L. Hunter, H. Keskkula, D.R. Paul, Polymer **43**, 5915 (2002)
308. M.I. Sarwar, S. Zulfiqar, Z. Ahmad, Colloid Polym. Sci. **285**, 1733 (2007)
309. B. Lepoittevin, N. Pantoustier, M. Alexandre, C. Calberg, R. Jerome, P. Dubois, J. Mater. Chem. **12**, 3528 (2002)
310. D.L. VanderHart, A. Asano, J.W. Gilman, Chem. Mater. **13**, 3781 (2001)
311. G. Gorrasi, M. Tortora, V. Vittoria, E. Pollet, B. Lepoittevin, M. Alexandre, P. Dubois, Polymer **44**, 2271 (2001)
312. P.B. Messersmith, E.P. Giannelis, J. Polym. Sci. A Polym. Chem. **33**, 1047 (1995)
313. S. Bourbigot, M. LeBras, F. Dabrowski, J.W. Gilman, T. Kashiwagi, Fire Mater. **24**, 201 (2000)
314. M.K. Akkapeddi, Polym. Compos. **21**, 576 (2000)
315. A. Usuki, M. Kawasumi, Y. Kojima, A. Okada, T. Kurauchi, O. Kamigaito, J. Mater. Res. **8**, 1174 (1993)
316. S. Zulfiqar, M. Ishaq, M.I. Sarwar, Surf. Interface Anal. **40**, 1195 (2008)
317. T.D. Fornes, D.R. Paul, Polymer **44**, 3945 (2003)
318. S. Wu, F. Wang, C.M. Ma, W. Chang, C. Kuo, H. Kuan, W. Chen, Mater. Lett. **49**, 327 (2001)
319. M.I. Sarwar, S. Zulfiqar, Z. Ahmad, J. Sol-Gel Sci. Technol. **45**, 89 (2008)
320. S. Zulfiqar, Z. Ahmad, M.I. Sarwar, Colloid Polym. Sci. **285**, 1749 (2007)
321. K.H. Tyan, T. Wei, E. Hsieh, J. Polym. Sci. B Polym. Phys. **38**, 2873 (2000)
322. H. Fong, W. Liu, C.S. Wang, R.A. Vaia, Polymer **43**, 775 (2002)
323. D.P.N. Vlasveld, H.E.N. Bersee, S.J. Picken, Polymer **46**, 10269 (2005)
324. L. Li, L.M. Bellan, H.G. Craighead, M.W. Frey, Polymer **47**, 6208 (2006)
325. Y. Liang, X. Xia, Y. Luo, Z. Jia, Mater. Lett. **61**, 3269 (2007)
326. S. Zulfiqar, I. Lieberwirth, M.I. Sarwar, Chem. Phys. **344**, 202 (2008)
327. S. Zulfiqar, M.I. Sarwar, High Perform. Polym. **21**, 3 (2009)
328. D.P.N. Vlasveld, P.P. Parlevliet, H.E.N. Bersee, S.J. Picken, Appl. Sci. Manuf. **36**, 1 (2005)
329. T. Liu, K.P. Lim, W.C. Tjiu, K.P. Pramoda, Z.-K. Chen, Polymer **44**, 3529 (2003)
330. D.M. Lincoln, R.A. Vaia, Z.-G. Wang, B.S. Hsiao, Polymer **42**, 1621 (2001)
331. A.B. Morgan, J.W. Gilman, J. Appl. Polym. Sci. **87**, 1329 (2003)
332. V.E. Yudin, G.M. Divoux, J.U. Otaigbe, V.M. Svetlichnyi, Polymer **46**, 10866 (2005)
333. Y.J. Li, H. Shimizu, Polymer **45**, 7381 (2004)

334. M. Mehrabzadeh, M.R. Kamal, Polym. Eng. Sci. **44**, 1152 (2004)
335. H. Zheng, Y. Zhang, Z. Peng, Y. Zhang, J. Appl. Polym. Sci. **92**, 638 (2004)
336. A. Usuki, A. Tukigase, M. Kato, Polymer **43**, 2185 (2002)
337. S. Sadhu, A.K. Bhowmick, J. Polym. Sci. B Polym. Phys. **42**, 1573 (2004)
338. S. Sadhu, A.K. Bhowmick, J. Polym. Sci. B Polym. Phys. **43**, 1854 (2005)
339. M.A. Kader, K. Kim, Y.S. Lee, C.J. Nah, Mater. Sci. **41**, 734 (2006)
340. A. Das, R. Jurk, K.W. Stöckelhuber, G. Heinrich, Macromol. Mater. Eng. **293**, 479 (2008)
341. A. Das, R. Jurk, K.W. Stöckelhuber, G. Heinrich, Expr. Polym. Lett. **1**, 717 (2007)
342. R.R. Tiwari, K.C. Khilar, U. Natarajan, Appl. Clay Sci. **38**, 203 (2008)
343. S. Siengchin, J. Karger-Kocsis, R. Thomann, Exp. Polym. Lett. **2**, 746 (2008)
344. J. Wang, K. Yang, N. Xu, J. Appl. Polym. Sci. **123**, 1293 (2012)
345. L. Celine, M. Fabien, A. Michael, D. Philippe, J. Nanosci. Nanotechnol. **9**, 2731 (2009)
346. G. He, Y. Chen, M.M. Zhang, D.X. Wang, K. Cong, H.B. Fan, F. Zhou, J. Polym. Mater. Sci. Eng. **27**, 150 (2011)
347. W.S. Mark, T.S. Keith, L.O. Duan, J. Inorg. Organomet. Polym. **18**, 364 (2008)
348. A.O. Maged, M. Vikas, M. Massimo, Macromolecules **36**, 9851 (2003)
349. K.G. Gatos, R. Thomann, J. Karger-Kocsis, Polym. Int. **53**, 1191 (2004)
350. A.B. Morgan, Mater. Matters. **2**, 20 (2007)
351. A.-R. Lee, H.-M. Park, H. Lim, T. Kang, X. Li, W.-J. Cho, C.-S. Ha, Polymer **43**, 2495 (2002)
352. H. Ishida, S. Campbell, J. Blackwell, Chem. Mater. **2**, 1260 (2000)
353. Y.H. Hyun, S.T. Lim, H.J. Choi, M.S. Jhon, Macromolecules **34**, 8084 (2001)
354. B.J. Ash, L.S. Schadler, R.W. Siegel, Mater. Lett. **55**, 83 (2002)
355. J.-C. Wang, Y.-H. Chen, R.-J. Chen, J. Polym. Sci. B Polym. Phys. **45**, 519 (2007)
356. B. Han, A.M. Cheng, G.D. Ji, S.S. Wu, J. Shen, J. Appl. Polym. Sci. **91**, 2536 (2004)
357. J.Y. Lee, M.J. Shim, S.W. Kim, Polym. Eng. Sci. **39**, 1993 (1999)
358. C. Zilg, R. Thomann, J. Finter, R. Mulhaupt, Macromol. Mater. Eng. **280**/**281**, 41 (2000)
359. H. Zhang, Z. Zhang, K. Friedrich, C. Eger, Acta Mater. **54**, 1833 (2006)
360. C. Karikal Chozhan, M. Alagar, P. Gnanasundaram, Polym. Polym. Comp. **16**, 283 (2008)
361. C. Karikal Chozhan, M. Alagar, R. Josephine Sharmila, P. Gnanasundaram, J. Polym. Res. **14**, 319 (2007)
362. S. Premkumar, C. Karikal Chozhan, M. Alagar, Polym. Eng. Sci. **49**, 747 (2009)
363. S.M. Lee, T.R. Hwang, Y.S. Song, J.W. Lee, Polym. Eng. Sci. **44**, 1170 (2004)
364. M. Quarmyne, W. Chen, Langmuir **19**, 2533 (2003)
365. H. Tu, L. Ye, Polym. Adv. Technol. **20**, 21 (2009)
366. I.A. Chmutin, P.N. Brevnov, G.R. Sabirova, O.D. Nazirova, N.G. Ryvkina, L.N. Novokshonova, Nanotekhnika **3**, 33 (2011)
367. K.S. Novoselov, A.K. Geim, S.V. Morozov, D. Jiang, Y. Zhang, S.V. Dubonos, I.V. Grigorieva, A.A. Firsov, Science **306**, 666 (2004)
368. M.S. Dresselhaus, G. Dresselhaus, Adv. Phys. **51**, 1 (2002)
369. A. Reina, X.T. Jia, J. Ho, D. Nezich, H.B. Son, V. Bulovic, M.S. Dresselhaus, J. Kong, Nano Lett. **9**, 30 (2009)
370. Y.B. Zhang, Y.W. Tan, H.L. Stormer, P. Kim, Nature **438**, 201 (2005)
371. K.S. Novoselov, A.K. Geim, S.V. Morozov, D. Jiang, Y. Zhang, M.I. Katsnelson, I.V. Grigorieva, S.V. Dubonos, A.A. Firsov, Nature **438**, 197 (2005)
372. D. Zhan, L. Sun, Z.H. Ni, L. Liu, X.F. Fan, Y. Wang, T. Yu, Y.M. Lam, W. Huang, Z.X. Shen, Adv. Funct. Mater. **20**, 3504 (2010)
373. I.I. Mazin, A.V. Balatsky, Philos. Mag. Lett. **90**, 731 (2010)
374. M. Nath, C.N.R. Rao, J. Am. Chem. Soc. **123**, 4841 (2001)
375. M. Lerner, C. Oriakhi, Layered metal chalcogenides, in *Handbook of Layered Materials*, ed. by S. Auerbach, K.A. Carrado, P. Dutta (Marcel Dekker, New York, 2004)
376. E. Benavente, M.A. Santa Ana, G. Gonzalez, Phys. Status Solidi B-Basic Res. **241**, 2444 (2004)

377. N. Mirabal, P. Aguirre, M.A. Santa Ana, E. Benavente, G. Gonzalez, Electrochim. Acta **48**, 2123 (2003)
378. M.A. Santa Ana, E. Benavente, P. Gómez-Romero, G. González, J. Mater. Chem. **16**, 307 (2006)
379. G. Alberti, M. Casciola, M. Pica, G. Di Cesare, Ann. N.Y. Acad. Sci. **984**, 208 (2003)
380. H.-L. Tsai, J.L. Schindler, C.R. Kannewurf, M.G. Kanatzidis, Chem. Mater. **9**, 875 (1997)
381. T. Hanaoka, T. Tago, K. Wakabayashi, Bull. Chem. Soc. Jpn. **74**, 1349 (2001)
382. J.-H. Zeng, J. Yang, Y. Zhu, Y.-F. Liu, Y.-T. Qian, H.-G. Zheng, Chem. Commun. **15**, 1332 (2001)
383. J.G. Winiarz, L. Zhang, J. Park, P.N. Prasad, J. Phys. Chem. B **106**, 967 (2002)
384. Z. Qiao, Y. Xie, M. Chen, J. Xu, Y. Zhu, Y. Qian, Chem. Phys. Lett. **321**, 504 (2000)
385. W. Guo, J.J. Li, Y.A. Wang, X. Peng, J. Am. Chem. Soc. **125**, 3901 (2003)
386. L. Li, E. Beniash, E.R. Zubarev, W. Xiang, B.M. Rabatic, G. Zhang, S.I. Stupp, Na. Mater. **2**, 689 (2003)
387. S.C. Tjong, Y.Z. Meng, Polymer **40**, 1109 (1999)
388. K.G.S. Ranmohotti, E. Josepha, J. Choi, J. Zhang, J.B. Wiley, Adv. Mater. **23**, 442 (2011)
389. W.H. He, J. Huang, X.F. Sun, A.J. Frontier, J. Am. Chem. Soc. **130**, 300 (2008)
390. K.A. Tarasov, V.P. Isupov, B.B. Bokhonov, Y.A. Gaponov, B.P. Tolochko, M.R. Sharafutdinov, S.S. Shatskaya, J. Mater. Synth. Proc. **8**, 21 (2000)
391. N.E. Kotelnikova, G. Vegner, T. Paakari, R. Sepimaa, V.N. Demidov, A.S. Serebryakov, A.V. Shchukarev, A.V. Gribanov, Z. Obshch, Zh. Obshch. Khim. **73**, 447 (2003)
392. V. Uskokovic, D.P. Uskokovic, J. Biomed, Mater. Res. B Appl. Biomater. **96B**, 152 (2011)
393. J.A. Shellman, H.R. Reese, Biopolymers **39**, 161 (1996)
394. R.D. Snyder, D.E. Ewing, L.B. Hendry, Environ. Mol. Mutagen. **44**, 163 (2004)
395. S. Letaïef, M.A. Martín-Luengo, P. Aranda, E. Ruiz-Hitzky, Adv. Funct. Mater. **16**, 401 (2006)
396. H. Haiyan, P. Mingwang, L. Xiucuo, S. Xudong, Z. Liucheng, Polym. Int. **53**, 225 (2004)